Escola Politécnica da Universidade de São Paulo
Departamento de Engenharia de Energia e Automação Elétricas

Harnessing electricity from salinity gradients: Pressure retarded osmosis

André de Oliveira
Projeto de Formatura 2011

Escola Politécnica da Universidade de São Paulo
Departamento de Engenharia de Energia e Automação Elétricas

Harnessing electricity from salinity gradients: Pressure retarded osmosis

Trabalho de conclusão de curso apresentado como parte dos pré-requisitos para a obtenção do diploma de Engenharia Elétrica com habilitação em Energia e Automação, à Escola Politécnica da Universidade de São Paulo.

Orientador: Prof. Dr. Luiz Natal Rossi
Coordenador: Prof. Dr. Carlos Márcio Vieira Tahan

André de Oliveira
Projeto de Formatura 2011

André de Oliveira

Harnessing electricity from salinity gradients: Pressure retarded osmosis

Energia dos gradientes de salinidade: Osmose retardada a pressão

Trabalho de conclusão de curso apresentado como parte dos pré-requisitos para a obtenção do diploma de Engenharia Elétrica com habilitação em Energia e Automação, à Escola Politécnica da Universidade de São Paulo.

São Paulo, 07/12/2011
Orientador: Prof. Dr. Luiz Natal Rossi
Coordenador: Prof. Dr. Carlos Márcio Vieira Tahan

Banca Examinadora: Prof. Dr. Lourenço Matakas Junior
Prof. Dr. Dorel Soares Ramos
Prof. Dr. Carlos Márcio Vieira Tahan

Agradecimentos

À Universidade de São Paulo e ao Politecnico di Torino.

Aos Professores Luiz Natal Rossi e Raffaela Gerboni pela oportunidade dada e pelo acompanhamento.

Aos meus parceiros de ultramar Marne Carlilo Schu e família, Jonathan Perez, Estefania Greco, Miguel Medrano, Elka Sierra e Emanuele Chiarello; pelos momentos de tranquilidade em terras estrangeiras.

Aos habitantes da Corso Peschiera número 271, Albert Lopes de Oliveira, Eduardo Sinato, Humberto Stein Shiromoto, Gabriel Neves, Vinícius Vitusso, Murilo Nagato e Rafael de Bessa; pela fraternidade.

Aos amigos politécnicos que permaneceram em terras tupiniquins, dentre eles Raoni Rugai Marinho, Marcos Zaparolli Ueocka, Daniel Nascimento Vivacqua e Renata Ito Horioka.

Aos amigos de longa data, do colégio, pela certeza do reencontro.

À minha família, pelo apoio incondicional.

À Taitana Teixeira Gomes, pela companhia inabalável.

"A sabedoria não se transmite, é preciso que nós a descubramos fazendo uma caminhada que ninguém pode fazer em nosso lugar e que ninguém nos pode evitar, porque a sabedoria é uma maneira de ver as coisas."
Marcel Proust

Resumo

A geração de energia elétrica a partir de fontes oceânicas sempre apresentou um enorme potencial para suprimir a demanda global com uma fonte de energia de proveniência sustentável e aparentemente infinita. A energia dos gradientes de salinidade refere-se à grande quantidade de energia liberada quando duas soluções com diferentes salinidades se misturam. Portanto, uma vez definidas as salinidades e a proporção de mistura é possível calcular, através de conceitos de termodinâmica, o potencial teórico de realização de trabalho a partir desta fonte. Avaliam-se seis diferentes tecnologias baseadas na energia dos gradientes de salinidade, cada uma em uma fase distinta de desenvolvimento. Em seguida focaliza-se no estudo da viabilidade técnica-econômica do processo de osmose retardada a pressão; identifica-se e dá-se devido tratamento aos pormenores técnicos do design de uma planta piloto durante as fases de posicionamento, dimensionamento e análise econômica. Finalmente, discute-se sobre a prospectiva de produção de eletricidade a partir desta tecnologia e as possíveis barreiras à sua penetração no mercado.

Palavras-chave: Energia oceânica, gradientes de salinidade, processos osmóticos, osmose retardada a pressão.

Abstract

Blue Energy, the production of electricity from oceanic sources, always presented an enormous potential to supply mankind with sustainable energy from an apparent infinite provenance. Salinity-gradient energy is another way to harness oceanic energy by using the chemical potential release from the mixing of solutions with different salinities. Once the salinities of each solution and the proportion of mixing are defined it is possible to calculate the theoretical potential for energy production from thermodynamics. Having this in mind, six different salinity-gradient energy technologies were evaluated, each in a distinguished development phase. Afterwards, techno-economic feasibility of pressure retarded osmosis is investigated. All major technicalities along preliminary design of a pilot plant were identified and unravelled, from power plant siting and sizing to its economic assessment. A final discussion on the theoretical and technical global potential for this technology is presented together with its future prospective.

Keywords: Blue Energy, salinity-gradient energy, osmotic processes and pressure retarded osmosis

Retratação

O autor, assim como a Escola Politécnica da Universidade de São Paulo, não favorecem nem dão suporte a quaisquer produtos ou produtores. A presença do nome de algumas marcas registradas ou fabricantes no texto se aplicam somente porque o autor as considera essenciais na consumação dos objetivos deste estudo.

Disclaimer

Neither the author nor the University of São Paulo's Polytechnic School endorses any products or manufacturers. Trademarks or manufacturers' names appear herein solely because they were considered essential to the objective of this study.

Contents

Table of figures

C1. Introduction

1.1 Salinity-gradient energy – Blue energy

Blue Energy is a term referring to the technologies of oceanic energy production; it can be harnessed through a variety of methods: tidal power, wave power, current power, thermal energy conversion and osmosis. It is a promising renewable energy source due to the common impression of an infinitely vast ocean, an infinite source of power. Predicted since 1950s (PATTLE, 1954), salinity-gradient power properly uses natural processes such as osmosis and salt diffusion to produce electricity; there are several interesting technologies that can harness such energy, some of them are introduced in the further sections of this study. Nonetheless, amongst those techniques there are two which deserve earlier mention for they are already tested at higher scale: Pressure retarded osmosis (PRO) and Reverse electrodialysis (RED).

Wherever a river runs into the ocean, huge amounts of energy are dispersed during the irreversible mixing of fresh and seawater; PRO, RED and some other techniques are able to harness this energy by intelligently controlling the mixing process; the final common by-product is brackish water. Carbon dioxide emission during plant operation is zero and possible environmental impacts are limited to the discharge of brackish water into the sea and mostly accounted for the construction phase of the power plant. Electricity production is as "green" as it can be.

Recently this energy source received renewed interest, however, obstacles such as high membrane cost and short life due to fouling are the main problems that prevented large-scale utilization of membrane-based techniques – PRO and RED – whereas other methods have challenging applications. For instance, the reverse vapour compression method (RVC) relies on a very small pressure difference to run; the submarine hydro-electric-osmotic power plants (SHEOPP) faces economic and viability problems; the electric double-layer capacitive method (EDL) and the hydrocratic generator (HYGEN) are still in their initial stages, producing very small amounts of electricity in laboratory scale.

1.2 Global theoretical and technical potential

Salinity-gradient techniques were first studied in the mid 50's and a global theoretical potential, based on annual river discharges and ocean salinity, was estimated to be between 1,4 and 2,6 TW (PATTLE, 1954). This potential is calculated from the theoretical non-expansion work produced by the mixing of fresh and salt water through a partly reversible process and estimated from the difference of Gibbs free energy of mixing as follow:

$$\Delta G_{mix} = \Delta G_b - (\Delta G_c + \Delta G_d)$$

$$\Delta G_{mix} = (n_c + n_d)(\Delta h_b - T\Delta s_b) - [\, n_c(\Delta h_c - T\Delta s_c) + n_d(\Delta h_d - T\Delta s_d)\,]$$

with subscript d for the diluted water, c for the concentrated water and b for the resulting mixed brackish water; the term n account for moles of each solution, T for temperature, Δh and Δs for the contributions of molar enthalpy and entropy of mixing to the respective total molar thermodynamic properties of the electrolyte solution. These subscripts and symbols are maintained throughout most of the study, remembering them will prove useful.

For ideal-dilute solutions, the total molar enthalpy of mixing is null since only the volume of the resulting solution changes on mixing. The resulting Gibbs free energy of mixing is then determined solely from the contribution of entropy:

$$\Delta G_{mix} = -(n_c + n_d)T\Delta s_{b_{mix}} + n_c T\Delta s_{c_{mix}} + n_d T\Delta s_{d_{mix}}$$

For each solution the entropy of mixing is calculated as a function of the molar fraction $\mathrm{x_i}$ of the component $\mathrm{i} = [\mathrm{Na}, \mathrm{Cl}, \mathrm{H_2O}]$ and the universal gas constant $\mathrm{R} = 8{,}314\ \mathrm{J/mol.K}$.

$$\Delta s_{mix} = -R \sum_{\mathrm{i}} \mathrm{x_i} \ln \mathrm{x_i}$$

The maximum theoretical work obtainable from the mixing of $1\ \mathrm{m^3}$ of freshwater with $1\ \mathrm{m^3}$ of seawater is calculated accordingly; assuming a salinity of $30\ g/L$ for

seawater – approximately $0{,}5\ mol/L$ – an ideal-dilute mixed solution and a temperature of $293\ K$.

One can also calculate the result for freshwater solutions with non-negligible salt concentration – around $0{,}01\ mol/L$ – leading to a more realistic maximum theoretical work of $1{,}4\ MJ$. It is thus practical to calculate maximum theoretical work for different salinity concentrations of both diluted and concentrated solutions, for a given constant temperature – usually $293\ K$, and plot a diagram such as the one in figure 1, taken from Post (2009).

Table 1: Entropy of mixing

Solution	$x_{Na} = x_{Cl}$	x_{H_2O}	n	$\Delta s_{mix} = -R \sum_i x_i \ln x_i$
Freshwater	$traces(10^{-6})$	1	55,5556 $kmol$	0
Seawater	0,0092	0.9816	55.8131 $kmol$	0,8688 J/mol. K
Mixed brackish water	0,0046	0.9908	111,3687 $kmol$	0,4877 J/mol. K

$$\Delta G_{mix} = -(n_c + n_d)T\Delta s_{b_{mix}} + n_c T\Delta s_{c_{mix}} + n_d T\Delta s_{d_{mix}} = -W_{max} = -1{,}709\ MJ$$

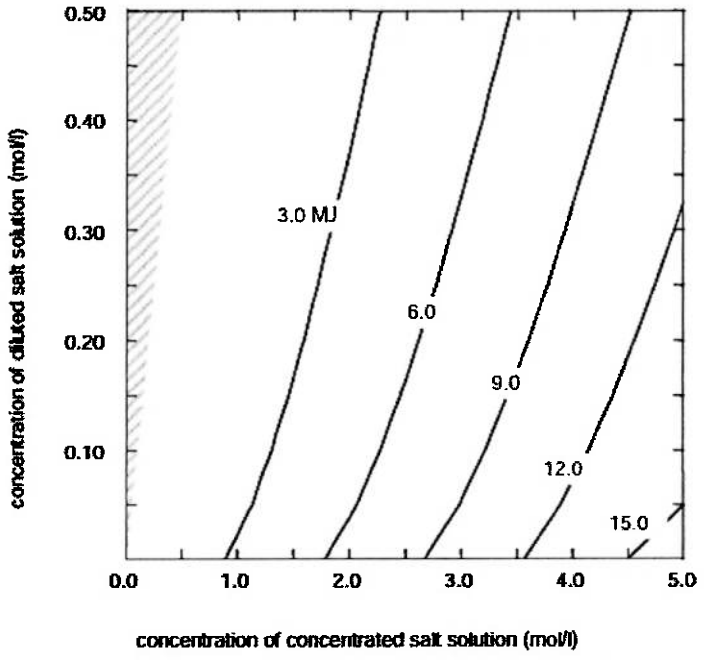

Figure 1: Maximum theoretical work for different salinity concentrations of solutions [1]

With an approximate value of maximum theoretical work per m^3 of freshwater and the total global river discharge into oceans, a picture of the worldwide potential for salinity-gradient energy is formed. According to Dai and Trenberth (2009) the total discharge of the world's 925 largest ocean-reaching rivers, covering around 80% of global ocean draining areas and 73% of global runoff excluding Antarctica and Greenland, was estimated $37288\ km^3/year$. Therefore, a rough $17701\ TWh$ – $6{,}3725.10^{19}\ J$ of global theoretical potential for energy production from salinity-gradient was calculated; this amounts to 90% of the world's total electricity consumption in 2007 (IEA, 2009). Furthermore, a policy of substitution of coal fired plants with salinity-gradient technologies could reduce the predicted 2030 levels of energy related greenhouse emissions as much as 40% (POST, 2009).

Although technical potential of energy production from salinity-gradients is known to be much lower than the rough estimates above, it remains clear that this technology can provide a significant fraction of our energy requirements in a sustainable, emission-free way. Technical potential is defined as the share of theoretical potential that can be harnessed using current technologies, regardless to other restrictions; it was estimated at $60\% - 10620{,}6\ TWh$.

With this promising perspective in mind, we briefly study some of the energy producing techniques that use salinity-gradient, and then focus on PRO systems and its constraints, technical difficulties and economic potential.

1.3 Outline of this study

In this **first chapter** we presented salinity-gradient energy, its global potential, and introduced the reader to a promising alternative to fossil fuel energy with a minute mention of the techniques employed to harness such power. Those techniques are further explained in the **second chapter** with considerable depth and closer attention to the two of them that are already being developed and in prototype phase: Pressure retarded osmosis (PRO) and Reverse electrodialysis (RED).

Table 2: Study outline

Chapter	Research question	Topic
2	What are the technologies available and/or predicted to possibly harness electricity from salinity-gradients?	Critical overview of different possible techniques and their development status.
3	What are the principles behind pressure retarded osmosis? What components are essential for its functioning?	Presentation of model plant schematics, discussion over membrane materials and technical aspects, overview of pressure exchanger unit and comparison of plant configurations.
4	How is the power plant siting planned and in what does it differ from other electricity production technologies?	In-depth analysis of plant siting through exemplification of a fictional 10 MW pilot power plant, most critical aspects are taken in consideration.
5	How is the power plant designed?	Practical approach for preliminary design through exemplification, plant modularity.
6	What are the economic perspectives and challenges of this technology?	Approach for preliminary economic evaluation, Total Cost of Investment per MW and Electricity Cost per kWh
7	According to the information gathered so far, what are the prospects of salinity-gradient energy?	Prospects, the role of marketing in promoting these technologies, final remarks

From the **third chapter** onwards we focus on the PRO technology and discuss the main technological aspects of it, presenting models equationing the system as a whole and also studying further the major components: the membrane and the pressure exchanger energy recovery unit. Thus, in the second and third chapter the theoretical foundation to understanding salinity-gradient technologies and pressure retarded osmosis is presented, the arguments exposed in these chapters should be credited to those whom over 60 years have dedicated their lives in leaving this knowledge behind.

An in-depth evaluation of the difficulties in power plant siting is presented in **chapter 4** altogether with an exemplification; the example considers a 10 MW pilot plant

to be placed somewhere in Sweden. Further reasoning as to why we have chosen Sweden is presented throughout the chapter.

Chapter 5 presents a guideline for preliminary design of power plant, as well as for net electricity output estimation. The calculations are done based on the pilot plant model and its fictional geographic position from chapter 4 and take into account a very important characteristic of PRO systems: modularity. Afterwards we evaluate the expected total cost of investment per kW and electricity production cost per kWh for a $10\ MW$ plant in **chapter 6**, critically pointing out major contributions for each parameter and future economic perspectives. **Chapter 7** discusses the prospects of salinity-gradient technologies in general, considering the important role of marketing in promoting them and leaving final remarks to proceed with their investigation and development.

C2. Salinity-gradient technologies

All across the globe freshwater runs into oceans and seas, releasing an impressive amount of energy estimated at around $17701\,TWh$ worldwide. Salinity-gradient energy, also referred as osmotic power or blue energy, is the tool with which that energy can be harnessed. There are several different concepts that can achieve this goal, many of them still at a very early research phase and predicted from reversing desalination techniques. In this chapter we explain the principles behind each method, trying to show as many details as possible. Nevertheless, given the restricted amount of articles and papers in this field, many are not openly available to the public, we always advise the reader to look at the bibliographic references for deeper comprehension of each technique.

2.1 Electric double-layer capacitive method (EDL)

Brogioli (2009) proposed a novel method based on the electric double-layer (EDL) capacitor technology. The capacitor is constituted by carbon electrodes which are immersed in a salt solution; the device operates in a charge-discharge cycle that has a net production of electricity.

Firstly, the electrodes immersed in seawater are charged. When the current flows through the capacitor, each porous electrode attracts ions of the opposite charge and repels those of the same; those charges are thus stored in the resulting electrical double-layer. The dielectric solution will not transport current as long as the capacitor is operated at voltages lower than the breakdown current, which is around $1V$ for water solutions.

The solution is then brought in contact with freshwater. Salt ions diffuse across the mixed solution effectively increasing the electrostatic energy of the system; this increase in electrostatic energy can be determined from electro-osmosis theory, taking in consideration water osmotic transport and ion diffusion-electrostatic transport (TIKHOMOLOVA, 1993). The equilibrium is described by Poisson-Boltzman equation and the analytic Gouy-Chapman solution can be determined for the ion concentrations.

The relation between the potential difference φ and the surface charge density σ is explicited below, taken from Brogioli (2009).

$$\varphi = \frac{2k_B T}{e} \sinh^{-1}\left(\frac{\sigma}{\sqrt{8CN_A\epsilon_o\epsilon_r k_B T}}\right)$$

where k_B is the Boltzmann's constant, T is temperature, e is electron charge, N_A is Avogrado's constant, $\epsilon_o\epsilon_r$ is the dielectric permittivity and C is solution concentration. Therefore, potential difference increases with decreasing solute concentration.

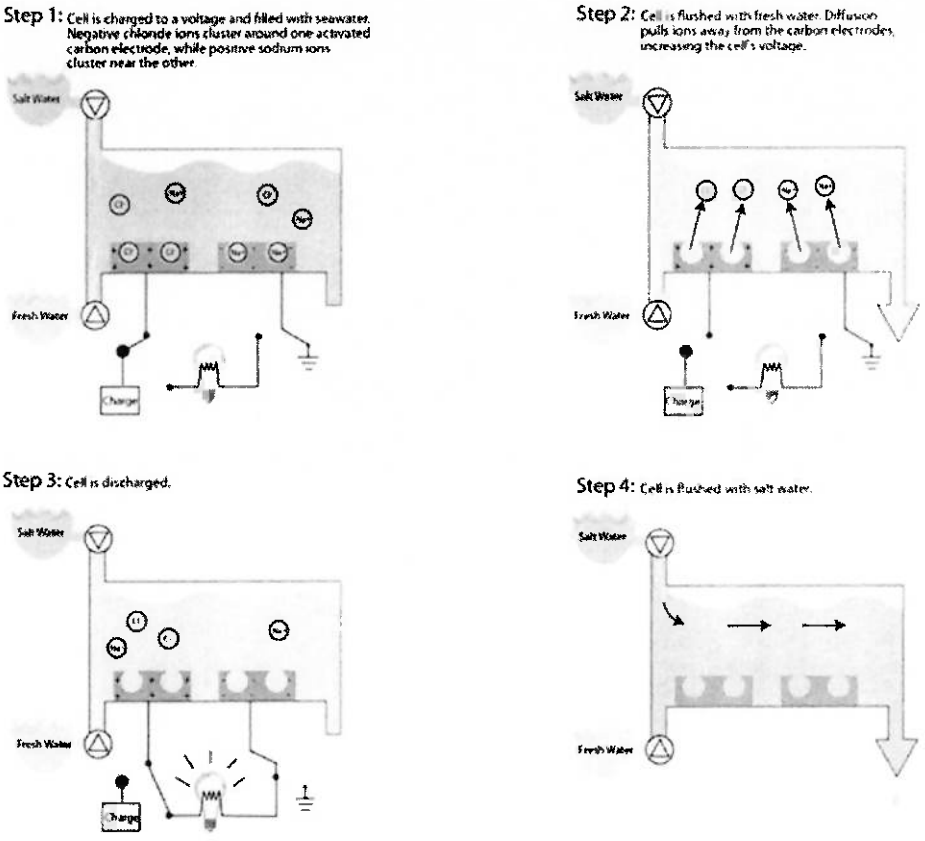

Figure 2: Step by step procedure for extracting energy [8]

The capacitor is then discharged and a net production of electricity is observed. Finally, the system is washed-up with seawater again with the electric circuit open, before recharge. A schematic view of the process is presented in figure 2. The following figures plot system voltage and current in time throughout charge-discharge cycles

(BROGIOLI, 2009). During discharge – Step 3/Phase C – a sudden drop in voltage is observed, followed by an exponential decay; those are the effects of the external resistance and internal capacitive circuit respectively. It is proven that the total incoming charge, calculated from the integral of the current in each cycle, is close to zero. That means that all energy dissipated in the external resistance was provided from salinity difference.

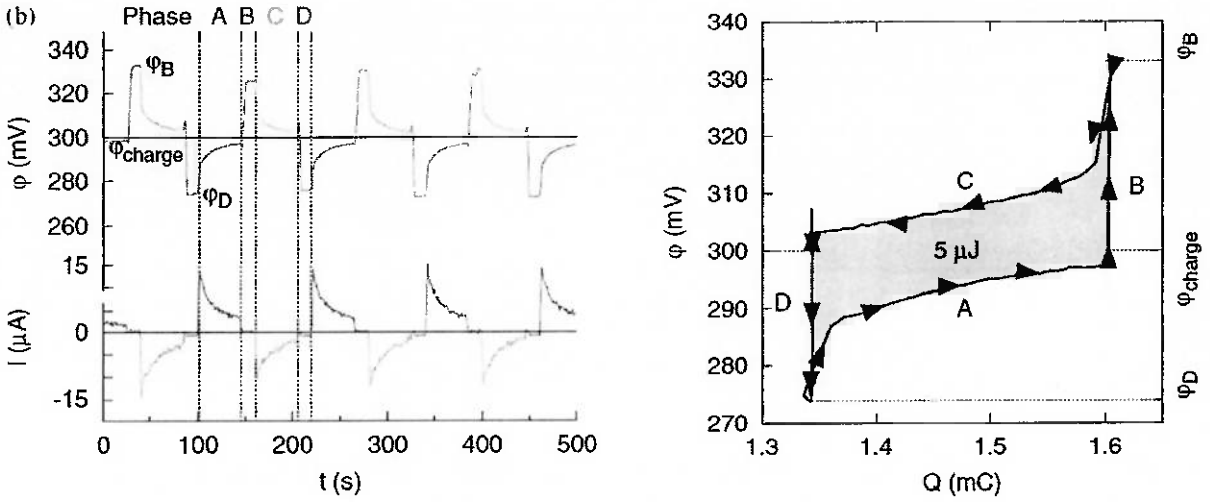

Figure 3: Process charge-discharge cycle and net energy production [8]

A single cycle plot is also presented, putting into evidence a net produced energy of $5\,\mu J$ from the enclosed surface; leakage losses must be carefully calculated as they increase with salinity. According to the graph in figure 4, total energy produced was around $10\,\mu J$, but half of this value was dissipated in the internal resistance of the capacitor.

The experimental device was able to provide 2,2% of the energy stored, working at a maximum $1Hz$ frequency. Increasing the working frequency would obviously lead to higher energy production; solution flushing is the most time-consuming phase at this early stage. Pumping expenditures must be discounted but are predicted to be lower than net produced energy.

A conceptual system is proposed, considering a large EDL salinity system that works at relative low frequencies such as the experimental device. The device would be connected to a flywheel through a motor; the pulsating low frequency energy produced would power the flywheel impulsively, keeping its rotational motion at higher levels.

Simultaneously, the flywheel would be coupled to an electrical engine, which could produce both AC and DC power. Therefore, apart from friction losses, the energy produced by the salinity device would have to be enough to sustain the resistant torque from the engine.

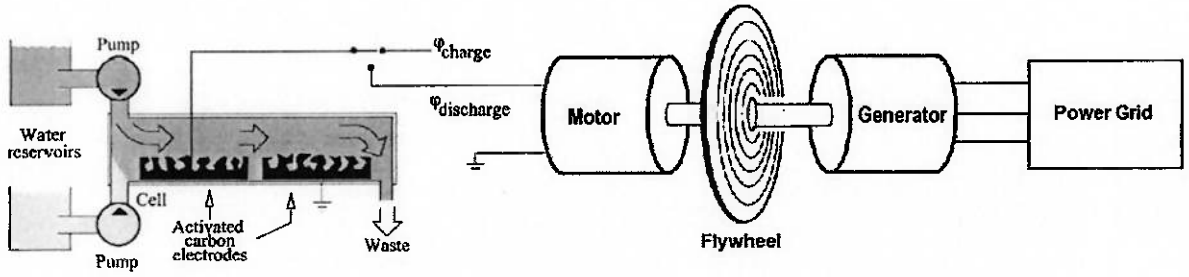

Figure 4: Possible design for harnessing energy from the EDL capacitive method

2.2 Reverse vapour compression (RVC)

This method exploits the pressure difference between boiling freshwater and boiling seawater; it is the reverse of vapour compression techniques used in desalination plants. In direct vapour compression, boiling saline water is in one side of a falling-film evaporator-condenser and condensing freshwater is in the other. Since saline water has a lower vapour pressure than freshwater, the pressure difference is maintained by a pump which also moves the vapour from the saline side to the other. By reversing the process and replacing the pump for a turbine, one could produce energy from the difference in vapour pressure. A schematic view of such engine is displayed in figure 5.

One of the advantages of this method is that developments in direct vapour compression technologies are adaptable to address challenges in RVC with relative ease. Moreover, RVC is a non-membrane based process and does not require any pre-treatment of water, thus having reduced construction costs when compared to the other salinity-gradient energy technologies.

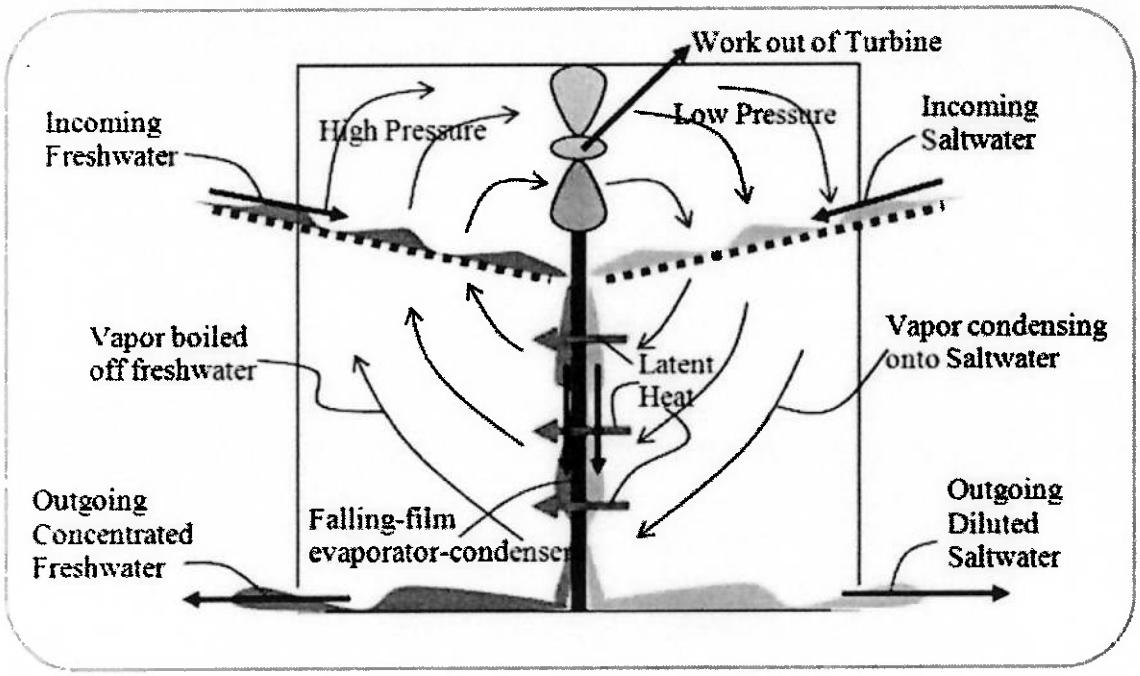

Figure 5: Schematic of a reverse vapour compression engine [14]

The heart of the RVC is the falling-film evaporator-condenser, through which only latent heat is exchanged, forcing vapours to run through the turbine. It also holds the key to making the method economically competitive. In order to resist the mechanical stresses from the pressure difference and fluid friction, heavy and expensive materials such as titanium and stainless steel are usually employed, however, Brewbaker (2006) shows that it is possible to use aluminium, plastic films and metal-plastic laminated films in RVC elements. The economy achieved by using these inexpensive materials allows the technology to compete with other energy producing plants.

A disadvantage of the RVC is that it is only practical when performed at temperatures close to those of the incoming liquids, which are around $293\ K$. This requires vacuum conditions of about 2% of atmospheric pressure (OLSSON et al., 1979), sharply decreasing the density of any vapour travelling along the device. In order to produce fair amounts of energy, the elements would have to deal with high volumes and yet be fortified against atmospheric pressure; Olsson et al. (1979) addressed to this problem by housing all operations inside a single vacuum chamber.

It is in the evaporator-condenser that saturated pure water is produced, in one side, and condensed in the other. As it condenses and diffuses into the saline solution it

reaches thermal equilibrium at a slightly higher temperature and releases its chemical potential energy, calculated from Gibbs free energy of mixing. Ideally, the energy released by the diffusion would match the one needed to warm the condensing freshwater, therefore, it is possible to calculate the difference in temperature between condensed freshwater vapour and saline solution (ΔT_b) for an infinite seawater sink (OLSSON et al., 1979):

Table 3: Gibbs free energy of mixing for different seawater to freshwater proportions

mixing proportions (sea/freshwater)	nH2O	nNa = nCl	ntot	xNa=xCl	xH2O	ds_mix brackish	dG_mix (MJ/m3 freshwater)
1	110,3431	0,5128	111,3687	0,004605	0,9908	-0,4882	1,7376
1,08	114,7260	0,5538	115,8337	0,004781	0,9904	-0,5039	1,7745
2	165,1306	1,0256	167,1818	0,006135	0,9877	-0,621	2,0338
5	329,4931	2,5641	334,6213	0,007663	0,9847	-0,7471	2,2873
10	603,4306	5,1282	613,6870	0,008356	0,9833	-0,8026	2,3918
25	1425,243	12,8205	1450,8841	0,008836	0,9823	-0,8404	2,4609
34	1918,3306	17,4359	1953,2023	0,008927	0,9821	-0.8475	2,4737
50	2794,931	25,641	2846,2126	0,009009	0,9820	-0,8539	2,4851
100	5534,306	51,282	5636,8696	0,009098	0,9818	-0,8608	2,4975
500	27449,31	256,41	27962,126	0,00917	0,9816	-0,8665	2,5075
1000	54843,06	512,82	55868,696	0,009179	0,9816	-0,8672	2,5088
10000	547930,6	5128,2	558186,96	0,009187	0,9816	-0,8678	2,5099
1E+10	5,479E+10	5,128E+8	5,581E+10	0,009188	0,9816	-0,8679	2,5100

Only $0{,}598\,K$ of difference between temperatures of condensed water and saline solution is expected. To cope with the amount of heat to be transferred the heat exchanger must have an enormous area, which also explains the major economic role of this element. The enthalpy diagram below, adapted from Olsson et al. (1979) apud Brewbacker (2006), shows in detail the energy barriers to vapour in an ideal process:

$$\Delta G_{mix} = -(n_c + n_d)T\Delta s_{b_{mix}} + n_c T\Delta s_{c_{mix}} + n_d T\Delta s_{d_{mix}} = -2{,}51\,MJ$$

$$\Delta G_{mix} = c_p \Delta T_b = 2{,}51\,\frac{MJ}{m^3} \qquad c_p = 4{,}2\,\frac{kJ}{kg.K} = 4{,}2\,\frac{MJ}{m^3.K}$$

$$\Delta T_b = \frac{1{,}709}{4{,}2} = 0{,}598\,K = T_s - T_c$$

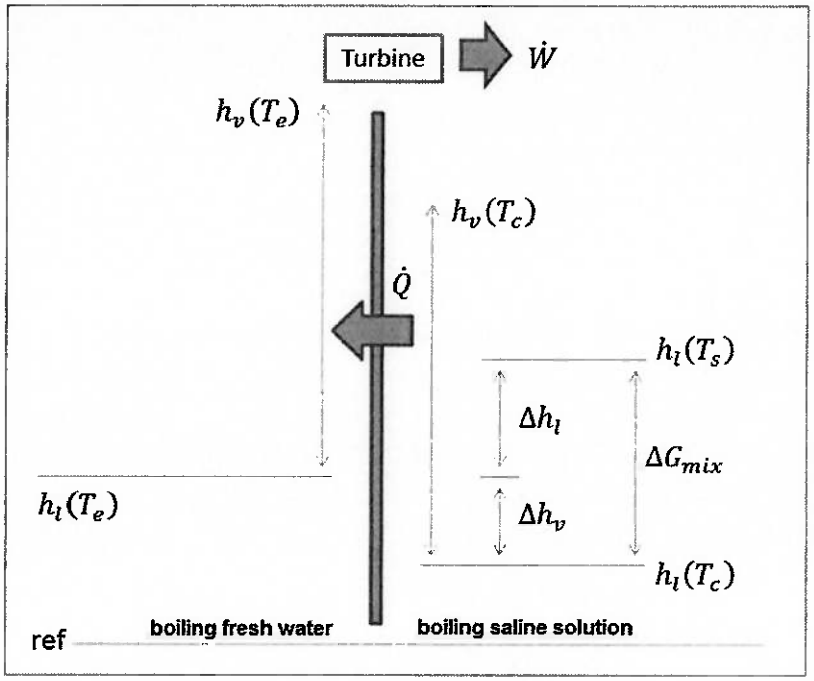

Figure 6: Enthalpy diagram for RVC process [11]

For an ideal process, all heat extracted at the condenser side is consumed in the evaporator and the difference between vapour temperatures on each side $\Delta T_v = T_e - T_c$ determines the amount of work extracted at the turbine. In order to maintain the RVC engine running, due to the finite area of the thermal interface, a gradient of temperature ΔT between boiling freshwater and boiling saline solution must be sustained.

$$\dot{Q} = \dot{m}\Delta h_{l-v} = \dot{m}[h_v(T_e) - h_l(T_e)] = \dot{m}[h_v(T_c) - h_l(T_c)]$$

$$\dot{W} = \dot{m}\Delta h_v = \dot{m}c_p\Delta T_v = \dot{m}c_p(T_e - T_c)$$

$$\dot{W} = \dot{m}c_p(T_s - T_c) - \dot{m}c_p(T_s - T_e) = \dot{m}\Delta G_{mix} - \dot{m}c_p\Delta T$$

At the equation above, the term with ΔT represents a loss in extractable work. It must never exceed ΔT_b and must be kept to a minimum; these are the first constraints when operating an RVC plant. Another constraint is revealed as we start considering a non-infinite seawater sink; the effect is visible in table 2 showing ΔG_{mix} as a function of the proportion of solutions, the smaller the value of ΔG_{mix} the more limited $\dot{W}$ will be.

Finally, a last challenge regards the fact that both solutions must be provided to the engine at specific temperatures which normally differ from those found at these water sources. Preconditioning of seawater to a temperature ΔT above that of freshwater is a non-trivial requirement that could be twice the actual power output of the RVC power plant. However, since this is a heat of relatively low intensity – room temperature – almost any heating source could be used to meet it.

A performance calculation found in Brewbaker (2006, 2007) estimates a power plant efficiency of 61% and a power density of $1\,W/m^2$ for $3{:}1$ seawater to freshwater proportion. The power density is an important parameter when comparing RVC with salinity-gradient membrane-based technologies. RVC is a promising cost-effective technology that, however, still faces some technical difficulties in its development. A small number of patents of RVC engines and power plants were produced with no experimental prototype device being produced so far.

2.3 Hydrocratic generator (HYGEN)

The Hydrocratic generator (HYGEN) is an apparatus developed for generating power using an innovative process which exploits the osmotic energy potential between two bodies of water with different salinity concentrations. An advantage of this method is that it does not require the use of semi-permeable membranes, other specially formulated material, heating, cooling or vacuum environment. It may recover energy from a variety of freshwater sources, as water quality does not concern the process execution.

The process in which solvent fluids having different osmotic potentials are put in direct contact and mixed with each other in the absence of a membrane is called hydrocasis; it is the basic concept in a HYGEN. It was already demonstrated that the mixing of saline and freshwater releases energy and that the amount of energy released depends on the proportion of mixing. The resulting brackish solution is less dense than the saline solution and, therefore, it is expected to occupy the uppermost area of a tank or the ocean. This causes a vertical stratification of salinity with higher salt

concentrations at deeper waters; a phenomenon well known to take place at river estuaries, solar ponds, etcetera.

The HYGEN explores both salinity solution stratification/buoyancy and the energy from mixing solutions with different salinities to produce power in a turbine. A source of relatively low salinity water is conducted to a predetermined depth through a DownTube. The DownTube is submersed in a body of relatively high salinity water and is discharging its contents in a vertical UpTube, where low and high salinity solutions are put in contact. The UpTube is fluidly connected to the source of relatively high salinity water through one or more openings, allowing high salinity solution to flow into it.

The mixture is pushed upwards in the UpTube due to buoyancy effects, making room for further mixing of high and low salinity solutions, continuously running the process. The upwelling mixture passes through a power generation unit, which is placed at a higher depth than the one in which buoyancy transport would cease, that is, the depth at which mixture density equals that of the surrounding water body. An illustration with one possible embodiment of the system is presented, taken from Finley and Pscheidt (2000).

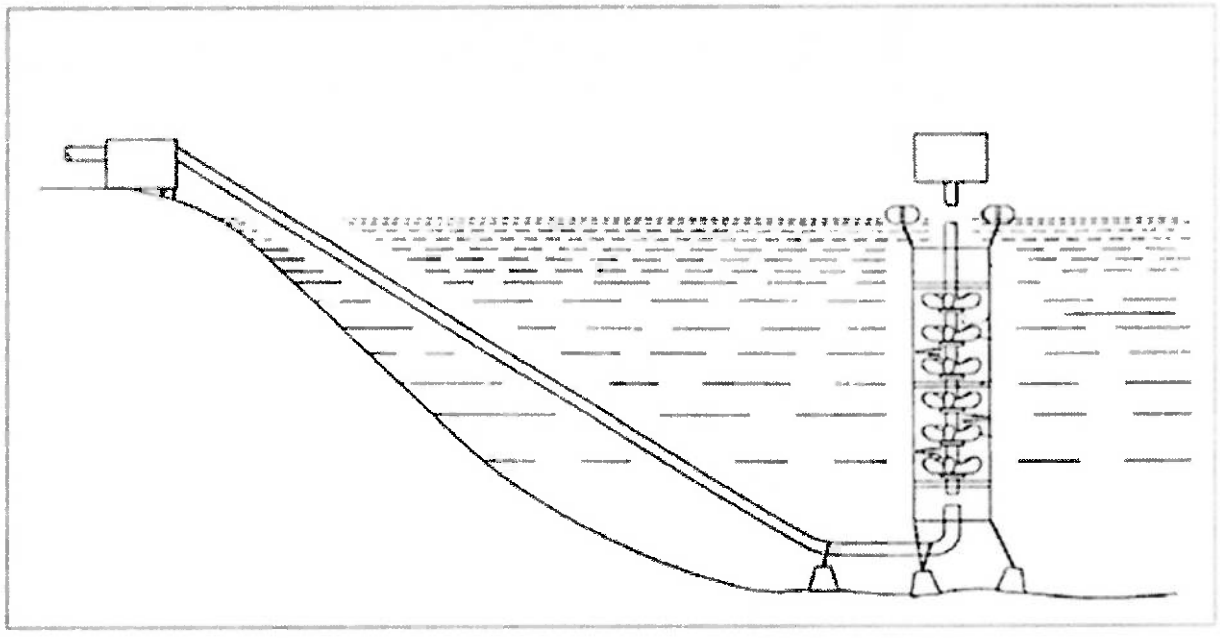

Figure 7: A possible embodiment for the HYGEN system [15]

The mixing of freshwater into saline seawater releases the freshwater chemical energy potential, resulting in a concomitant pressure drop across the hydraulic turbine. This pressure drop in conjunction with the induced water flow upwelling through the UpTube allow the generation of significant hydro-power for commercial power production applications without adversely affecting surrounding marine culture.

The device was developed during mariculture enhancement studies, while testing a prototype by injecting nutrient-rich freshwater at the bottom of the vertical UpTube as previously described. The researchers noticed that the mixture flowed upwards with a much higher speed than that which could be accounted for buoyancy or kinetic energy transfer. It was presumed that that energy would come from the same released energy of mixing that drives osmotic and diffusion processes.

A laboratory scale prototype was built and tested, the experiment aimed and succeeded to determine hydrocratic effect as the cause of the apparent unbalanced kinetic energy transfer previously calculated from energy conservation principle. The experimental apparatus operated with an estimated $34:1$ proportion of seawater to freshwater and generated $0.98\,W$ with a freshwater flow of $2{,}4.10^{-4}\,m^3/s$. This is equivalent to $4\,kW$ per m^3/s of freshwater, about 0.16% efficient considering the theoretical potential of $2{,}4737\,MW$, taken from table 3. A schematic of the experimental apparatus is present along with some tables with the data retrieved, provided by Finley and Pscheidt (2000).

An interesting fact is that the device can operate in both upwards and downwards flow directions with some minor adaptations by providing solutions with salinities ranging from pure freshwater to brine. If the feed solution has a lower salinity than the water body – the sea for example – the induced flow will be in the upward direction; if the feed solution has a higher salinity than the water body, the induced buoyancy flow will be in the downward direction. It is just a matter of knowing feed water salinity and placing DownTubes and turbines accordingly.

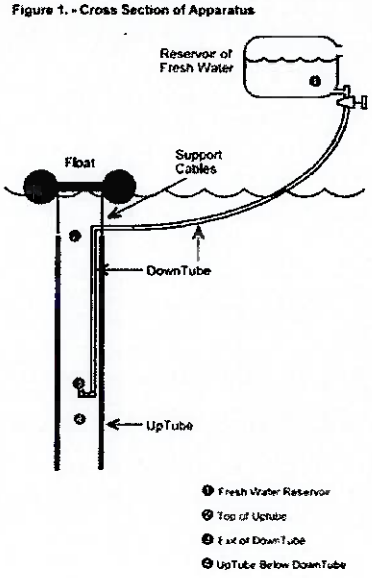

Table 1 - Expected vs. Observed Flow at Top of UpTube

Height of Reservoir (meters)	Flow of Fresh Water (10^{-4} m³/sec)	Salinity of Brine at Top of UpTube (ppt)	
		Expected	Observed
0.23	1.3	17	34
0.55	2.4	17	34

Salinity of Salt Water (ppt) 35
Salinity of Fresh Water (ppt) 0.3
Density of Salt Water (Kg/l) 1.035
Expected Maximum Salinity . . . . . $S_s/(1+\rho_s)$

Table 3 - Demonstration Device

	DownTube Flow (10^{-4} m³/sec)	Turbine Speed (rpm)
Fresh Water (0.3 ppt)	2.4	5.6
Salt Water (36 ppt)	2.3	2.3

Reservoir Height (meters) 0.55
Flow (10^{-4} m³/sec) 2.4

Table 2 - Flow and Kinetic Energy

Height of Reservoir (meters)	Salinity at Point 2 (ppt)	Flow (10^{-4} m³/sec)				Kinetic Power (watts)			
		Point 1	Point 2	Point 3	Point 4	Point 1	Point 2	Point 3	Point 4
0.23	34	1.3	45.5	1.3	44.2	0	0.16	0.02	0.14
0.55	34	2.4	84.0	2.4	81.6	0	0.98	0.11	0.90

Figure 8: HYGEN experimental design and results [16, 17]

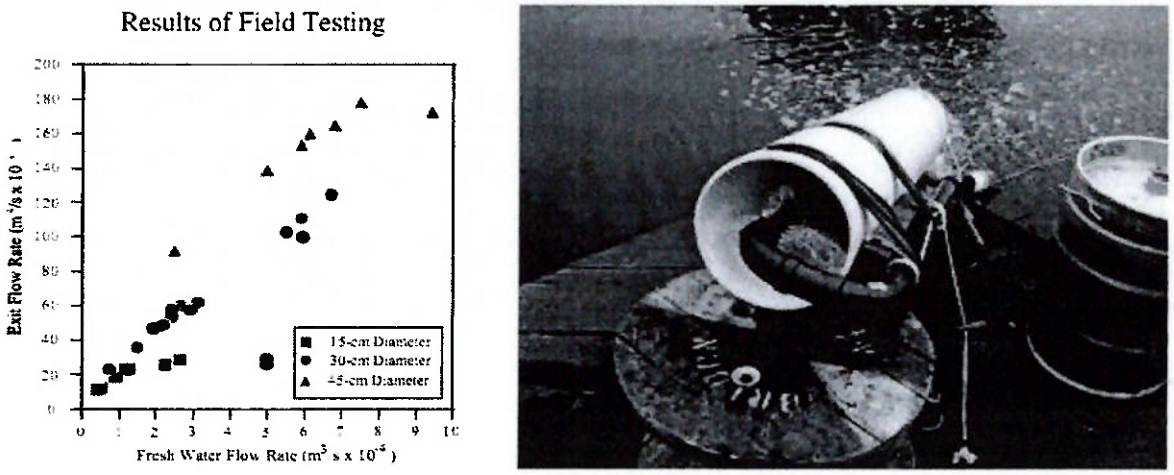

Figure 9: HYGEN field testing and results [17]

It is thus possible to place the HYGEN at the discharge of desalination or PRO plants, further recovering and producing electricity. In such designs it is important to evaluate the apparatus economic feasibility separately. Wader LCC is the company applicant to most of the HYGEN patents and responsible for the experimental development and for the results obtained so far; further improvement in the energy recovery capacity of the device is still needed before proceeding to the next phase. Field testing in California was executed with bigger scale elements: flow rates and power were

studied as a function of UpTube diameter and length; flow rates increases with increased diameters and power increases with increased length.

It was also found that reducing the difference in osmotic potential between the freshwater exiting the DownTube and the water of high salinity entering the UpTube reduces the amount of energy available. It is therefore generally advantageous that the body of water have a large volume. According to the words of Wader LCC:

> We have determined that our next step in the development of this project requires us to operate in the marine environment (...), we need continuous access to an ocean environment and we need continuous access to a brine line from a desalination plant (...). We are currently attempting to entering (sic) into a joint venture arrangement with a financially responsible party for the purposes of financing the developing (sic) of prototype plants for both a brine into Ocean device and a brine into "Fresh" Water – effluent from a Waste Water Treatment Plant – device. Spain, Malta or Kuwait would be good locations for this development of the prototype devices. We can construct these prototypes at a cost not to exceed $2,000,000US. (Email)

Therefore, the hidrocratic generator tecnology is in seach for international partnerships and financing in order to take the next step in the evaluation of the technical feasibility of its prototype. The prospectives of success will be better estimated after it is confirmed that the deviced can operate in more realistic environments.

2.4 Submarine hydro-electric-osmotic power plant (SHEOPP)

SHEOPPs were first considered when re-examining pressure retarded osmosis power plants. Pumping expenses could drastically reduce net power output and efficiency; aiming to avoid such expenses the concept of a submersed hydroelectric plant was developed.

According to Reali (1980) it is possible to achieve better efficiencies if osmotic flow is not used for direct generation of electric power. Instead, a submarine hydroelectric plant is anchored to the sea floor and freshwater from a river estuary is conveyed through a penstock to the hydraulic turbine. After generating power, it is discharged, depressurized and diffused into the sea by osmosis, through a barrier of semi-permeable membranes. The membranes prevent salt diffusion into the power

plant, proving this method to have an advantage concerning protection from the corrosive effects of salt.

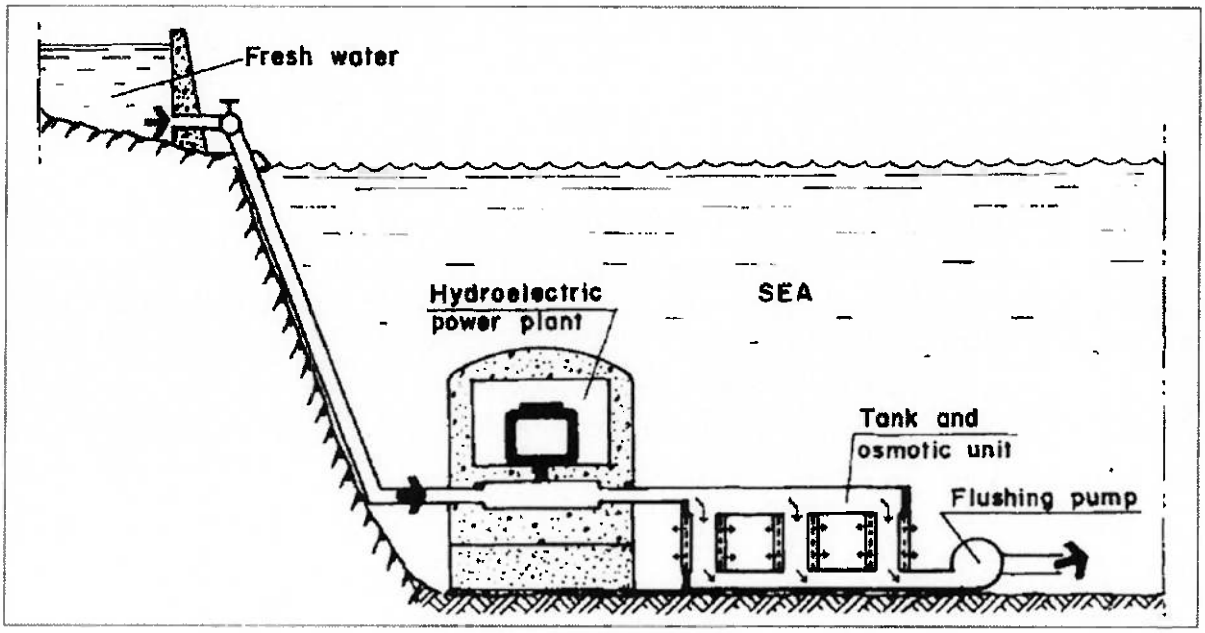

Figure 10: Submarine hydro-electric-osmotic power plant embodiment [18]

Table 4: Osmotic pressure difference between sea and fresh water

Seawater molar composition [19]			Hypothetical freshwater molar composition		
Component	Concentration (mol/kg)	Osmotic pressure (atm)	Component	Concentration (mol/kg)	Osmotic pressure (atm)
H_2O	53,6	----	H_2O	55,4	----
Cl^-	0,546	13,6330	Cl^-	0,0512	1,2492
Na^+	0,469	11,7105	Na^+	0,0512	1,2492
Mg^{2+}	0,0528	1,3184	TOTAL	55,5024	2,4984
SO_4^{2-}	0,0282	0,7041			
Ca^{2+}	0,0103	0,2572		$\Delta\pi\ (atm)$	25,4664
K^+	0,0102	0,2547			
C_T	0,00206	0,0514			
Br^-	0,000844	0,0211			
B_T	0,000416	0,0104			
Sr^{2+}	0,000091	0,0023			
F^-	0,000068	0,0017			
TOTAL	54,719979	27,9648			

Ideally, no flushing pump requirements would be necessary to prevent accumulation of unwanted solutes and contaminants on the freshwater side of the membrane; nevertheless, river water usually contains non-negligible amounts of dissolved salts, particulate matter and other contaminants. The flushing pump would not necessarily have to work continuously since special membranes and geometric configurations may ultimately be designed to reduce its effects to a minimum. Also, the discharge from flushing will be only a small fraction – 10% – of the working fluid which flows through the turbine (REALI, 1980). The net power output is thus the difference between generated power and pumping expenses.

A general equation describing water transport in osmotic devices is presented, flux is dependent on the membrane water permeability (A) and difference in pressure of each solution. Here, pressure is composed by two elements, the first related to dilute concentration also known as osmotic pressure (π); the second related to external action, namely, external pressure (p). For a SHEOPP mounted at sea bed, $\Delta\pi$ is calculated to be around $24\ atm$ for seawater and freshwater with simplified compositions of $0{,}5\ mol/L$ and $0{,}05\ mol/L$; Δp is purely a function of depth. The power to be produced, per square meter of membrane, is the product of the water flux with the resulting pressure.

$$J_w = A(\Delta\pi - \Delta p)$$

$$\pi = CRT \qquad p = \rho g h$$

$$\dot{w} = \dot{W}/S = A(\Delta\pi - \Delta p)\Delta p$$

Differentiating the equation above we observe that maximum power is obtained when $\Delta p = \Delta\pi/2$. A value of $12\ atm$ is necessary to optimize conditions for a power plant working with the salinity differences of sea and river water; that is equivalent to $110\ m$ of water column pressure and also the optimal depth for a SHEOPP siting.

The power plant could be built at a depth less than $110\ m$ if lower efficiencies of energy conversion are found to be acceptable or more convenient. The SHEOPP may be of the rock-bored type, completely underground and below the sea surface if the nature of the terrain favours this solution (REALI, 1980). It must then be connected by a special conduit to the osmotic unit anchored to the sea floor at about the same depth. A

last "brutal-force method" is proposed by the author, in which an enormous dam would separate freshwater from the sea; freshwater is then transported underground to produce electricity at the hydroelectric plant and discharged into an artificial buffer lake under the sea surface and finally diffuse through semi-permeable membranes.

The expected performance of a SHEOPP is to produce around $1\,MW/m^3$ of freshwater; about 1/10 of the turbine flux would be pumped out to prevent accumulation of undesirable substances. Further development of this technology is related to the employment of materials less likely to suffer from corrosion and fouling. Membrane performance and life-time still can be further improved to reduce operation and maintenance costs; underwater construction costs must be carefully analysed not to prohibitively increase investments.

2.5 Reverse electrodialysis (RED)

Reverse electrodialysis is a membrane-based salinity-gradient energy technology that explores the electrochemical potential of solutions with different salinities. Cation and anion-exchanging membranes are stacked in an alternating pattern, forming a series connection of electrochemical modules; the membrane is impermeable to water. Compartments filled with either saline or freshwater are placed between membranes alternately; when using river and seawater the salinity-gradient results in a potential difference of around $80\,mV$ per membrane; this value is also called the membrane potential (POST et al., 2007).

The system basically works as a salt battery: the chemical potential gradient causes the transport of ions across the membranes and electro-neutrality is maintained via oxi-reduction reactions in the extreme anode and cathode compartments. Electrons can flow from anode to cathode through an external circuit, transferring power to the load connected to its terminals.

According to Post et al. (2007), the driving force of the process is a gradient of free energy. When ion transport is present, calculation of the theoretical amount of free energy obtained from mixing of solutions must account the electric potential difference ($\Delta\varphi$) produced. The molar free energy (μ) of a component of an ideal solution is:

$$\mu_i(T,p) = \mu_i^0(T,p) + RT\ln x_i + |z_i|F\Delta\varphi$$

where μ_i^0 is the molar free energy under standard conditions, x_i is the molar fraction of the component, z_i is the component ion valence, $i = [Na, Cl, H_20]$ represents each solution component, $F = 96485\ C/mol$ is the Faraday constant, $R = 8{,}314\ J/mol.K$ is the universal gas constant and T is temperature.

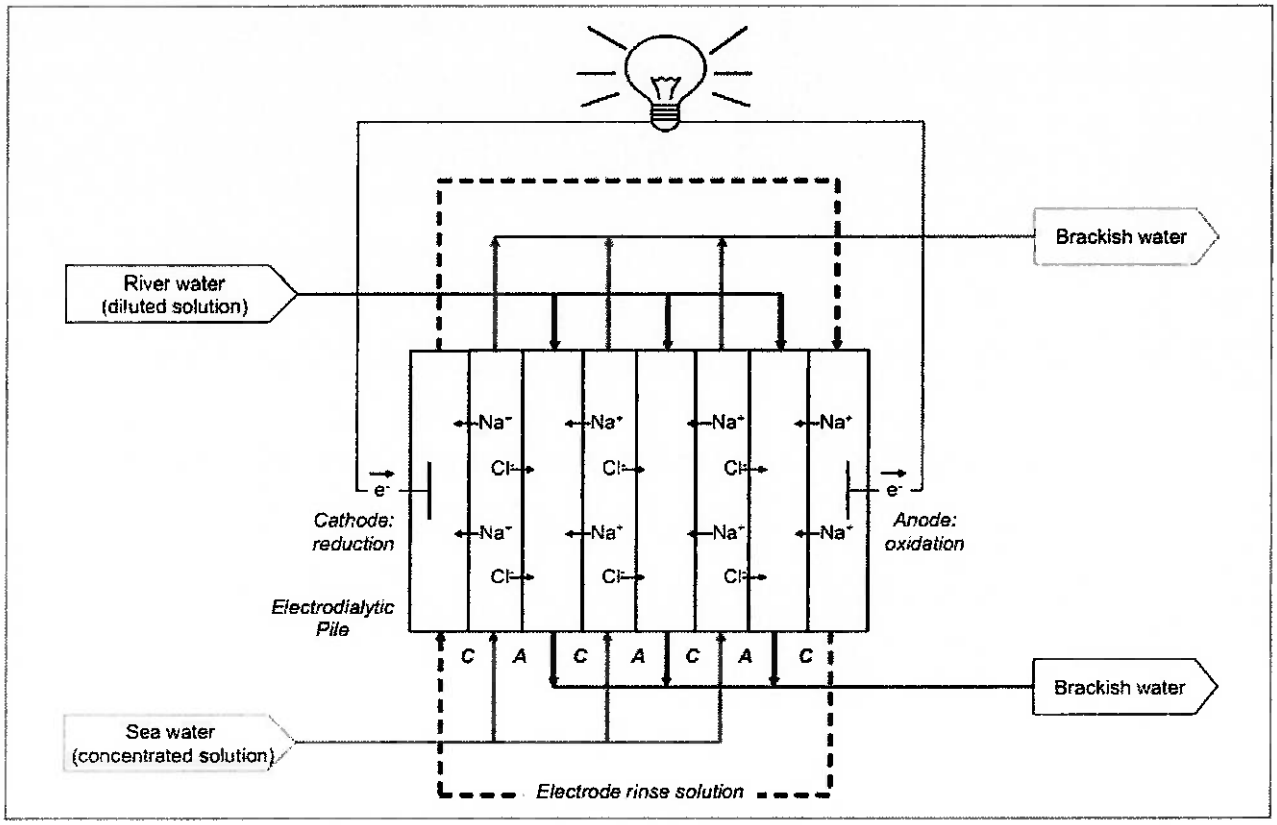

Figure 11: Reverse electrodialysis [20]

Water does not flow across the membrane, there is no pressure difference between solutions, and therefore, at equilibrium conditions we have:

$$\mu_{NaCl,c} = \mu_{NaCl,d}$$

$$RTlnx_{Na,c} + |z_{Na}|F\Delta\varphi_{Na,c} + RTlnx_{Cl,c} + |z_{Cl}|F\Delta\varphi_{Cl,c}$$

$$= RTlnx_{Na,d} + |z_{Na}|F\Delta\varphi_{Na,d} + RTlnx_{Cl,d} + |z_{Cl}|F\Delta\varphi_{Cl,d}$$

Knowing that $x_{Na,k} = x_{Cl,k} = x_k$ and $z_{Na} = z_{cl} = z$, one could simplify the equation above, gathering all terms related to the electric potential to obtain the total electric potential between both solutions ($\Delta\phi$):

$$zF\Delta\phi = RTln\left(\frac{x_{Na,c} \cdot x_{Cl,c}}{x_{Na,d} \cdot x_{Na,d}}\right) = RTln\left(\frac{{x_c}^2}{{x_d}^2}\right) = 2RTln\left(\frac{x_c}{x_d}\right)$$

$$\Delta\phi = \frac{2RT}{zF} ln\left(\frac{x_c}{x_d}\right)$$

Electric potential must then be corrected to account for the effect of ion concentration at membrane interface ($x_{m,k}$) and transport of counter-ions through the membrane. The resulting $\Delta\phi_{eff}$ is the membrane potential mentioned earlier.

$$\Delta\phi_{\text{eff}} = \frac{2RT}{zF}\left(ln\left(\frac{x_c}{x_{m,c}}\right) + \ln\left(\frac{x_{m,d}}{x_d}\right)\right) = \frac{2RT}{zF} ln\left(\frac{x_c(\bar{x} + \sqrt{4x_c^2 + \bar{x}^2})}{x_d(\bar{x} + \sqrt{4x_d^2 + \bar{x}^2})}\right) = \alpha\Delta\phi$$

where $\bar{x}$ is the mean mole fraction of active groups crossing the membrane and α the perm-selectivity of the membrane. The perm-selectivity expresses the membrane discrimination between counter-ions and co-ions and also is a parameter of membrane quality.

In analogy to battery systems, $\Delta\phi_{\text{eff}}$ is the effective open-circuit potential. When the circuit is closed through an external load connected to the RED stack terminals, current (I) is formed, a potential difference (ΔV) at load terminals is presented, and the effective driving force moving ions through the membrane is reduced to ($\Delta\phi_{\text{eff}} - \Delta$V). It is then possible to calculate the molar flow of sodium chloride from Faraday's relation:

$$\dot{n}_{Na,Cl} = \frac{I}{Fz_{Na,Cl}} = \frac{1}{Fz_{Na,Cl}}\left(\frac{\Delta\phi_{\text{eff}} - \Delta\text{V}}{\text{R}}\right)$$

This is not, however, the way that molar flow is usually represented. In order to explicit some important RED parameters we consider the molar flow per square meter of

membrane area $J_{Na,Cl}\,(mol/m^2s)$; and, consequently, $i\,(A/m^2)$ current density and r (Ωm^2) internal area specific resistance.

$$J_{Na,Cl} = \frac{\dot{n}_{Na,Cl}}{Area} = \frac{i}{FZ_{Na,Cl}} = \frac{1}{FZ_{Na,Cl}}\left(\frac{\Delta\phi_{\text{eff}} - \Delta V}{r}\right)$$

$$r = r_{AEM} + r_{CEM} + r_{seaH2O} + r_{freshH2O}$$

There are two fundamental performance parameters for membrane-based salinity-gradient technologies: power density and energy recovery. Power density is defined as the power output corresponding to one square meter of membrane area, it equals the product of half the current density (current passes through both anion and cation-exchange membranes) with the electrical potential over the stack terminals. Differentiating power with respect to ΔV one finds the value which maximizes power output: $\Delta V = \Delta\phi_{\text{eff}}/2$. Energy recovery is defined as the efficiency of the device with respect to the total amount of Gibbs free energy of mixing theoretically available, it evaluates the exhaustion of the available energy over time. Using the parameters introduced and the applied membrane surface (S_m), we have:

$$\dot{w} = \frac{\dot{W}}{S_m} = \frac{i}{2}\Delta V = \frac{1}{2}\left(\frac{\Delta\phi_{\text{eff}} - \Delta V}{r}\right)\Delta V \qquad \dot{w}_{opt} = \frac{1}{2}\frac{\Delta\phi_{\text{eff}}}{4r}$$

$$\eta = \frac{\int_{to}^{t} \dot{w}_{opt}\, S_m dt}{\Delta G_{mix}}$$

Post et al. (2007) compared the performances of RED and PRO modules using the best membrane characteristics available at that time; the conclusion reached was that reverse electrodialysis fitted best when operating with standard river and seawater whereas pressure retarded osmosis would be best allocated when higher salinity brine and river water were available. The results of such analysis are shown in figures 12 and 13. Although this study was done recently, many developments in membrane design for PRO systems occurred in the last years and power densities of around $3\,W/m^2$ were reached experimentally using salinity levels of sea and river water. The importance of

frequently updating experimental results in these new fast-developing technologies is clear.

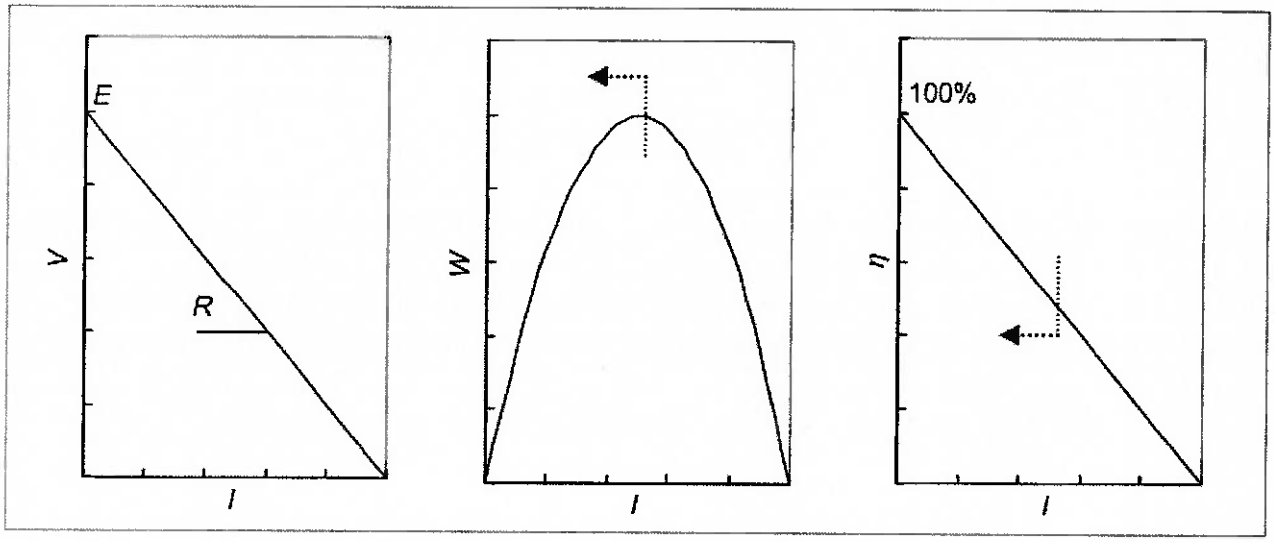

Figure 12: RED stack voltage, power and energy recovery rate as functions of load current [20]

Before entering the RED stack, pre-treatment of water is necessary to prevent performance losses and membrane fouling. According to Post (2009), reverse electrodialysis membranes are less susceptible to fouling than those of pressure retarded osmosis and submarine hydro-electro-osmotic applications. Sea/river-bank and mechanical filtration are most adequate for their ability to deal with larger fluxes and reduced cost.

In 2005 the Dutch team WETSUS – centre for sustainable water technology – started the Blue Energy project aiming to produce electricity from reverse electrodialysis. Since then, a number of scientific articles regarding this technology aroused and membrane performance on laboratory scale improved considerably. The state-of-art is a stack with an active membrane area of $25x75\ cm^2$ and 50 cell-pairs which produces around $16\ W$; the manufacturer is a spin-off company from WETSUS called REDstack.

A module of $200\ kW$ was designed and a preliminary economic evaluation proposed by Post (2009). The expected power density is of $2\ W/m^2$ with an energy recovery of 70%; gross power output is $220\ kW$ but expenses in pumping and DC/AC conversion accounts for 10% of that value; river and seawater would be evenly consumed at a rate of $0{,}2\ m^3/s$. For the economic evaluation a power plant composed of 1000 such modules was considered, it was proven that with favorable conditions

electricity could be produced at a break-down cost of $0{,}08\ €/kWh$ and power plant cost would be around $4{,}45\ M€/MW$. The plant would provide $1{,}6\ TWh$ of energy per year, working with a load factor over 90%.

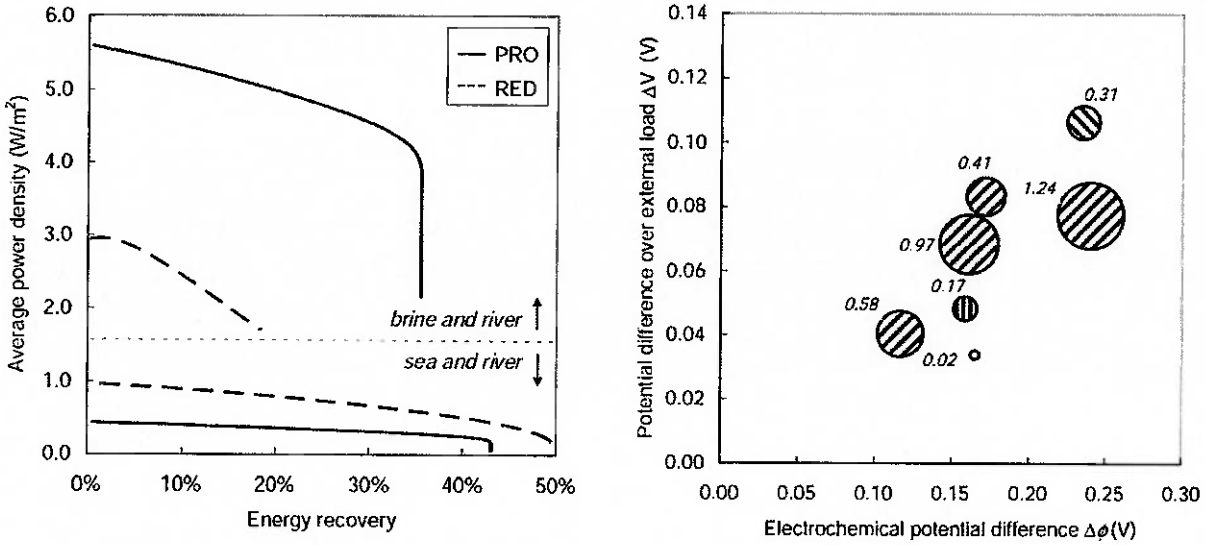

Figure 13: Power density and energy recovery rates of PRO and RED processes, taken from [20]

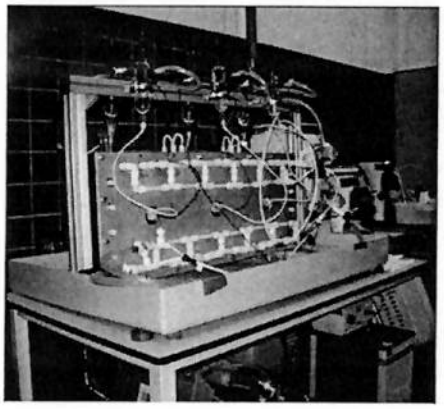

Author	Year	Power density (W/m^2)	Spacer thickness (mm)
Pattle	1954	0.05	0.7
Weinstein and Leitz	1976	0.17	1.0
Jagur-Grodzinski and Kramer	1986	0.41	0.55
Turek	2007	0.46	0.19
Suda	2007	0.26	1.0
Veerman et al.	2008	0.95	0.2
Veerman et al.	2009	1.18	0.2

Figure 14: Evolution in RED technology and state-of-art stack [20]

There are several locations being studied as potential sites for a pilot power plant in the Netherlands; Afsluitdijk is however being considered the ideal spot for RED on a short-term evaluation. The biggest challenges of the scaling-up phase of RED technology is to prepare membrane manufactures for the square kilometre demand a full-sized power plant would require. A development path for the scale-up is already in action, with the mutual agreement of researches and investing companies.

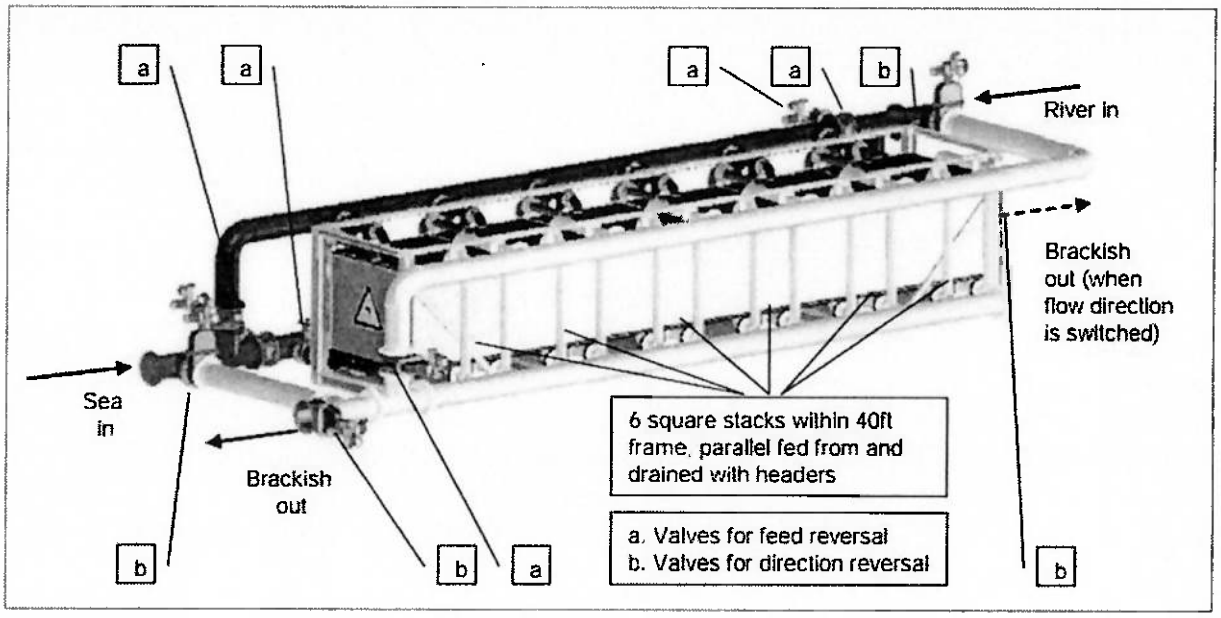

Figure 15: State-of-art in RED [20]

Table 5: Prospective for RED development, taken from [20]

Project	Scale	Aim
2008-2010 Pilot on industrial water flows	kW-scale	First step out of the laboratory. Pilot on saline flows in a salt factory of Frisia in Harlingen (Financial supported by SenterNovem, Innowator project).
2008 Engineering of pilot on surface waters	-	Feasibilty study and definition of requirements for a communal pilot on the Afsluitdijk (Private funding, 2008).
2010-2012 Pilot on surface waters	20-50 kW	Communal pilot on sea water and river water at the Afsluitdijk. Focus on 'design to work'.
2013-2015 Demonstration plant on surface waters	1 MW	Communal demonstration on sea water and river water at the Afsluitdijk. Focus on 'design to cost'.

2.6 Pressure retarded osmosis (PRO)

Osmosis is a natural process that occurs when two solutions with different solute concentrations are separated by a semi-permeable membrane, permeable only to water. In response to the gradient in free energy, water is transported from one solution to the other across the membrane. Pressure retarded osmosis explores this effect to produce electricity: low salinity feed solution water permeates through the membrane into a pressurized high salinity draw solution. Power is obtained by depressurizing the permeate flow through a turbine. Pre-treatment of water before entering the pressurized vessel with the membrane is mandatory for PRO applications as fouling can sharply reduce membrane life. A more detailed explanation over the most important components of a PRO power plant will be given in the next chapter.

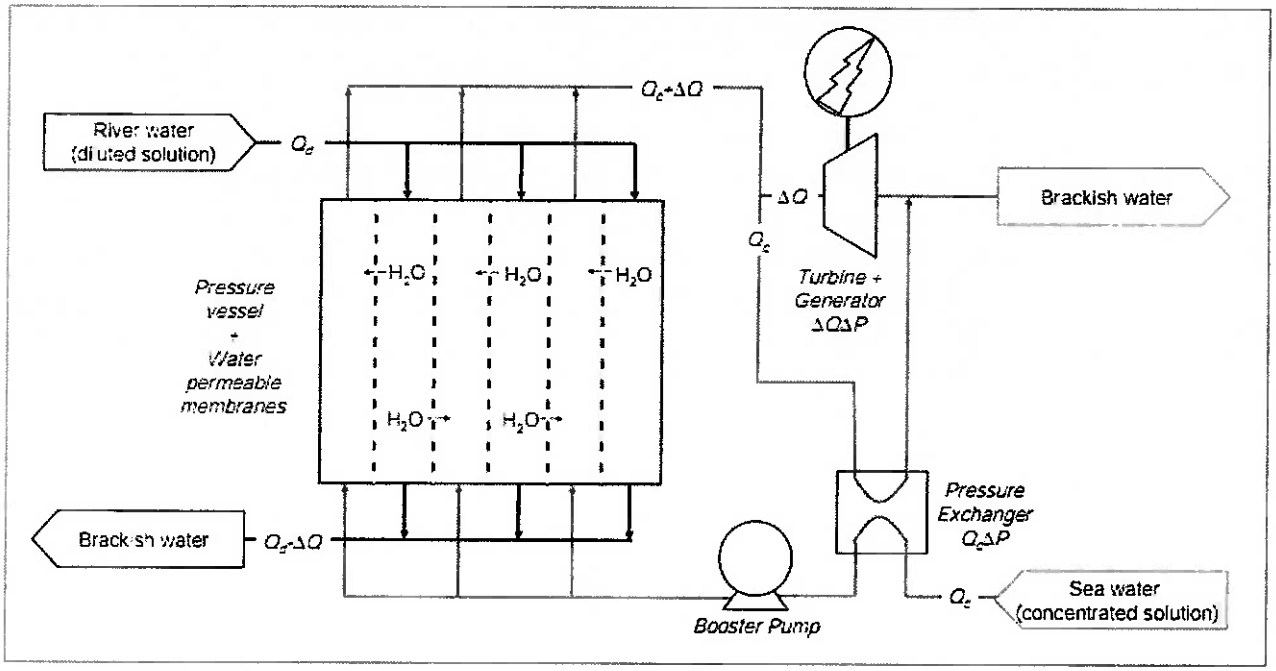

Figure 16: Pressure retarded osmosis [20]

The osmotic pressure difference can be estimated either from Morse's equation or from the thermochemical equilibrium theory. The condition for equilibrium is that the chemical potential of the solvent in both sides of the membrane to be equal, given that the membrane is impermeable to solutes. We remind that the chemical potential of any

solution component can be calculated from the equation below and that the term $|z_i|F\Delta\varphi$ for water equals zero, since no ionic transport occurs:

$$\mu_i(T,p) = \mu_i^0(T,p) + RT\ln x_i + |z_i|F\Delta\varphi$$

$$\mu_{H2O,c}(T,p+\Delta\pi) = \mu_{H2O,d}(T,p)$$

$$\mu_{H2O,c}(T,p+\Delta\pi) = \mu_{H2O,c}(T,p) + \int_p^{p+\Delta\pi}\left(\frac{d\mu_{H2O,c}}{dp}\right)_T dp$$

From thermodynamics $\left(d\mu_{H2O,c} / dp\right)_T$ equals the partial molar volume of solvent in the high salinity draw solution. The partial molar volume (v) of any substance X in a mixture is the volume contribution of one mole of X when added to the mixture; hence, it not only depends on the substance being added but also on the mixture solution. For ideal dilute-solutions, such as seawater being added to brackish water, the partial molar volume is equal to the volume of one mole of X substance/solution. In these conditions it is calculated to be approximately $17{,}7594\ cm^3$. Returning to the chemical equilibrium discussion, we had:

$$\mu_{H2O,c}(T,p+\Delta\pi) = \mu_{H2O,d}(T,p)$$

$$\mu_{H2O,c}^0(T,p) + RT\ln x_{H2O,c} + v_{H2O,c}\,\Delta\pi = \mu_{H2O,d}^0(T,p) + RT\ln x_{H2O,d}$$

Standard conditions of pressure and temperature with which the PRO power plant operates are $1\ atm$ and $293\ K$. Furthermore, these are also the reference for chemical potential measurements for which reason $\mu_{H2O,c}^0 = \mu_{H2O,c}^0 = 0$. Osmotic pressure for average sea and river water salt concentrations – 0,5 and 0,05 mol/L respectively – are then obtained. Results from thermodynamic equilibrium theory and Morse's equation application slightly differ.

$$\Delta\pi = \frac{1}{v_{H2O,c}} RT\ln\left(\frac{x_{H2O,d}}{x_{H2O,c}}\right) = \frac{1}{v_{H2O,c}} RT\ln\left(\frac{1-2x_d}{1-2x_c}\right) = 22{,}94\ atm$$

Contribution of only sodium chloride – taken from table 3 : $\Delta\pi = 22{,}85\ atm$

The osmotic pressure ($\Delta\pi$) is the pressure which, if applied as a hydraulic pressure (Δp) to the high salinity draw solution, would cease water transport across the membrane. The application of an external Δp defines which different type of osmotic process is used: for forward osmosis $\Delta p = 0$, for reverse osmosis $\Delta p > \Delta\pi$ and for pressure retarded osmosis $\Delta p < \Delta\pi$. Total pressure difference $\Delta\pi - \Delta p$ and water flux per m^2 across the membrane are related through the membrane water permeability parameter (A).

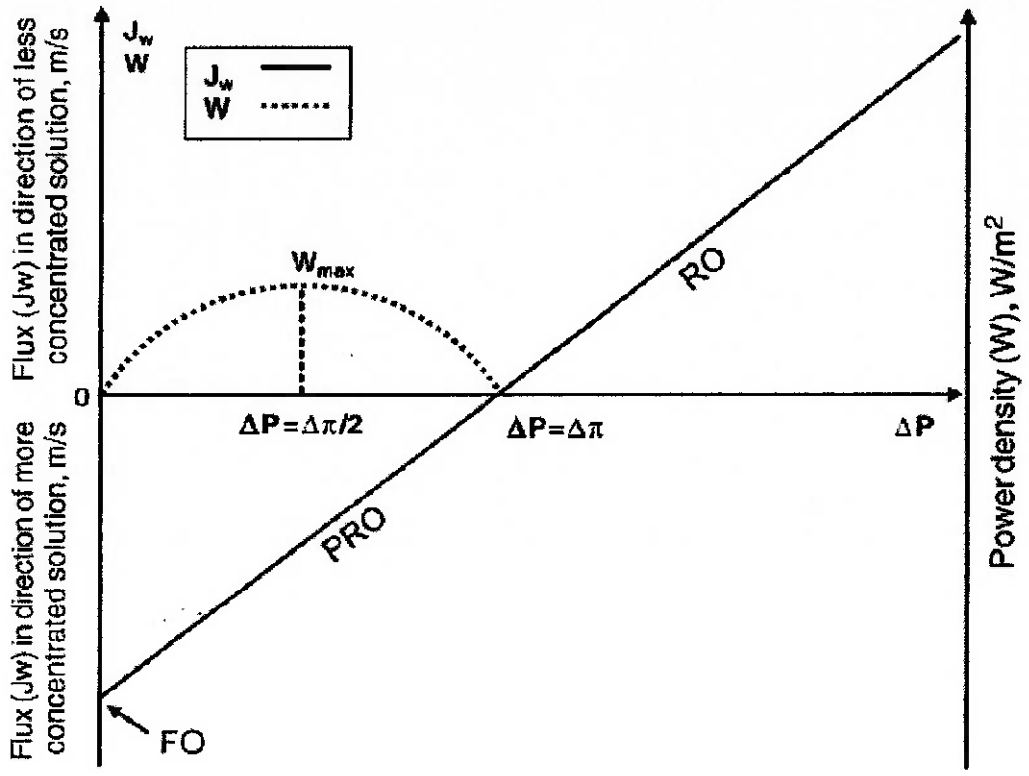

Figure 17: Water flux and power density as a function of applied pressure [22]

The general equation describing water transport in osmotic devices is presented once again. Permeating flux is dependent on the membrane water permeability (A) and differences in osmotic ($\Delta\pi$) and applied pressure (Δp) of each solution. The power density achieved is the product of the water flux with the external pressure applied.

$$J_w = \frac{\dot{V}_{H2O}}{S} = A(\Delta\pi - \Delta p)$$

$$\dot{w} = \frac{\dot{W}}{S} = J_w \Delta p = A(\Delta\pi - \Delta p)\Delta p$$

$$\dot{w}_{opt}\left(\Delta p = \frac{\Delta\pi}{2}\right) = A\frac{\Delta\pi^2}{4}$$

Many developments in membrane technology have occurred in the direction of increasing power densities; figure 18 portraits these historical advancements. Recent studies were able to increase power density values tenfold for seawater systems and threefold for brine systems. Membrane parameters linked to inefficiencies in osmotic transport other than the energy recovery rate will be introduced in detail in the next chapter where PRO is discussed in-depth.

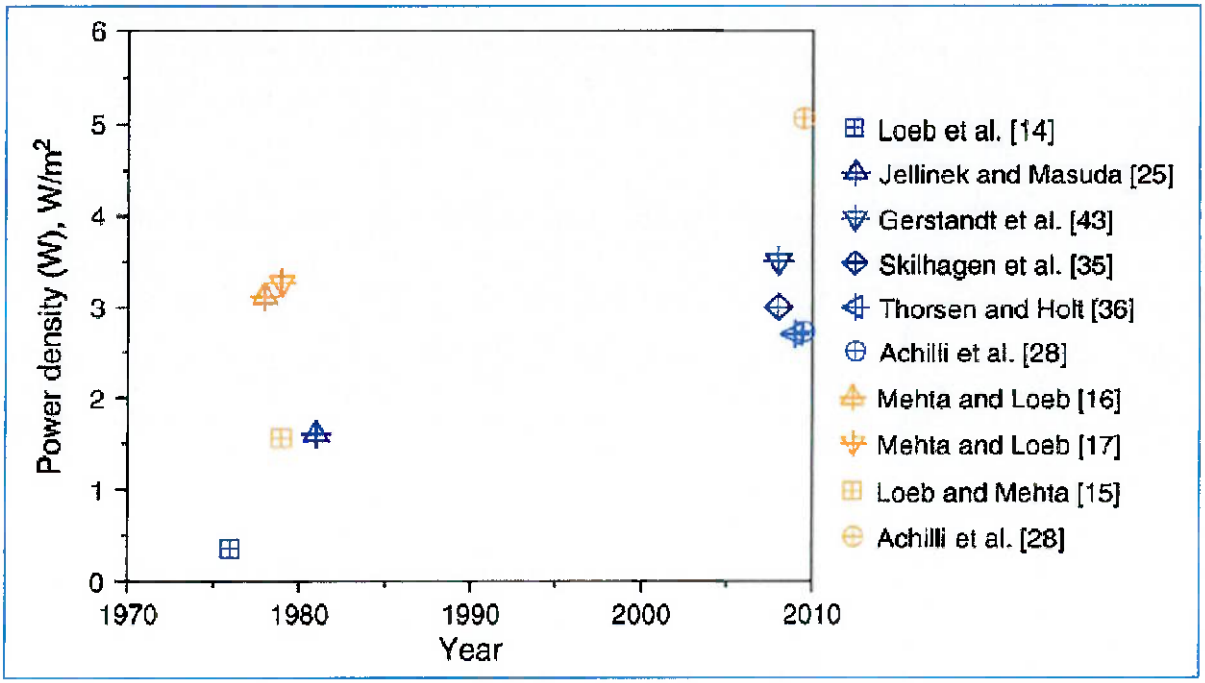

Figure 18: Historical power density values achieved by mixing freshwater with seawater (blue) or brine (orange) [22]

The energy recovery rate can be calculated in the same way proposed for reverse electrodialysis; however, a much simpler way is also possible when we consider the water flux and power density membrane parameters:

$$\eta = \frac{\int_{to}^{t} \dot{w}_{opt}\, S_m dt}{\Delta G_{mix}} = \frac{\dot{w}}{J_w \Delta G_{mix}}$$

Pressure retarded osmosis was invented in the early 70's when Professor Sidney Loeb designed the first membrane for seawater desalination by RO and considered the possibility of harnessing electricity using that same membrane. Studies were carried out and PRO was considered economically unfeasible at that time due to technological constraints. Membranes were costly, with low power density values and the second most important component for the power plant, the energy recovery pressure exchanger unit, was also at a non-optimal design.

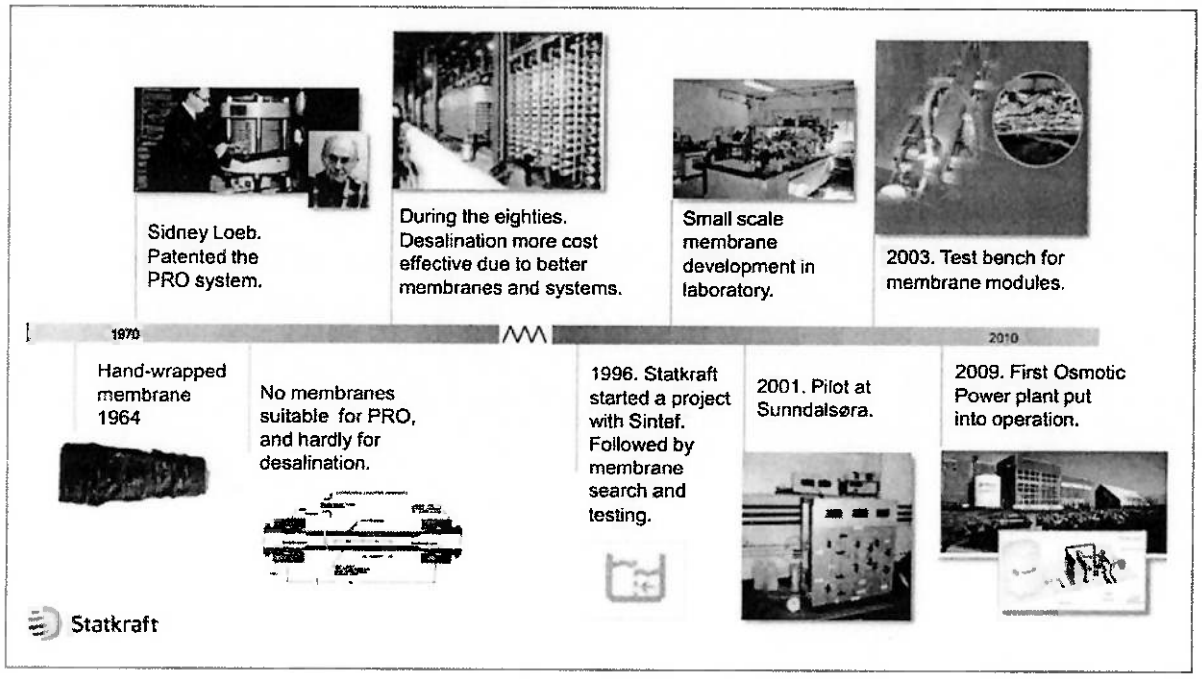

Figure 19: History of PRO

Torleif Holt and Thor Thorsen at SINTEF – the largest group of research organization in Scandinavia – worked on the theoretical potential of osmotic power during the 1980s, and not until 1995 did they obtain financing for a feasibility project. In 1996, the Swedish company Statkraft contacted both researchers and a collaboration project was established. From there onwards great developments in membrane technology were achieved; osmotic power was awarded EU funding and won the attention of researchers and specialists as a new promising alternative.

The first PRO power plant prototype was put in operation in late November 2009; originally designed to produce $4\ kW$, the power plant has a net output of $2-4\ kW$. This reduction is caused by pumping expenses necessary to run the power plant, which impact is carefully assessed in the following chapters. Power densities of $3\ W/m^2$ has already been achieved for seawater and freshwater mixing, but Statkraft claims that they should be of the order of $5\ W/m^2$ for the power plant to be economically competitive; they expect to reach this value by 2015.

C3. Harnessing electricity with pressure retarded osmosis

In the previous chapter pressure retarded osmosis was introduced along with other salinity-gradient energy technologies. Those brief explanations gave only some insights on how these processes worked at basilar level; when further studying and actually applying this knowledge one will discover that there are numerous technicalities involved that effectively alter the amount of energy produced. This chapter aims to present a in-depth study of the main components of a PRO system: the membrane and the pressure exchanger energy recovery unit; furthermore, mechanical efficiency is evaluated in four different power plant (PP) configurations, following the footsteps of Loeb et al. (1990): continuous flow – terrestrial PP, continuous flow – terrestrial PP with PX, continuous flow – underground PP and alternating flow – terrestrial PP.

3.1 PRO Membrane

The first membranes used in PRO experiments by Prof. Sidney Loeb were cellulose acetate membranes adapted from Reverse Osmosis (RO) processes. Those membranes were found to be semipermeable to seawater electrolytes in the same period by Sourirajan, Reid and Breton. Sourirajan reported his findings to the University of California while Breton and Reid worked at the University of Florida. At the late 50's, Loeb and Sourirajan partnership allowed them to experimentally notice membrane asymmetry, previously assumed to be isotropic, which led to many more findings regarding membrane effective thickness, porosity, pre-treatment and tailoring (LOEB, 1981).

An ideal membrane for PRO would have a high water permeability, low salt permeability, low resistance to water flux in the support layer, high structural resistance to withstand operating pressure, high tolerance to pH and temperature variability and high resistance to the attack of bacteria, chemicals and fouling substances; those criteria must be met with reduced membrane thickness and pore diameter. Overall, there are numerous material engineering trade-offs to be considered when designing membranes and studies in this area will clearly open new pathways and possibilities for

PRO and other membrane based technologies. Nowadays, there are three types being considered for such application: cellulose acetate/triacetate membranes (CA/CTA), aromatic polyamide membranes (PA) and thin film composite membranes (TFC). A brief qualitative comparison between membrane characteristics is presented. This study does not intend to further discuss membrane design concerning material engineering, if any interest in such matters arises we recommend reading the work of Sourirajan (1970) and other references indicated in the bibliography.

Table 6: PRO membrane main characteristics

Membrane	CA/CTA	PA	TFC
Membrane polymer	cellulose acetate / triacetate	polyamide	multiple (polyimide, polysulfone, etc.)
Water permeability and flux	M / L	L	H
NaCl rejection	M / H	H	H
Compaction tendency	H	H	L
pH tolerance	4-7 / 3-8	3-10	2-11
Temperature stability	max 35°C / 40°C	max 45°C	max 45°C
Organic rejection	L	M	H
Oxidant tolerance (chlorine, etc.)	H	L	L
Biodegradability	H	L	L
Cost	L	M	H

H = High, M = Medium, L = Low

There are several design configurations for the membrane and its pressurized vessel. The design can significantly alter the performance and costs of an operating power plant, some are based on simplicity, others are more cost, assembly or even performance-oriented.

The **spiral wound** configuration consists of two or more layers of semi-permeable membrane normally separated by a woven fabric, the edges of the membranes are sealed in three of the four sides in order to form a flexible envelope that can be spiralled around the collector tube; the open end of the envelope is attached to the perforated

collector tube. A sheet of plastic netting, which function is to promote turbulence and separate membranes during assembly, is placed adjacent to the envelope. After the enveloped is spiralled around the perforated collector tube, the whole device is inserted in a pressure container.

The spiral wound configuration has a high packing density, low manufacturing cost and can be cleaned both chemically and hydraulically with relative ease; its primary disadvantage is that it is not adequate for highly turbid waters without extensive pre-treatment. Freshwater flow passages are small and subject to clogging.

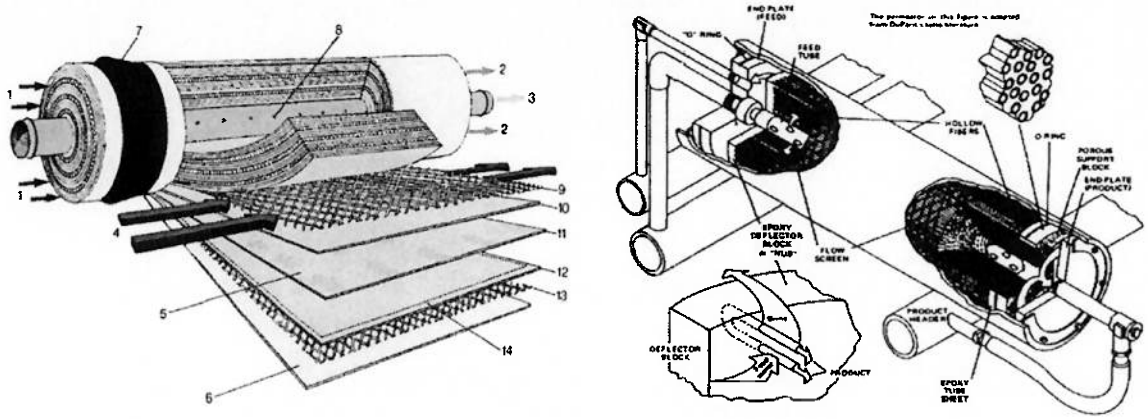

Figure 20: Spiral wound and hollow fibre membrane configurations

The **hollow fibre** configuration consists of a very large number of hollow membrane fibres which are assembled into a cylindrical bundle, evenly spaced about a central feed distributor tube. The ends of the fibres are put into an epoxy tube sheet so that the pores are exposed; finally, the bundle is inserted in a pressure vessel. Freshwater is introduced through the distributor tube and flows through the membrane into the holes of each hollow fibre. This design has an extremely high packing density and relatively low manufacturing cost; however, it is also very susceptible to fouling and difficult to clean. Pre-treatment is required even on relatively clean feedwaters.

The **tubular** configuration is the simplest of all; membrane is either placed within a porous tube and sealed into place or cast on its inner surface. Water passes through the membrane and the porous tube before dropping off in a convenient receptacle for removal. This configuration has the advantage of being able to operate at extremely turbid feedwaters and to be cleaned either mechanically or hydraulically with ease,

nevertheless, capital costs are much higher than those of the hollow fibre and spiral wound configurations. A last possible design, the **flat** configuration, is composed of membranes attached to both sides of a rigid plate. The plate/membrane units are stacked in a pressure vessel; water passes through the membrane and is collected in the porous media. Due to its complexity and high capital cost, it is unlikely to be used in large-scale applications.

The characteristics of an ideal membrane were listed above, nonetheless, for any real osmotically-driven process imperfections and their consequent inefficiencies are always present. There are three major phenomena that cause membrane performance to fall: reverse salt diffusion, internal concentration polarization and external concentration polarization.

An important note to the reader is necessary; from here onwards we start dealing with local physical quantities, or in other words, quantities that no longer apply for the solution as a whole. A distinct identification of subscripts will be necessary to fit this new treatment. The uppercase subscripts D, F and B will be used to label the *high salinity draw solution*, *low salinity feed solution* and *brackish solution*, respectively. The lowercase subscripts m and b will be used to label quantities at *membrane dense layer interface* and at *bulk solution*, that is, distant enough from the membrane so that no concentration polarization phenomena are observed.

Reverse salt diffusion is characterized by the passage of small amounts of salt from the draw solution to feed solution through the membrane (ACHILLI et al., 2009). It reduces the effective osmotic pressure obtainable by increasing the salinity level of the feed solution and it is measured with the salt permeability membrane coefficient (B):

$$J_{NaCl} = B\left(C_{D,b} - C_{F,b}\right) \cong BC_{D,b}$$

Salt flux through the membrane – usually expressed in mol/m^2s, is independent on the pressure applied to the system, unlike water flux. It depends only on the gradient in salinity of draw and feed solutions at membrane interface. Membrane selectivity is usually measured in terms of salt rejection (R), a term already introduced in table 5. Since salt concentration in draw solution is many times higher than that in feed solution,

salt rejection is normally close to unity. Referencing table 5 in a quantitative way, low salt rejection would be for $R < 0{,}96$; medium for $R = 0{,}96 - 0{,}99$; and high for $R > 0{,}99$.

$$R = 1 - \frac{C_{F,b}}{C_{D,b}}$$

It is possible to experimentally determine B if other membrane parameters are known. Salt concentration in the feed solution can be expressed in terms of J_{NaCl} and J_w in the following way:

$$C_{F,b} = \frac{J_{NaCl}}{J_w}$$

$$R = 1 - \frac{C_{F,b}}{C_{D,b}} = 1 - \frac{\frac{J_{NaCl}}{J_w}}{C_{D,b}} = 1 - \frac{B(C_{D,b} - C_{F,b})}{A(\Delta\pi - \Delta p)C_{D,b}} = 1 - \frac{RB}{A(\Delta\pi - \Delta p)}$$

$$B = \frac{A(1-R)(\Delta\pi - \Delta p)}{R}$$

Overall, reverse salt diffusion could be a more serious problem if membrane technologies weren't developed as they are today and salt rejection levels were lower. On the other hand, minimizing concentration polarization does pose itself as the new breakthrough in membrane technology to be achieved. It occurs in both sides of the membrane but, given its asymmetry, effects in each solution side are defined distinctly.

Dilutive external concentration polarization is the phenomenon that occurs on the more dense side of the asymmetric membrane, which must be placed facing the draw solution for structural reasons. It results from local reduction in salt concentration in the saline solution at membrane vicinity due to solvent transport across the membrane prior to its complete diffusion (ACHILLI et al., 2009). The external concentration polarization is calculated as shown:

$$\frac{\pi_{D,m}}{\pi_{D,b}} = \exp\left(-\frac{J_w}{k}\right)$$

$$k = \frac{S_h D}{d_H} = \frac{0{,}2 R_e^{\,0{,}57} S_c^{\,0{,}4} D}{d_H}$$

where π is the local osmotic pressure and k is the mass transfer coefficient in the draw solution. The transfer coefficient is estimated from the diffusion coefficient (D), the hydraulic diameter of the flow channel (d_H) and Sherwood number (S_h). The osmotic pressure at membrane interface ($\pi_{D,m}$) results smaller than that at bulk solution ($\pi_{D,b}$) due to dilutive external concentration polarization. This effect is also shown graphically in figure 21.

Concentrative internal concentration polarization is the local increase in solute concentration along the porous support of the membrane. As observed in the graph above, this phenomenon has a severe contribution to the reduction of the effective osmotic pressure difference across the membrane. An experimental expression for this effect is presented (LEE et al., 1981 apud ACHILLI et al, 2009).

$$J_w = A\left[\pi_{D,m}\frac{1 - \frac{C_{F,b}}{C_{D,m}}\exp(J_w K)}{1 + \frac{B}{Jw}[\exp(J_w K) - 1]} - \Delta p\right]$$

$$K = \frac{t\tau}{D\varepsilon}$$

The term K represents solute resistivity for diffusion in the porous layer of the membrane, it is a function of membrane porosity (ε), tortuosity (τ) and thickness (t) as well as of the diffusion coefficient (D).

The expression for internal concentration polarization takes into account reverse salt diffusion across the membrane, as one can notice from the term B included; including dilutive internal concentration polarization in the formula as well is simple. A final expression for water flux in a PRO process is thus obtained, water flux across the membrane is a function of the membrane characteristics (A and B), bulk solutions osmotic pressure ($\pi_{F,b}$ and $\pi_{D,m}$), mass transfer coefficient (k), solute resistivity to diffusion (K) and applied hydraulic pressure (Δp).

$$\pi = CRT \rightarrow \frac{\pi_{F,b}}{\pi_{D,m}} = \frac{C_{F,b}}{C_{D,m}}\frac{T_F}{T_D}$$

$$J_w = A\left[\pi_{D,b}\exp\left(-\frac{J_w}{k}\right)\frac{1-\frac{\pi_{F,b}}{\pi_{D,m}}\frac{T_D}{T_F}\exp(J_wK)}{1+\frac{B}{J_w}(\exp(J_wK)-1)} - \Delta p\right] = A(\Delta\pi_{eff} - \Delta p)$$

$$\dot{w} = A\left[\pi_{D,b}\exp\left(-\frac{J_w}{k}\right)\frac{1-\frac{\pi_{F,b}}{\pi_{D,m}}\frac{T_D}{T_F}\exp(J_wK)}{1+\frac{B}{J_w}(\exp(J_wK)-1)} - \Delta p\right]\Delta p$$

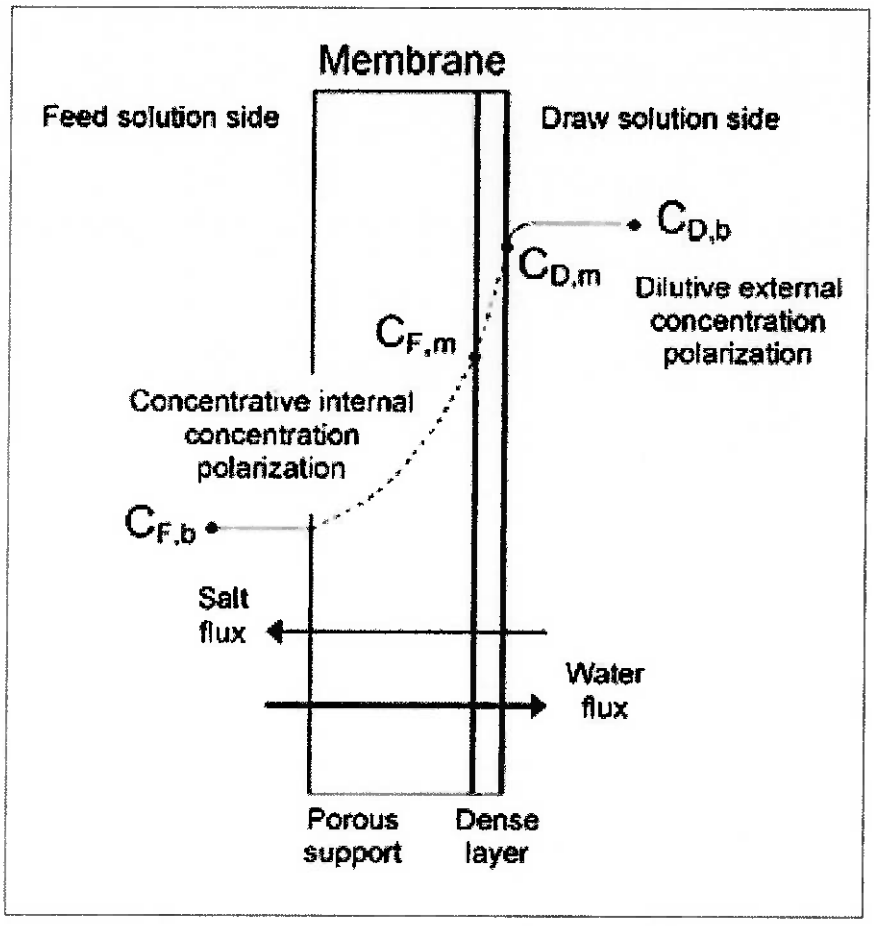

Figure 21: Effects of concentration polarization [23]

After a numerical solution to J_w is found it is possible to algebrically calculate the membrane power density ($\dot{w}$). As expected, under real circumstances, membrane performance is obviously affected by the effects of reverse salt diffusion and concentration polarization; Achilli et al. (2009) provided a graphic where the performance drop for real membranes is visible.

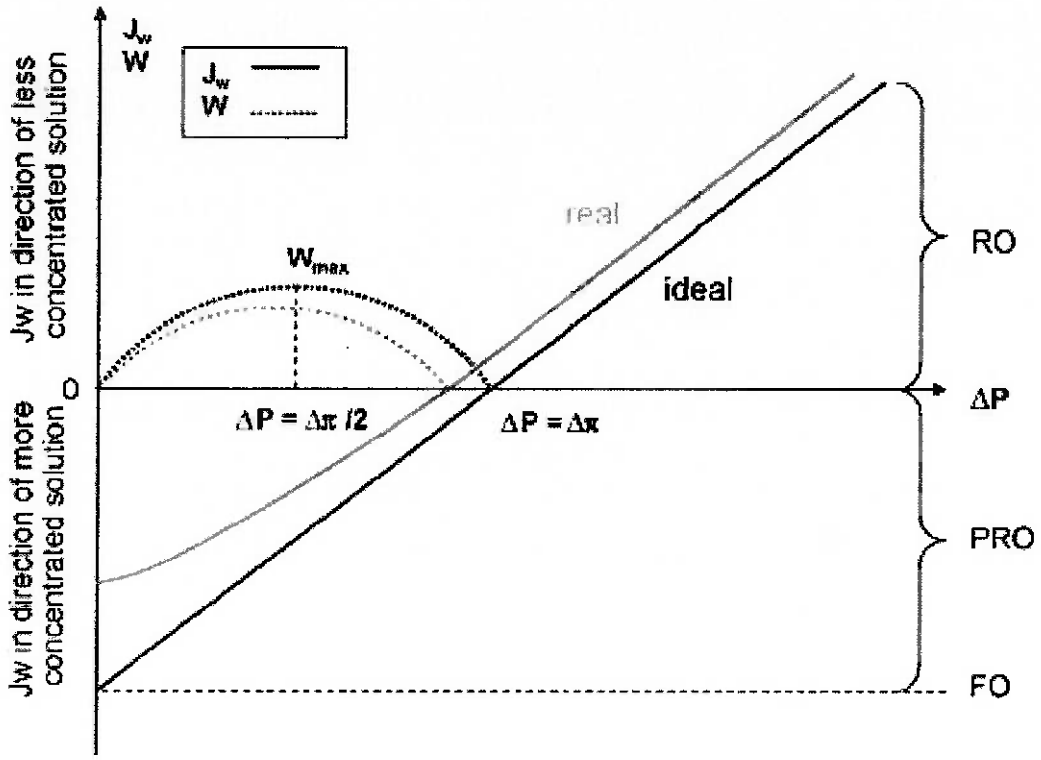

Figure 22: Performance drop in real PRO membranes [23]

Achilli et al. (2009) also studied the combined effects of external concentration polarization, internal concentration polarization, and salt passage for different salinity levels of both feed and draw solutions. The most important result of such study observed that decreasing draw solution salinity level is less harming to membrane performance than increasing the salinity in feed solution by the same value; therefore, freshwater provision to the power plant must be prioritized.

3.2 Pressure exchanger energy recovery unit (PX)

The pressure exchanger facilitates pressure transfer from a high-pressure fluid to a low-pressure one by putting both in direct, temporary contact. It is a direct application of positive displacement technology and Pascal's law which states that when pressure is applied to an enclosed fluid, it is transmitted undiminished to every portion of the fluid and to the walls of the pressurized vessel.

Energy Recovery Inc. developed a high efficiency device to meet such target. It is composed of a ceramic rotor with ducts which perfectly fit into ceramic sleeves and endcovers so as to create an almost frictionless hydrodynamic bearing when pressurized. There are no physical barriers between fluids interface inside the rotor ducts, the mixing of solutions is a function of their velocity and of the duration of exposure. The exposure is longer at lower rotational speeds, which in turn depends on the velocity of the streams. No electrical motor is necessary; the device is rotated by means of momentum conservation between the rotor and the fluids passing through its ducts. The PX is designed so that the interface between solutions, called the plug, never reaches the end of the rotor duct before they are sealed. A schematic representation is presented in figure 24 (STOVER, 2004, 2007).

At any given instant, half of the rotor ducts are exposed to the high-pressure stream and half to the low-pressure stream. As the rotor turns, the ducts pass a sealing area that separates high and low pressure. Thus, the ducts that contain high pressure are separated from the adjacent ducts containing low pressure by the seal that is formed with the rotor's ribs and the ceramic end covers.

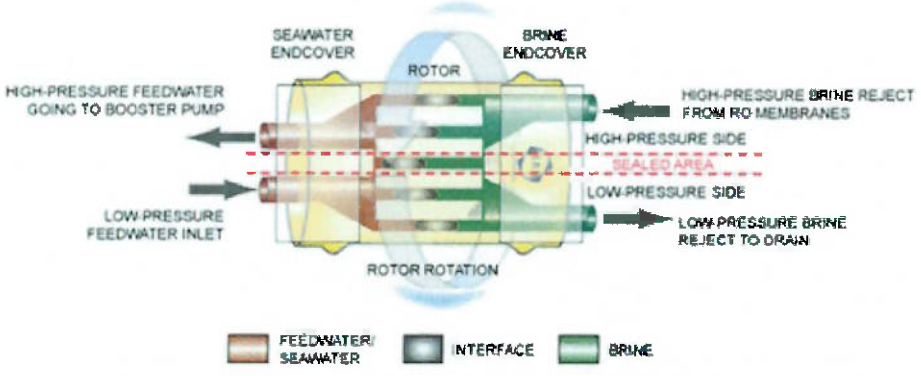

Figure 23: Working mechanism of a PX unit [31]

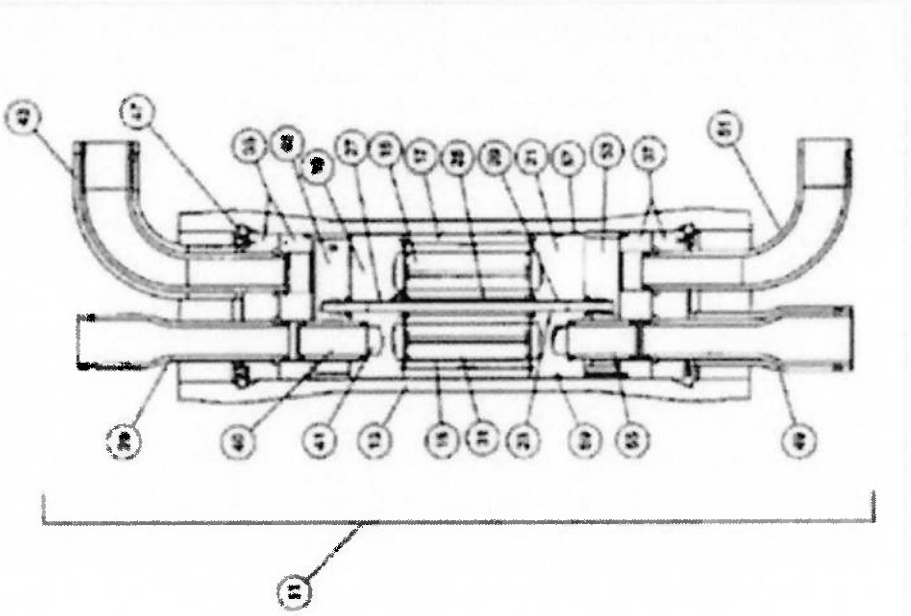

Figure 24: Technical scheme of a PX unit [30]

As observed from figure 24, the interface between solutions travels back and forth inside the rotor duct. The relationship amidst rotational speed, flow rate, plug travel velocity and distance is illustrated below. As flow increases so do plug velocity and rotation and equilibrium is maintained through intelligent design; if the interface reached the duct end before complete sealing, the fluids would inevitably mix and plant operation could be compromised; actually, a minor percentage of mixing is always present.

Originally designed for RO applications, brochures and datasheets do not provide information about the amount of mixing if sea and brackish water were used nor the eventual reduction in seawater salinity. One can, however, estimate this value from data provided when seawater and brine are employed: 2,5% of salinity variation. The driving force for mixing is the salinity-gradient between solutions; making it simple, one can consider brine to be twice as saline as seawater which in turn is twice as saline as brackish water. Brine-seawater salinity difference is, therefore, twice the difference between sea-brackish water; hence, the same proportion could be assumed for salinity variation. Alternatively, one could simply consider the same 2,5% value provided for conservative design.

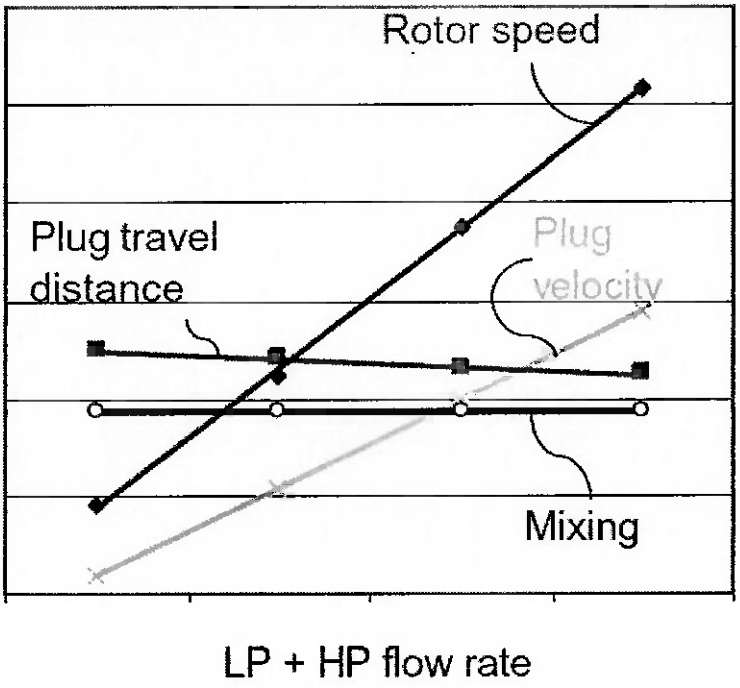

Figure 25: Various parameters as functions of flow rate in a PX unit [31]

The PX efficiency can be as high as 98% in some models; the main sources of performance loss are seawater compression, viscous friction inside the reduced cross-sectional area of rotor ducts and lubrication flow through the hydrodynamic bearing. It can be calculated with the following expression (STOVER, 2004):

$$\eta_{PX} = \frac{\sum(Pressure * Flows)_{out}}{\sum(Pressure * Flows)_{in}}$$

In the next section we compare performances of PRO power plant configurations, one of which employing the PX unit in its design. The extent of the so far supposed improvement due to the use of the PX will be shown then.

3.3 Power plant (PP) configurations

Loeb et al. (1990) studied the mechanical efficiency of several PRO plant configurations; in order to do so they relied on data obtained by Honda (1989) in a previously sized hollow-fibre membrane PRO system. In this section we compare the results obtained by them with ours, given that assumptions in both cases slightly differ. Four configurations are studied: continuous flow – terrestrial PP, continuous flow – terrestrial PP with PX, continuous flow – underground PP and alternating flow – terrestrial PP.

Due to its simple design and reduced number of elements, there are only a few sources of losses in mechanical efficiency for a PRO power plant. Frictional pressure drop in piping, losses in rotating pairs and membrane inefficiencies are all met by higher pumping requirements, which directly affect the net amount of electricity produced.

A series of assumptions must be done before proceeding with the study. In order to solely evaluate the contribution of plant configuration to mechanical efficiency other loss sources must be kept constant. The amount of water permeating through the membrane will be denoted $\Delta\dot{V} = J_w S$ and the amount of seawater used at the process will be denoted $\dot{V}$.

Table 7: Assumptions in power plant configuration analysis

	(LOEB et al., 1990)	This study
(ZERO)	Freshwater hydraulic pressure, p_f, and osmotic pressure, $\pi_{F,b}$, are both assumed to be zero gauge.	Idem
(A)	The concentrated and diluted solutions entering the permeator will be salt water and freshwater respectively. The salt water enters the permeator at a rate $\dot{V}\ m^3/day$ and an osmotic pressure of 28 atm.	Idem
(B)	The ratio $\dot{V}/\Delta\dot{V}$ is 1,08, it represents a mixture of freshwater and salt water leaving the permeator at a rate $(\dot{V} + \Delta\dot{V})$ with a concentration of about 1,8% NaCl and an osmotic pressure of about 15 atm.	The ratio $\dot{V}/\Delta\dot{V}$ is 1. Resulting brackish water will have a concentration of about 1,75% NaCl and an osmotic pressure of about 14 atm.
(C)	The pressure change through the hydroturbine will be from 9 to 0 $atms$ in each scheme. As a corollary to this requirement the approximate hydraulic pressure p_s on the salt water side of the PRO permeator will also have the value $p_s = 9\ atm$ in each of the schemes, a value appropriate for $\dot{V}/\Delta\dot{V} = 1{,}08$. The maximum available power will be: $P_s\Delta\dot{V}$.	$p_s = 10{,}5\ atm$, reasons as to why this value is used are presented further ahead.

(D)	The frictional pressure drop across the salt water side of the PRO permeator will be $0{,}007p_s$.	Idem
(E)	The frictional pressure drop across the freshwater side of the PRO permeator will be $0{,}011p_s$.	Idem
(F)	The freshwater entering the low pressure side of the permeator is assumed to have some salt in it. Furthermore some salt may diffuse from the seawater side to the freshwater side due to imperfections in the membrane. Therefore, to prevent the freshwater solution being concentrated to a high osmotic pressure due to $\Delta\dot{V}$, the water permeation rate, a flushing solution leaves the low pressure side of the permeator at a rate $\dot{FS}$. The freshwater enters the permeator at a rate $(\dot{FS} + \Delta\dot{V})$ so as to satisfy mass conservation requirements.	An ideal membrane is considered, no flushing solution is necessary.
(G)	The ratio $\dot{FS}/\Delta\dot{V}$ is 0,39. This is high enough to prevent a significant and undesirable osmotic pressure in the flushing solution stream, but low enough to prevent excessive pumping power requirements for $\dot{FS}$, particularly in the underground plant.	$\dot{FS}/\Delta\dot{V} = 0$ as consequence of assumption **(F)**.
(H)	The efficiency of all the rotating pairs is 80%. These pairs include the hydroturbine-generator, the freshwater pump-motor, the seawater pump-motor, and the flushing solution pump motor.	Idem

It was already shown that $\Delta p = \Delta\pi_{eff}/2$ maximizes power output for a PRO power plant. Loeb et al. (1990) approximate the value of $\Delta\pi_{eff}$ with the arithmetic average osmotic pressure on the saline water side. Following assumptions (ZERO) and (B), the osmotic pressure of the produced brackish water is:

$$\pi_{B,b} = \frac{\pi_{F,b}\Delta\dot{V} + \pi_{D,b}\dot{V}}{\Delta\dot{V} + \dot{V}} = \frac{\pi_{F,b}}{2} = 14\ atm$$

$$\Delta\pi_{eff} \cong \frac{\pi_{D,b} + \pi_{B,b}}{2} = 21\ atm$$

$$\Delta p = \frac{\Delta\pi_{eff}}{2} = 10{,}5\ atm$$

Based on these conditions, the mechanical efficiency of these different configurations will be calculated. It is defined as the ratio between net power produced and maximum available power of the power plant.

$$\eta_m = \frac{net\ power}{p_s \Delta \dot{V}}$$

A schematic of the **continuous flow – terrestrial PP** is presented to the reader. Salt water at a rate $\dot{V}$ passes through two rotating pairs, the pump-motor and turbine generator, and it is subject to losses in these elements. Freshwater permeates through the membrane at a rate $\Delta \dot{V}$, but pumping requirements must account parasitic power consumed and the flushing solution $\dot{FS}$ as well.

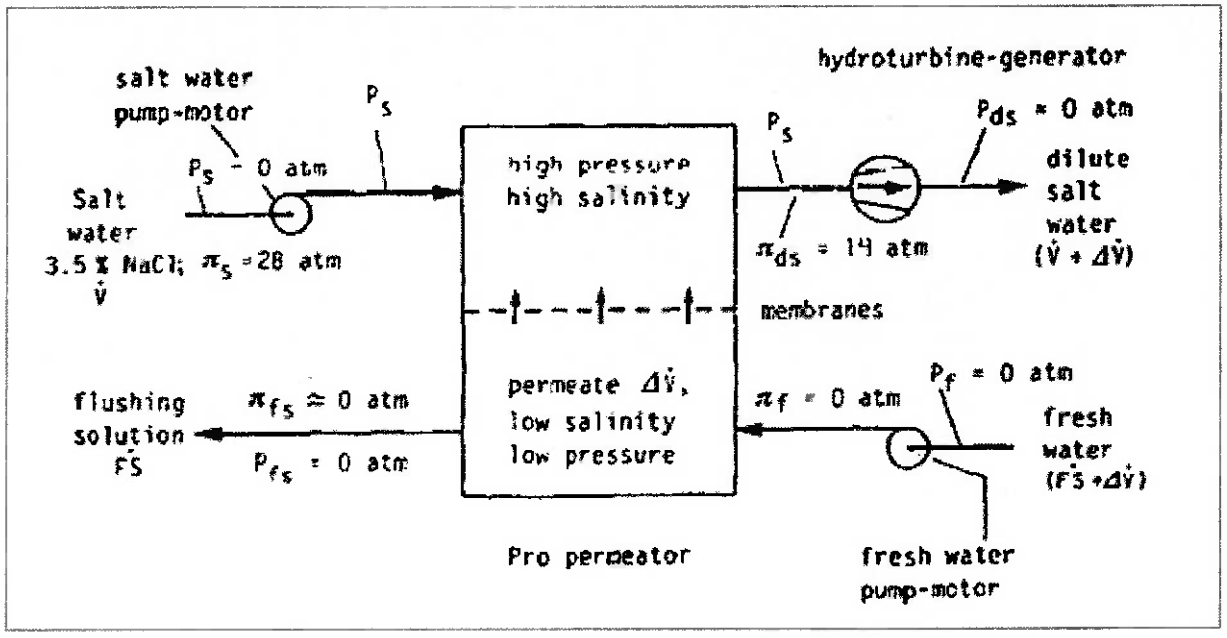

Figure 26: Continuous flow - terrestrial power plant layout [26]

For this configuration, the net power produced will be the difference between the generated power at the turbine-generator pair and the pumping requirements from both fresh and saline water sides. Using assumptions (B), (G) and (H), we have:

$$net\ power = \eta_T(\dot{V} + \Delta\dot{V})p_s - \frac{p_s\dot{V}}{\eta_p} - \frac{0{,}007 p_s \dot{V}}{\eta_p} - \frac{0{,}011 p_s(\Delta\dot{V} + \dot{FS})}{\eta_p}$$

$$\eta_m = \frac{net\ power}{p_s \Delta\dot{V}} = \eta_T \left(\frac{\dot{V}}{\Delta\dot{V}} + 1\right) - \frac{1{,}007}{\eta_p}\frac{\dot{V}}{\Delta\dot{V}} - \frac{0{,}011}{\eta_p}\left(1 + \frac{\dot{F}S}{\Delta\dot{V}}\right) = 0{,}3275$$

Mechanical efficiency for the continuous flow – terrestrial PP configuration is prohibitively low. Increasing the ratios $\dot{V}/\Delta\dot{V}$ and $\dot{F}S/\Delta\dot{V}$ would only worsen the system performance; one may suggest reducing the value of $\dot{V}/\Delta\dot{V}$ but along with it the value of the hydraulic pressure p_s that maximizes work would also drop, nullifying the benefits from mechanical efficiency improvement.

For the **continuous flow – terrestrial PP with PX** configuration, salt water and freshwater intake remain the same. However, after exiting the membrane pressurized vessel, the total brackish water flow $(\dot{V} + \Delta\dot{V})$ is again divided: $\dot{V}$ is directed to the Pressure Exchanger unit to provide salt water pressurization and $\Delta\dot{V}$ is directed to the turbine for power generation. However, the energy recovery unit is not sufficient for salt water to reach the desired working pressure p_s, a booster-pump is used to achieve it. A schematic of this design is shown:

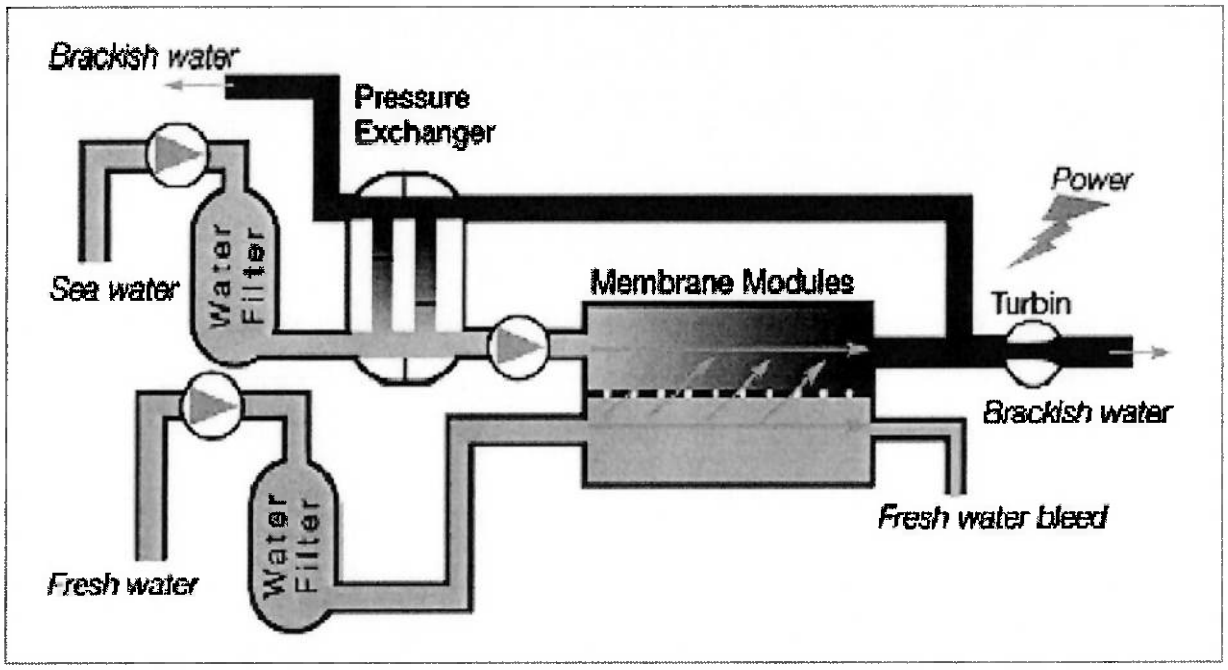

Figure 27: Continuous flow - terrestrial power plant with PX layout, adapted from [26]

The values of hydraulic and osmotic pressure of the flows passing through the pressure-exchanger are obtained from the device efficiency and mixing rate defined by the producer. For the mixing rate a typical value found was a difference of 2,5% in salinity due to direct contact of both flows inside the device. The efficiency of the energy recovery unit is defined as follows (STOVER, 2004):

$$\eta_{PX} = \frac{\sum(Pressure * Flows)_{out}}{\sum(Pressure * Flows)_{in}} = \frac{p_{PX}}{p_s} = 0{,}95$$

Therefore, if high and low pressure flows are balanced the device efficiency is determined by the ratio between the sum of the outlet fluids pressure and the sum of the inlet fluids pressure. In this study specific case, the efficiency corresponds to the ratio between the pressure achieved at the low pressure side and the pressure available at the high pressure side. The pressure-exchanger energy recovery unit has high efficiency values, typically around 0,95. Net power produced by this configuration is calculated just as it was for continuous flow – terrestrial PP, however, losses at the salt water side are supposed to be lower due to the use of a pressure-exchanger device.

$$net\ power = \eta_T p_s \Delta\dot{V} - \frac{(p_s - p_{PX})\dot{V}}{\eta_p} - \frac{0{,}007 p_s \dot{V}}{\eta_p} - \frac{0{,}011 p_s(\Delta\dot{V} + F\dot{S})}{\eta_p}$$

$$\eta_m = \frac{net\ power}{p_s \Delta\dot{V}} = \eta_T - \frac{1,}{\eta_p}\left(1 - \frac{p_{PX}}{p_s}\right)\frac{\dot{V}}{\Delta\dot{V}} - \frac{0{,}007}{\eta_p}\frac{\dot{V}}{\Delta\dot{V}} - \frac{0{,}011}{\eta_p}\left(1 + \frac{F\dot{S}}{\Delta\dot{V}}\right) = 0{,}7150$$

Although we already expected mechanical efficiency to be higher in this configuration, the value has more than doubled thanks to the energy recovery unit. Actually, it is noticeable that the efficiency limiting factors were not losses due to pumping requirements but those in the turbine-generator rotating pair, given $\eta_T = 0{,}8$. We have left the expression fully developed with the terms $\dot{V}/\Delta\dot{V}$ and $F\dot{S}/\Delta\dot{V}$ aiming to compare with the results obtained if the conditions specified by Loeb et al. (1990) were applied. The calculated mechanical efficiency was $\eta_m = 0{,}7040$; no significant variations took place when more realistic membrane performance and requirements were considered.

In the **continuous flow – underground PP** configuration, freshwater at sea level runs vertically downward in a penstock at a rate $(\dot{FS} + \Delta\dot{V})$, reaching a depth of around $100\,m$, so that the hydraulic head equals the required pressure p_s; it then drives the turbine-generator placed at the same depth producing electricity and depressurizing from p_s to $0\,\text{atm}$. This is basically a land-based variation of the SHEOPP proposed by Reali (1981).

Given the depth at which the power plant is built it is necessary to re-pressurize the freshwater flux in order to expel it from the power plant, osmotic membranes are then used to provide the pressurization needed. Seawater is collected and pressurized by the hydraulic head in the same manner as freshwater was and then directed into the membrane module. However, only $\Delta\dot{V}$ is able to permeate through the membrane; the remaining fraction $\dot{FS}$ must be pressurized by an external pump. Brackish water is produced at a rate $(\dot{V} + \Delta\dot{V})$ and pressure close to p_s, so parasitic power expenses are negligible. A schematic of the power plant is shown in figure 28 with the original hydraulic and osmotic pressure values assumed by Loeb et al. (1990).

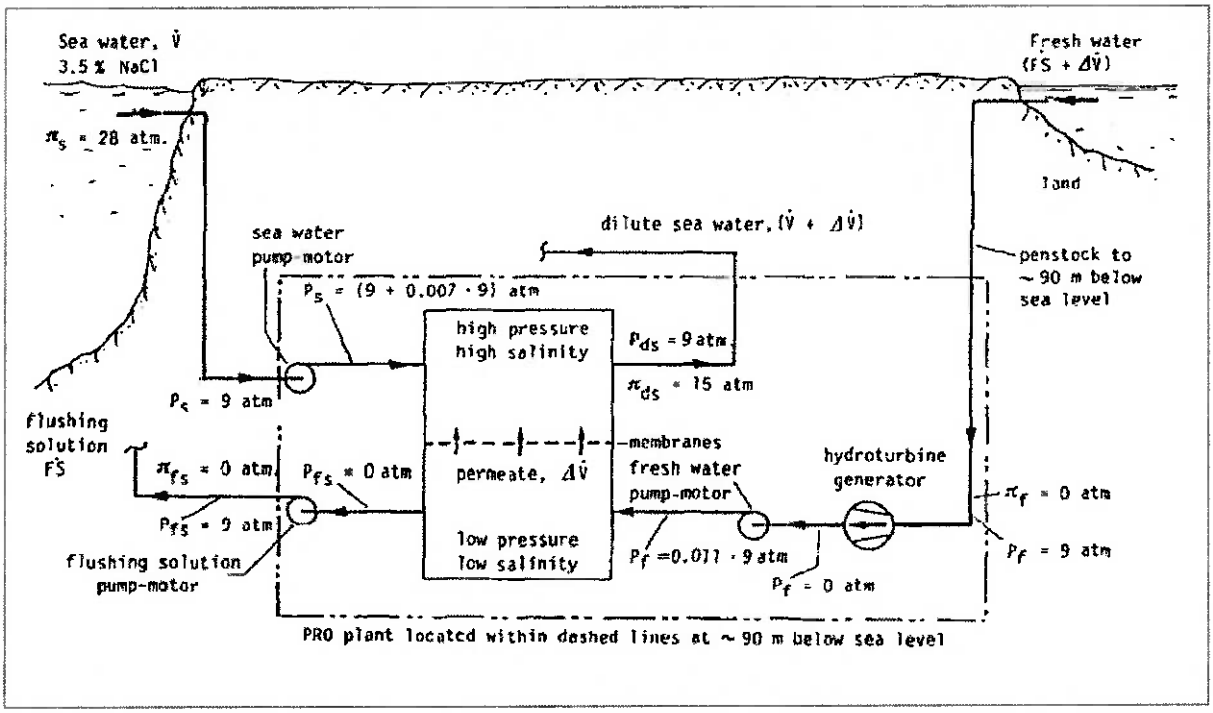

Figure 28: Continuous flow - underground power plant layout [26]

$$net\ power = \eta_T p_s(\Delta\dot{V} + \dot{FS}) - \frac{0{,}007 p_s \dot{V}}{\eta_p} - \frac{0{,}011 p_s(\Delta\dot{V} + \dot{FS})}{\eta_p} - \frac{p_s \dot{FS}}{\eta_p}$$

$$\eta_m = \frac{net\ power}{p_s \Delta\dot{V}} = \eta_T\left(1 + \frac{\dot{FS}}{\Delta\dot{V}}\right) - \frac{0{,}007}{\eta_p}\frac{\dot{V}}{\Delta\dot{V}} - \frac{0{,}011}{\eta_p}\left(1 + \frac{\dot{FS}}{\Delta\dot{V}}\right) - \frac{1}{\eta_p}\frac{\dot{FS}}{\Delta\dot{V}} = 0{,}7775$$

Again, the mechanical efficiency calculated was very high and basically limited to losses in the turbine-generator rotating pair. However, this configuration is much more sensitive to variations in the ratio $\dot{FS}/\Delta\dot{V}$ as concluded from the expression above itself and from comparison to the result obtained by Loeb et al. (1990), where $\eta_m = 0{,}5960$. According to their study, there might be some sites at which, due to their special location, the underground configuration is economically more interesting even when its higher capital amortization energy cost is considered.

The **alternating flow – terrestrial PP** configuration was proposed by Loeb in 1985. The system consists of two salt water tanks that are filled with seawater from the bottom while open to the atmosphere, one at a time. While one of the tanks is being filled, the other is sealed and pressurized by the produced brackish water from the membrane vessel, poured into it from a higher location. Mixing does not occur due to the difference in density of both solutions and a vertical stratification of solutions is observed inside the sealed tank.

The pressurized water from the sealed tank passes through the membrane vessel at a rate $\dot{V}$ absorbing permeating flux at a rate $\Delta\dot{V}$, so that $(\dot{V} + \Delta\dot{V})$ of brackish solution emerges from the high pressure side. This flux is again divided, $\Delta\dot{V}$ being used to produce electricity at the turbine-generator rotating pair and $\dot{V}$ being used at salt-water pressurization. When the sealed tank is emptied it is drained from a valve, opened to atmosphere and refilled with seawater. Meanwhile, the other tank is sealed, pressurized by the brackish water and used in the PRO process as described above. The alternating pattern is repeated during plant operation.

In practical terms, Prof. Loeb has invented a feedback system that works in a similar manner to that of a pressure exchanger energy recovery unit. The physical principles behind both technologies are the same; pressure is exchanged in accordance to Pascal's law. Mixing is prevented, or at least minimized, by controlling the interface

between solutions in this configuration through vertical solution stratification and in the PX device through plug interface displacement control.

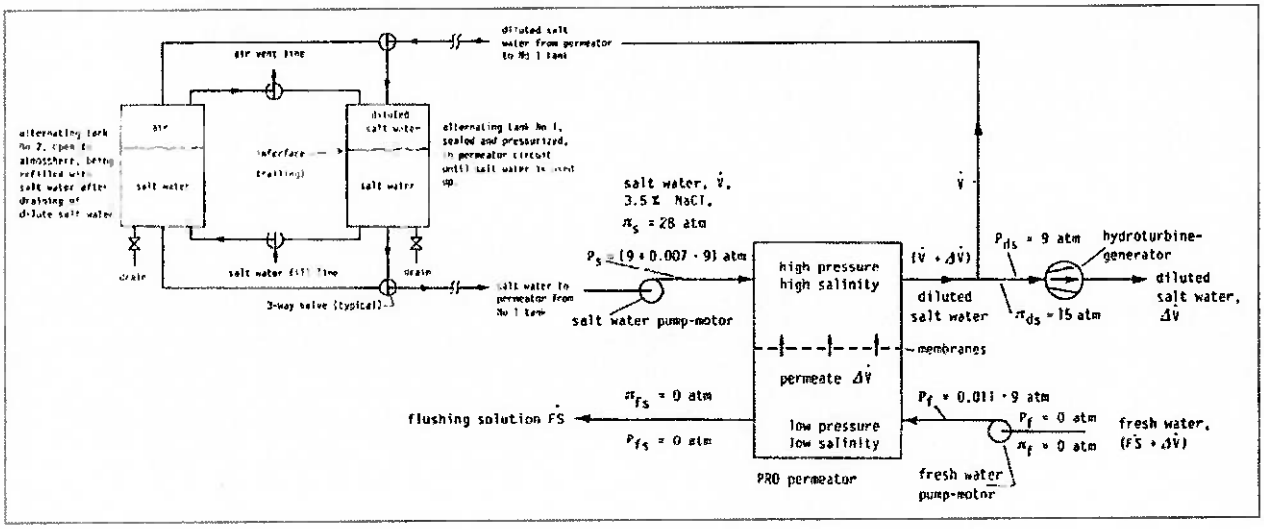

Figure 29: Alternating flow - terrestrial power plant layout, adapted from [26]

Assuming $H = 2\,\mathrm{m}$ of average tank filling, the average seawater tank head would be around $p_H = 0{,}2\,\mathrm{atm}$; seawater pumping requirements must meet this value plus frictional losses in the salt water side. Freshwater pumping requirements compensate solely the frictional losses in the freshwater side. The net power produced is:

$$net\ power = \eta_T p_s \Delta\dot{V} - \frac{0{,}007 p_s \dot{V}}{\eta_p} - \frac{0{,}011 p_s (\Delta\dot{V} + \dot{FS})}{\eta_p} - \frac{p_H \dot{V}}{\eta_p}$$

$$\eta_m = \eta_T - \frac{0{,}007}{\eta_p}\frac{\dot{V}}{\Delta\dot{V}} - \frac{0{,}011}{\eta_p}\left(1 + \frac{\dot{FS}}{\Delta\dot{V}}\right) - \frac{1}{\eta_p}\frac{p_H}{p_s}\frac{\dot{V}}{\Delta\dot{V}} = 0{,}7537$$

The mechanical efficiency calculated was only slightly higher than that obtained by Loeb et al. (1990), where $\eta_m = 0{,}7457$. As said previously, the alternating flow – terrestrial PP functions similarly to the continuous flow – terrestrial PP with PX; both configurations are more robust to variations in $\dot{V}/\Delta\dot{V}$ and $\dot{FS}/\Delta\dot{V}$ ratios and highly efficient. Nonetheless, this configuration has a disadvantage from the operational point of view which is the pressure drop that occurs when shifting from one tank to the other. A final table is presented summarizing all that has been demonstrated in this section.

Table 8: Power plant configuration analysis summary

Power Plant configuration	continuous flow terrestrial PP	continuous flow terrestrial PP + PX	continuous flow underground PP	alternating flow terrestrial PP
This study	$\eta_m = 0{,}3275$	$\eta_m = 0{,}7150$	$\eta_m = 0{,}7775$	$\eta_m = 0{,}7537$
(LOEB et al., 1990)	$\eta_m = 0{,}2854$	$\eta_m = 0{,}7040$	$\eta_m = 0{,}5960$	$\eta_m = 0{,}7457$

Results obtained in this study were always higher as a result we assuming the membrane to be ideal from the very beginning, whereas Loeb et al. (1990) assumed a more realistic model, in which a flushing solution was used to prevent salt concentration in the freshwater side and a ratio $\dot{V}/\Delta\dot{V}$ bigger than unity was employed .

Conclusions

The continuous flow – terrestrial PP configuration proved to be unfeasible with its extremely low mechanical efficiency even when an ideal membrane is considered. Other configurations proved to be over twice as much effective, however, the continuous flow – terrestrial PP + PX and the alternating flow – terrestrial PP presented greater robustness to variations in $\dot{V}/\Delta\dot{V}$ and $\dot{FS}/\Delta\dot{V}$ ratios than the continuous flow – underground PP.

For all three configurations, a common trade-off for higher efficiency is a higher capital cost. Properly assessing its value during power plant project is determinant to whether or not energy producing costs will be competitive. It is expected that terrestrial power plants have the advantage in this matter except in a few very particular sites, where natural conditions favour the underground configuration.

Finally, it was concluded that the pressure-exchanger energy recovery device and the alternating feedback pressurization in the alternating flow – terrestrial PP functioned analogously. Nevertheless, from the operational point of view the last one is in disadvantage thanks to the pressure drop that occurs during tank shifting.

C4. Pressure retarded osmosis power plant siting criteria

Salinity-gradient energy power plants harness the energy released from the mixing of fresh and saline water, a natural process that occurs all across the world wherever a river flows into the sea; not surprisingly, proximity to those water sources are the two basic criteria for siting any salinity-gradient power plant. However, the solution is not that simple; a complete three bottom-line analysis – social, environmental and economic – must be performed to properly assess the impact of placing the power plant at the chosen location. In this section we provide insight in such matters by means of an exemplification, a fictional 10 MW power plant to be placed somewhere in Sweden.

Tsiourtis (2008) published an article that gave insight in criteria and procedures for properly siting desalination plants which are taken in consideration throughout this study. According to him, the site comprised of inland and offshore parts:

(i) must be located in a place where access and interconnections to the power supply grid or independent power production and to the water supply networks are technically and economically feasible;

(ii) must be appropriate in terms of area extent and shape (size and geometry) so that the marine intake head structures, the marine pipelines, the inland pit, the seawater pumping station, the inland pipelines, the main facility structures, the post treatment system, the product delivery sub-system and the power supply system (IPP or national grid substation) are adequately accommodated and optimally located so that civil, electrical, piping interconnections and other works costs are minimized;

(iii) must be suitably located in a marine environment where adequate quantity of seawater with a reasonable good, uniform and steady quality is abstracted at a reasonable cost;

(iv) must be at a location where the backwash wastewater and other wastes are disposed without adverse environmental effects;

(v) must be geologically and topographically suitable for the construction and erection of the various structures at reasonable costs;

(vi) must meet environmental, town planning and rural planning regulations, law requirements and restrictions;

(vii) shall have social acceptance of the neighbouring communities and other authorities;

(viii) shall be located where local taxes are not prohibitive and the existing infrastructure makes project implementation easier and cheaper.

In order to evaluate all those topics during power plant siting, Tsiourtis (2008) proposed the following flow chart indicating the step-by-step procedure developed. Apart from the creation of the special committees and the use of external consulting groups to assess power plant impacts mentioned in his work, this study tries to follow these guidelines in the best way possible.

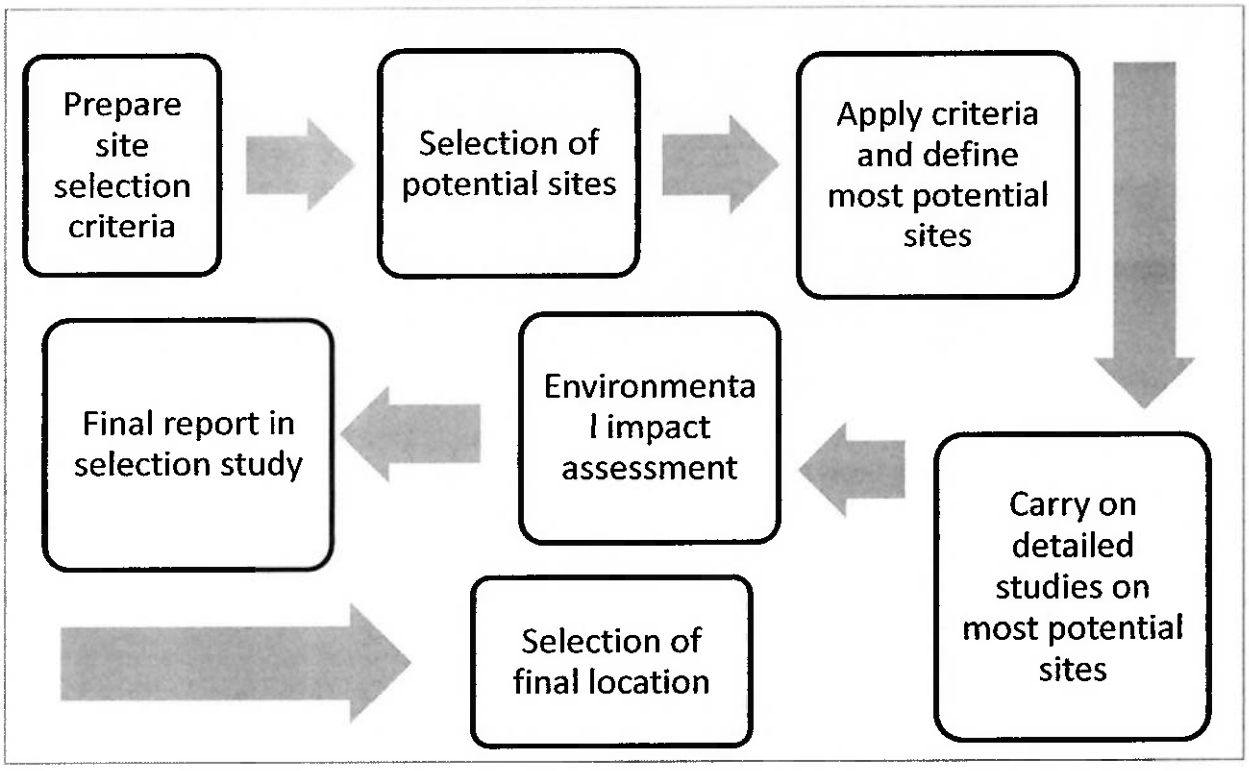

Figure 30: Diagram for desalination plant siting - also valid for PRO power plants, adapted from [32]

The two basic criteria for PRO power plant siting are proximity to high and low salinity water sources such as river estuaries; the power plant shall be placed somewhere in Sweden. Sweden is known to be very developed, placing seventh in

Human Development Index – $HDI = 0{,}963$ – and also was one of the first nations to demonstrate deep concern toward environmental issues. Sweden has been continuously proposing incentives and investments in the diversification of the energy matrix and in proper treatment of residuals, which allow us to assume that it would be open to research and investments in salinity-gradient energy technologies as other Nordic countries such as Norway and Netherlands are.

There are no infrastructural problems harsh enough to prevent PRO technology development in Swedish territory; the areas close to shore are well populated and provided with decent road transport, portuary, aeroportuary and electricity transmission services. Several eco-incentives were already put to use to promote waste recovery technologies and other renewable energy sources and it is also safe to assume that, once interest from the government is taken, similar incentives will be used to in the development of PRO technologies and their competitive insertion in the market.The Swedish coast is bathed by the Baltic Sea which, according to the Swedish Meteorological and Hydrological Institute, has much lower salinity levels than that of oceanic water due to abundant freshwater runoff from the surrounding land in addition to the shallowness of the sea itself. These natural conditions combined with the introduction of salt from the South build up a gradient of salinity along the Baltic Sea.

Near the Danish straits the salinity is close to that of the Kattegat, but still not fully oceanic, because the saltiest water that passes the straits is already mixed with considerable amounts of outflow freshwater. The salinity steadily decreases towards East and North. At the northern part of the Gulf of Bothnia the water is no longer salty and many freshwater species live in the sea. Official data states that the salinity is around $3 - 4\,psu$ in the Bothnian Bay, $5 - 6\,psu$ in the Sea of Bothnia, $6 - 9\,psu$ in the Baltic Proper and $15 - 30\,psu$ in the Skagerrak and Kattegat region.

Pressure retarded osmosis is dependent on the salinity-gradient between feed and draw solutions, thus higher concentration of salt in seawater increases the potential for producing electricity. The most saline water is vertically stratified in the water column to the north, the Skagerrak region, making it the most appropriate site for placing the power plant. There are several interesting potential sites for positioning the power plant

along the northwestern Swedish coast; their main relevant characteristics are listed in table 9.

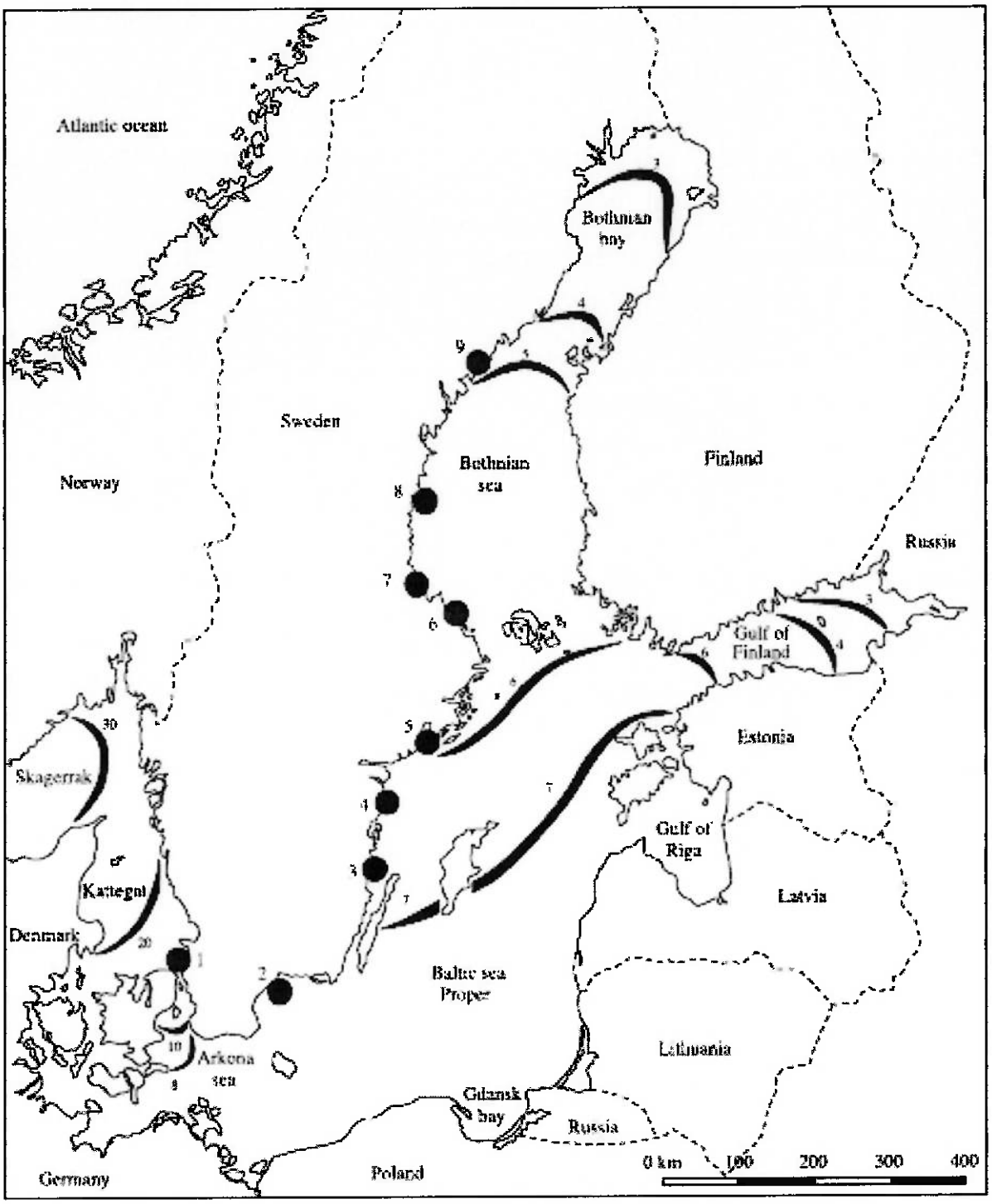

Figure 31: The Baltic Sea salinity

Table 9: Possible sites for PRO plant location along the western Swedish coast - pros and cons

	Pros	Cons
Strömsån River (Strömstad)	Nothernmost location = saltiest water	Stromsvattnet Nature Reserve - 213 hectares of protected land and water
	Small urban infrastructure nearby	Strömsån river is a migration route for salmons
	The municipality is interested in supporting new activities within its territory	Potential for salmon habitat expansion
	Portuary, railway and motorway infrastructure - 45min to closest airport (Rygge)	Oslo is the closest large city to the location (133 km)
		Second closest is Göteborg (164 km)
	Small freshwater flux of 4,5 m3/s - appropriate for a prototype	Freshwater flux not enough for an economically interesting power plant
Anråsälven River (Långö)	Small urban infrastructure nearby	No data found
Kleveån (Bovallstrand)	Small urban infrastructure nearby	No data found
Orekilsälven River (Munkedal)	Average Freshwater flux of 22 m3/s	Orekilsälven river is a migration route for salmons
	Freshwater flux enough for a small sized power plant	Salmon habitat area reached yield point, no expansion potential available
	Medium urban infrastructure nearby	
Bäveån River (Uddevalla)	Located at the bay Byfjorden	Göteborg is the closest large city to the location (89 km)
	Medium urban infrastructure nearby	Freshwater flows into a brackish water bay
	Sweden´s first EMAS (Eco Management and Audit Scheme) registered municipality	Bäveån river is a migration route for salmons. Salmon habitat area reached yield point, no expansion potential available
	Small freshwater flux of 3,4 m3/s - appropriate for a prototype	Freshwater flux not enough for an economically interesting power plant
Anråse ä River (Stora Höga)	Small urban infrastructure nearby - portuary facilities within 30 km	Anråse ä river is a migration route for salmons. Salmon habitat area reached yield point, no expansion potential available
	Small freshwater flux of 1 m3/s - appropriate for a prototype	Freshwater flux not enough for an economically interesting power plant

Nordre älv River (Municipalities along)	Railway and motorway infrastructure - airport and portuary facilities within 20-30 km	Researchers and technicians would have to commute from Göteborg to the Power Plant regularly
	Huge freshwater flux of 550 m3/s - power plant would leave the river environment nearly undisturbed	
	The municipalities are interested in supporting new activities within its territory	No riverside infrastructure, investments needed for opening roads
	Small urban structures near Göteborg (20km)	
Göta älv River (Göteborg)	Big urban infrastructure	Southernmost location of the Skagerrak sea - salinity levels are lower
	Airport, portuary, railway and motorway infrastructure	Competition with others river using activities
	Freshwater flux of 150-250 m3/s – environmental impacts are minimal	Water at Göta älv river's delta has a much higher concentration of domestic and industrial waste due to Göteborg urban activities
	Seven water quality monitoring stations along the Göta älv river	Göta älv river is a migration route for salmons. High potential for salmon habitat expansion available
	Proximity to research facilities and technical universities	Expensive pre-treatment of freshwater needed

Most of the world's rivers run into the sea at places where people have already built cities or industrial areas such as harbours, ergo, most of the potential sites for osmotic power generation can be utilised without affecting pristine areas. Moreover, plants can be constructed partly or completely underground – in the basement of an industrial building or under a park – reducing visual pollution. In these areas the environmental impacts onshore are often considered to be of minor importance. Environmental impacts will mainly be related to the building of access roads, channels, the power plant itself and connections to the electricity grid.

Nonetheless, one area where there has been some discussion is whether or not there will be negative effects on the marine environment due to the discharge of brackish water by the osmotic power plant. A local change in salinity levels could result in displacement of marine life forms such as algae or fishes that are more sensitive to it. The impact, however, will also depend on how much of the river flow is used. A quick

estimate of water requirements can be done once membrane water flux J_w and power density $\dot{w}$ are known. This study uses data from Achilli et al. (2009).

$$\Delta G = \frac{\dot{w}}{J_w} = \frac{2{,}73\ W/m^2}{2{,}81E^{-6}\ m/s} = 0{,}9715\ \frac{MJ}{m^3} = 0{,}9715\ \frac{MW}{m^3/s}$$

The ratio expressed above is a direct measure of water volume requirements per MW of electricity produced and an indirect measure of membrane efficiency. Comparing the value of ΔG for the experimental membrane to that of ΔG_{mix} of sea and fresh water in a $1:1$ proportion one finds that the average experimental energy recovery was $\eta = 0{,}5685$. For a $10\ MW$ power plant, freshwater requirements are a little over 10 m^3/s , that alone excludes several options along the northwestern Swedish coast. Among the data found only Orekilsälven, Nordre älv and Göta älv rivers have enough flux to provide the power plant with the water flow it needs.

So far all three options are feasible according to sea and fresh water requirements but environmental impacts are expected to differ a lot from location to location. Although they cannot be precisely measured at this early stage, they are expected to be proportional to the amount of water being used as previously mentioned. Over 45% of the average flux of the Orekilsälven river would be deviated into the power plant; less than 2% would be used for the Nordre älv river; and around $5-6\%$ for the Göta älv river.

Both Orekilsälven and Göta älv rivers have been pointed out as important migration routes for salmons (NASCO, 2009), and significant interferences in these habitats could certainly affect the species survival. A power plant placed along the Göta älv using only 6% of the river flow will produce minimal harm to salmon migration; on the other hand, a power plant placed along the Orekilsälven will most certainly trample with the species reproduction given that almost half of the average river flow would be used. With the remaining options left at hand, it is time to analyse the social and economic perspectives of each location at depth.

Figure 32: Locations of three best river estuaries along the Skagerrat sea

The Nordre älv is a branch of the Göta älv that is formed when it reaches the island of Hisingen. The Göta älv flows from the enormous Vänern lake with a mean average flow of $800\ m^3/s$ and an average precipitation of $910\ mm$ in its source area. At Kungälv, in the downstream part, flows the northern river branch named the Nordre älv; it carries the main flow, about 75% of the yearly total. The southern branch, still referred to as the Göta älv, carries a flow in the range of $150 - 250\ m^3/s$ over the year.

There are seven water monitoring stations along the Göta älv, of which five are upstream of the river branch (ZHAN, 2009); and none along the Nordre älv. These stations measure basic raw water parameters such as pH (acidity), conductivity (salinity), turbidity (cloudiness) and redox potential (oxygenation). The closest station to the Nordre älv estuary is the Södra Nol station located in Nol municipality, $6\ km$ away

from the river branch and around 22 km away from the estuary. Södra Nol also tests for microbial organisms' concentration, an important feature to be controlled in PRO power plants to prevent membrane fouling. The closest station to the Göta älv estuary is the Lärjeholm station, 13 km away. With zero investments it is possible to control the water quality of both rivers to have an accurate forecast of production.

Parameter	Unit	Min	Median	Max
Temperature	°C	0.5	7.1	22.5
Turbidity	FNU	2.4	4.7	40
Conductivity	mS/m	8.9	9.8	112
pH		7.0	7.2	7.5
Alkalinity	mmol/l	0.27	0.30	0.35
Ca^{+2}	mg/l	7.2	7.9	14
Mg^{+2}	mg/l	1.6	1.8	20
Total Fe	mg/l	0.08	0.17	1.8
Total Mn	mg/l	0.004	0.008	0.042
NH_4^+-N	µg/l	<50	<50	50
PO_4-P	µg/l	<4	<4	8
Colour	mg/l Pt	15	20	100
Extinction 254 nm	ae/cm	0.100	0.113	0.277
TOC	mg/l	4.1	4.6	5.5
Coliforms	CFU/100ml	36	350	6500
Thermoresistant coliforms	CFU/100ml	<10	100	1300
E.coli	CFU/100ml	5	86	1300

Figure 33: Water monitoring stations along the Göta älv and test results from Lärjeholm station [33, 34]

The Nordre älv estuary is only 14 km away from Göteborg whereas the Göta älv runs through the city, the second largest of Sweden. When it comes to siting the power plant, being close to a huge urban centre is more advantageous than being in the urban centre itself. The first advantage is that competition for terrains along the Göta älv in Göteborg is much more aggressive than along the Nordre älv, making prices considerably higher. Another one is that the PRO plant should be positioned close to the delta of the river; therefore it could interfere with many other river using activities.

Göteborg has two universities: The University of Göteborg, one of the largest universities in Scandinavia, and Chalmers University of Technology, a well known university. Qualified workers, researchers and technicians are available from both universities to participate in all phases of plant project and operation. Furthermore, as it happens to many metropolitan centres, Göteborg is supporting activities within its

peripheral zone to prevent infrastructural problems and help city planning. Moreover, the municipalities along the Nordre are interested in expanding their economic bounds towards industrialization by diversifying their industry profile, and energy provision plays a key role in this issue. Having a regular traffic of people between both cities can be favourable to the tourism industry as well, by making the city known, improving transportation, etcetera.

Finally, the concentrations of domestic and industrial waste in Göta älv's water are much higher than those from the Nordre älv, given the size of Göteborg urban centre. In order to guarantee a reliable membrane performance with longer life-time, expensive pre-treatment of Göta's water are required. That adds not only to PRO power plant capital cost but also to the cost of operation and maintenance and, consequently, to the cost of electricity produced. Hence, the best place to produce electricity from PRO process taking into account techno-economic, environmental and socio-political restraints is in the Nordre älv river estuary.

To decide the exact location along the Nordre älv where to site the Power Plant it is important to consider how long the piping system that supplies water to the power plant will be. It can be kilometres long to secure the desired salinity levels, especially in rivers where salinity intrusion is enhanced by the terrain. Salinity intrusion is the gradient in water salinity that presents itself at the encounter of river and seas. A natural force opposing the generated salinity-gradient acts on dissolved salts to move upstream. Since salted water is denser, the intrusion occurs at the bottom of the river.

Salinity intrusion is known to reach long distances upstream, for instance, $11\ km$ in the Tanshui River in Taiwan (LIU et al., 2001); $20\ km$ in the Red River in Vietnam (CA, 1996); and $7\ km$ upstream in the Göta älv (SELMER; RYDBERG, 1993). It depends on complex mass transport models but have as basic parameters the river's cross-section, width and discharge; the salt concentration gradient and dispersion coefficients. Simplifying, salinity intrusion rises with increased salt concentration gradient and drops with bigger discharges and shallower waterflows. The results obtained from the mass transport and fluid-dynamics model of salinity intrusion for the Nordre älv river would then be displayed in graphs such as figure 34 (SELMER; RYDBERG, 1993).

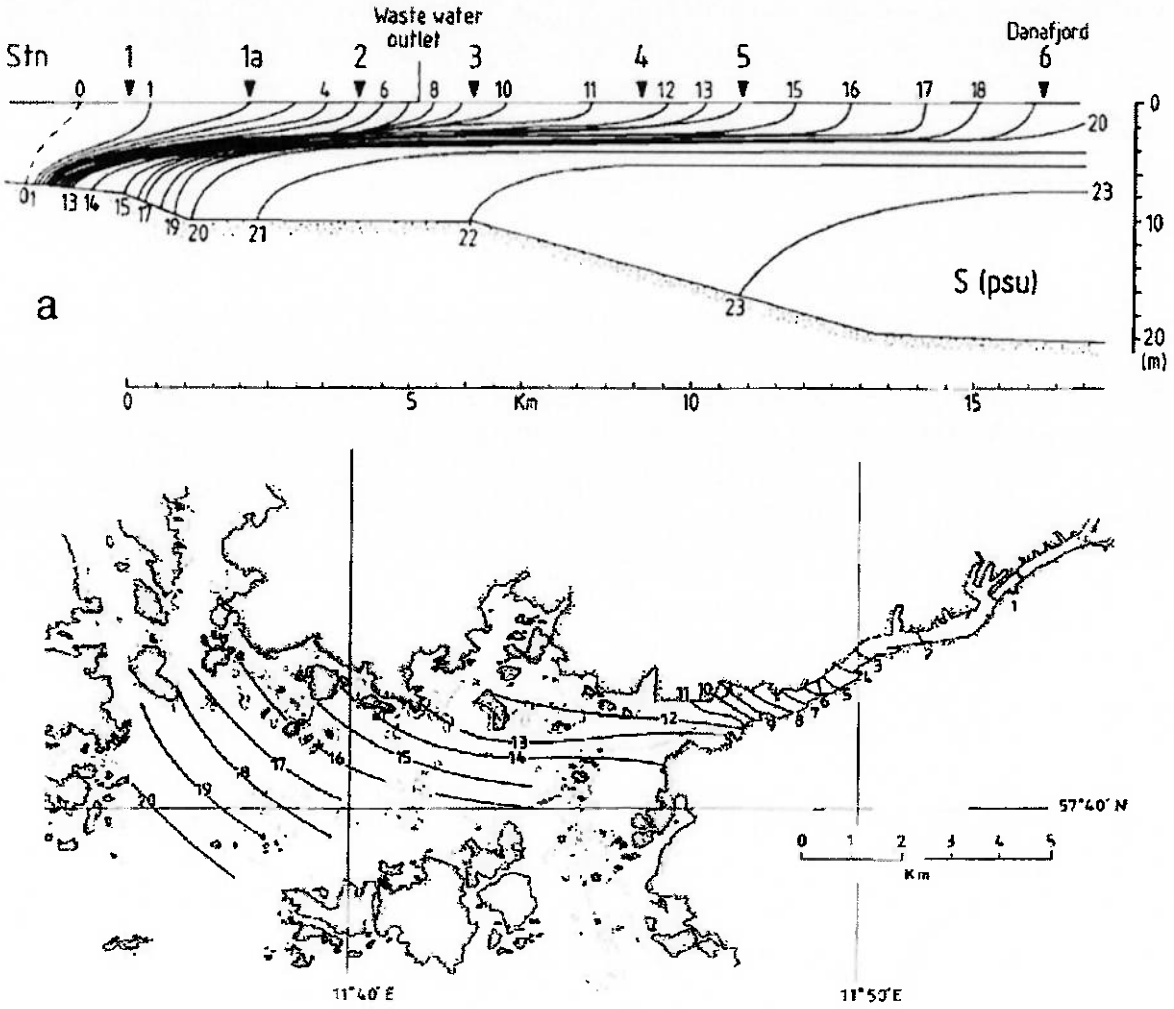

Figure 34: Results from salinity intrusion simulation in the Göta älv [37]

As previously mentioned, for PRO processes the effects of increasing feed water salinity are much more severe than those of reducing salinity at the draw water side, which is why river water provision must be prioritized. As a consequence, PRO power plant positioning is done regarding the worst case of salinity intrusion – minimal discharge – rather than the average case. In this study, since salinity intrusion simulation results for the Nordre älv could not be found, salinity levels were considered from speculation, based on the bathymetry and surface salinity levels (DHI, 2005).

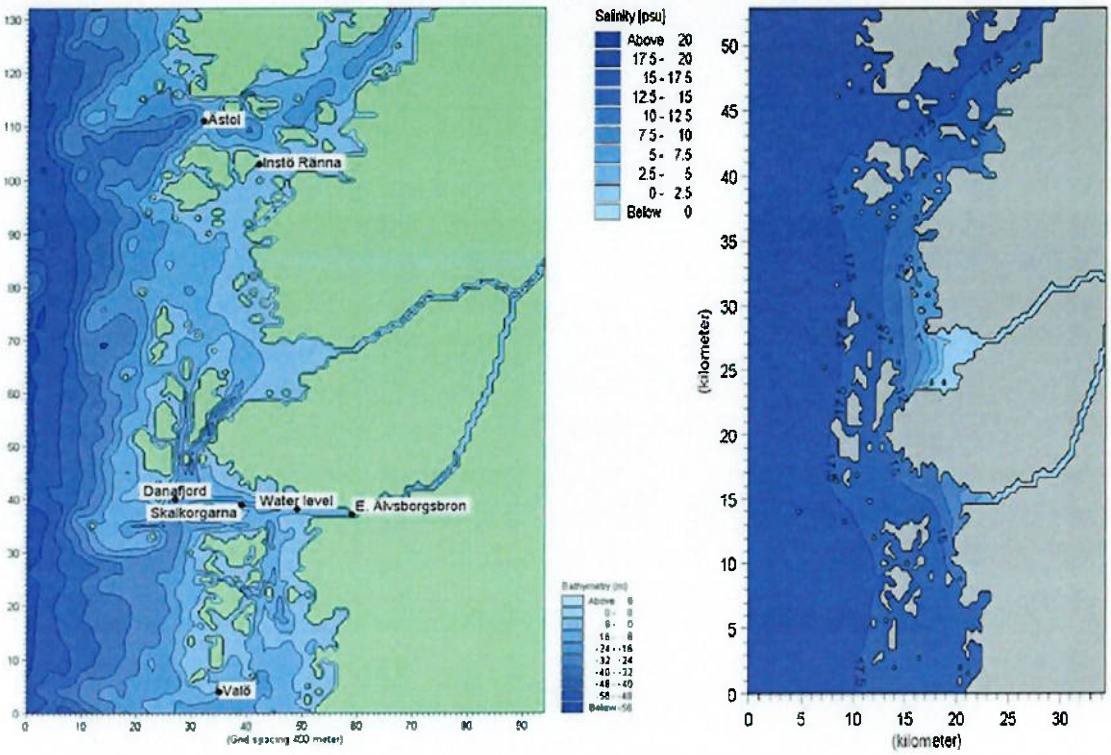

Figure 35: Surface salinity and bathymetry measurements in the Nordre älv estuary [38]

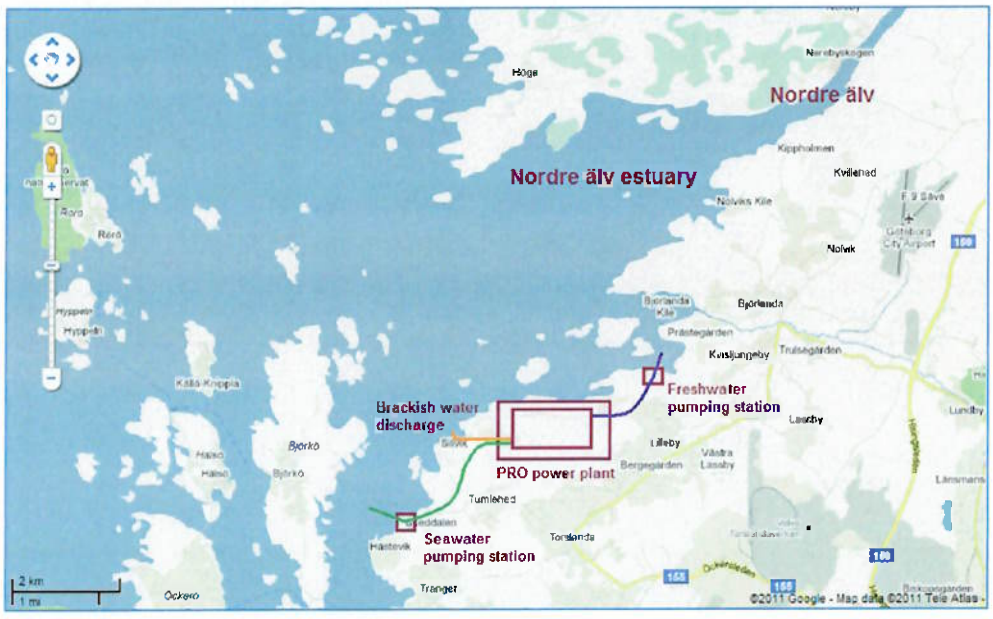

Figure 36: Exact location for PRO power plant

After collecting these data it is finally possible to place the power plant. The exact location is shown in detail in figure 36. We took advantage of the deeper waters around Björkö and Öckerö island to reach saltier levels in a location still close to the shore.

Seawater will be drained from a depth of $30\,m$ guaranteeing adequate salinity and pollution levels; a pumping station is positioned as close as possible from the Björkö isle. Freshwater will be taken from shallower waters, this time we take advantage of the natural freshwater flow at bay pushing salt intrusion further away from the coast to secure the water's quality. The resulting brackish water is discharged at a point with matching salt concentration, minimizing environmental problems.

A schematic representation of a desalination plant is provided by Tsiourtis (2008): it divides the plant into several sub-sectors each with its own desired characteristics and functions. The layout can be easily adapted to PRO power plants and, more specifically, to our hypothetic $10\,MW$ pilot plant. Sub-site A represents the land where the main components of the PRO facility shall be placed; they are also represented in red in the figure with the exact power plant location, marked by PRO power plant tag. The other subsites regard to the structures needed for water provision and disposal which are also represented in figure 36.

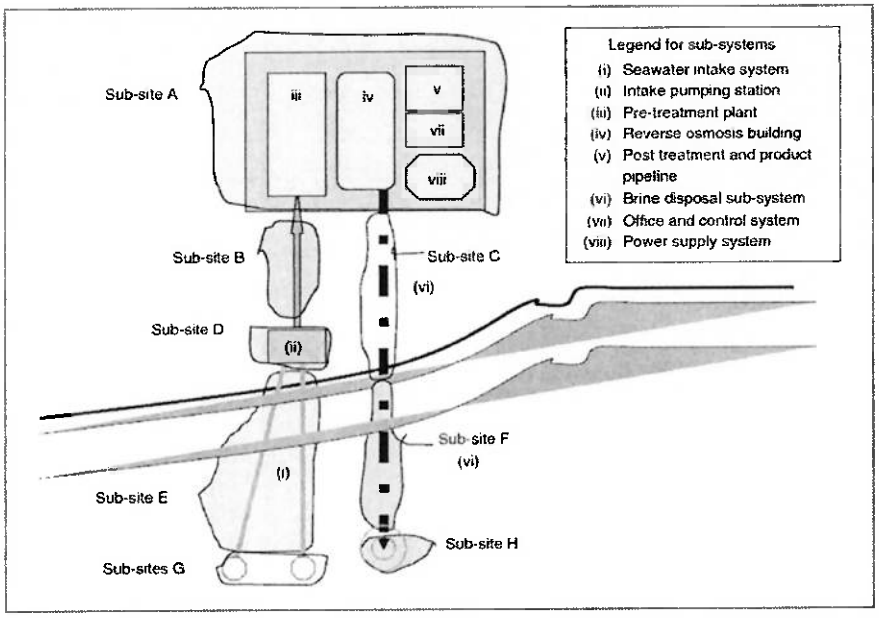

Figure 37: Desalination plant sub-site division - applicable to PRO power plants [32]

Dividing the power plant in sub-sites is very important to the assessment presented in the next chapter, where the hypothetical PRO facility have its most essential components – its primary equipment – sized and thoughtfully considered. For

example, at feed and draw solution intake mouths, pre-treatment technologies play an important role in extending membrane life and reducing operational costs; losses in external pipelines can sum up to unacceptable values if not correctly sized; pumping stations and pipelines construction and operation can significantly alter the environmental impacts of the plant.

C5. Guideline to pressure retarded osmosis power plant design

In the chapter 4 a proper site to a $10\,MW$ PRO power plant was found in the Nordre älv river estuary. Having at hand data regarding freshwater quality, seawater salinity levels and membrane performance; it is now possible to present a preliminary plant design. An important feature of osmotic processes plants is modularity: components are designed to run in parallel with smaller fluxes rather than having a few, plant-customized elements running the whole process. Modular design has at least two big advantages: increased power plant reliability and decreased component cost due to scale production.

Out of the four power plant configurations studied in chapter 3, the **continuous flow – terrestrial PP with PX** was chosen. This configuration presented high efficiency, robustness to membrane performance regulation – $\dot{V}/\Delta\dot{V}$ and $\dot{F}S/\Delta\dot{V}$ ratios – and potentially lower capital costs than the other highly-efficient configurations available. The design will consider a net $1\,MW$ power plant and then will be scaled-up to the actual capacity, the membranes used in the study are those found in Achilli et al. (2009).

Achilli et al. (2009) do not provide us with information regarding the ratios $\dot{V}/\Delta\dot{V}$ and $\dot{F}S/\Delta\dot{V}$ used in their studies, instead, the values proposed by Loeb et al. (1990) will be used. The internal piping friction loss coefficients considered are those from Honda (1989) apud Loeb et al. (1990); all of them were already exposed in chapter 3. External piping friction losses will be determined along with pipeline sizing, but it is anticipated to the reader that proper diameter selection can drastically reduce this source of parasitic loss. A table with all assumptions considered so far and a schematic of the power plant configuration are displayed.

Table 10: Assumptions for PRO power plant sizing

	Assumptions
(ZERO)	Freshwater hydraulic pressure (p_f) and osmotic pressure ($\pi_{F,b}$) are both assumed to be zero gauge. Salt water is pumped from a depth of $30\,m$ into the power plant; no additional pumping requirements apart from frictional pressure drop in external pipes are added. Membrane performance parameters are all taken from Achilli et al. (2009)

(A)	The concentrated and diluted solutions entering the permeator will be salt water and freshwater respectively. The salt water enters the permeator at a rate $\dot{V}$ and an osmotic pressure of $28\ atm$.
(B)	The ratio $\dot{V}/\Delta\dot{V}$ is $1{,}08$. This ratio represents a mixture of freshwater and salt water leaving the permeator at a rate $(\dot{V}+\Delta\dot{V})$.
(C)	The pressure change through the hydroturbine will be from p_s to $0\ atms$ in each scheme. As a corollary to this requirement the approximate hydraulic pressure p_s on the salt water side of the PRO permeator will be $9{,}7\ atm$, a value appropriate for $\dot{V}/\Delta\dot{V} = 1{,}08$. The maximum available power is: $p_s\Delta\dot{V}$.
(D)	The internal piping frictional pressure drop across the salt water side of the PRO permeator will be $0{,}007p_s$.
(E)	The internal piping frictional pressure drop across the freshwater side of the PRO permeator will be $0{,}011p_s$.
(F)	The freshwater entering the low pressure side of the permeator is assumed to have some salt in it. To prevent the freshwater solution being concentrated to high osmotic pressure due to $\Delta\dot{V}$, a flushing solution leaves the low pressure side of the permeator at a rate $\dot{FS}$. The freshwater enters the permeator at a rate $(\dot{FS}+\Delta\dot{V})$ so as to satisfy mass conservation requirements
(G)	The ratio $\dot{FS}/\Delta\dot{V}$ is $0{,}39$. This is high enough to prevent a significant and undesirable osmotic pressure in the flushing solution stream, but low enough to prevent excessive pumping power requirements for $\dot{FS}$.
(H)	The turbine generator, freshwater pump-motor, the seawater pump-motor and the flushing solution pump-motor pairs all have efficiencies of 85%. The PX unit efficiency is 97%.
(I)	Initially, external piping frictional losses were estimated supposing constant $\Delta\mathrm{p/m} = 2$; from the pressure loss diagram one can notice that this is a reasonable value. Sea and fresh water external pipelines are approximately $\mathrm{L_D} = 2{,}5$ and $L_F = 1{,}5\ km$ long – check power plant exact location and water provision spots in chapter 4.

5.1 Total membrane area and main flows

PRO power plant sizing starts with calculating the membrane area required for electricity production, taken from gross power conditions. Plant mechanical efficiency can be estimated for each configuration according with the equations elaborated in chapter 3, however, they must be corrected to account external piping pressure losses as predicted from assumption (I). Under these conditions, we have:

$$\eta_m = \eta_T - \frac{1}{\eta_p}\left(1 - \frac{p_{PX}}{p_s}\right)\frac{\dot{V}}{\Delta\dot{V}} - \frac{0{,}007}{\eta_p}\frac{\dot{V}}{\Delta\dot{V}} - \frac{0{,}011}{\eta_p}\left(1 + \frac{\dot{FS}}{\Delta\dot{V}}\right) - \frac{\frac{\Delta p}{m} L_D}{\eta_p p_s}\frac{\dot{V}}{\Delta\dot{V}}$$

$$- \frac{\frac{\Delta p}{m} L_F}{\eta_p p_s}\left(1 + \frac{\dot{FS}}{\Delta\dot{V}}\right)$$

$$\eta_m = 0{,}78317 = \frac{net\ power}{gross\ power} = \frac{P_{net}}{P_{gross}}$$

$$P_{gross} = 1{,}27685\ MW = S\dot{w}$$

$$S = 467\,712\ m^2 \qquad and \qquad \begin{bmatrix} \Delta\dot{V} = 1{,}3142\ \frac{m^3}{s} = 4731{,}2\ \frac{m^3}{h} \\ \dot{V} = 1{,}4194\ \frac{m^3}{s} = 5109{,}8\ \frac{m^3}{h} \\ \dot{FS} = 0{,}5125\ \frac{m^3}{s} = 1845{,}0\ \frac{m^3}{h} \end{bmatrix}$$

5.2 Membrane and PX units arrangements

A common membrane arrangement found is the use of the spiral wound configuration loaded in groups of five into a pressure vessel, each membrane having a length of $1{,}55\ m$, diameter of $45\ cm$ and membrane area of $S_m = 90\ m^2$. A rack is then assembled and two configurations are possible: 5 vessels – 25 membranes vertically positioned or 25 vessels – 175 membranes array; the array with 175 vessels was chosen for its $8m\ x\ 2{,}7\ m$ compact footprint. The number of membrane racks for a $1\ MW$ power plant would be:

$$no._m = \frac{S}{175\ S_m} \approx 30\ \left[\frac{racks}{MW}\right]$$

With the volume of salt water necessary for a $1\ MW$ module, it is possible to calculate the number of PX units. The PX is said to have its highest efficiency when operating at higher water fluxes and a single unit flow is only a small fraction of the total

mass flow requirement. The unit with best compatibility is the PX-300, which has a maximum allowable flow of $68\ m^3/h$, produced by Energy Recovery Inc.

$$no._{PX} = \frac{\dot{V}}{\dot{V}_{PX,max}} = \frac{5109{,}2}{68} = 75{,}13 \approx 78\ \left[\frac{PX\ units}{MW}\right]$$

$$\dot{V}_{PX} = 65{,}5\ \frac{m^3}{h}$$

$$p_{PX} = p_s \eta_{PX} = 9.409\ atm$$

5.3 Turbine and power equipment configuration

To increase power plant reliability, three turbine - generator pairs of $5\ MW$ nominal will be used. Under normal conditions they will work with 80% load; during alternating maintenance periods two of them will work very close to overload; nonetheless, nominal overload condition can be sustained through the short maintenance period without harm to equipment. This way the power plant can provide net $10\ MW$ of electricity non-stop.

Regarding which turbine configuration would be most adequate for PRO processes, an extensive argumentation is possible, particularly when the power plant capacities are lower and, consequently, so are water flow rates. Unless the project is planned to work with draw solutions of higher salinity than that of seawater – brine for example – the net pressure head produced will not be over $120\ m$; for high flow rates the most reasonable choice would be a Francis turbine, however, under conditions of medium pressure head and lower flow rates both Pelton and Francis turbine configurations are feasible – see figure (RUBBO, 1967).

Figure 40 shows turbine efficiency as a function percentual load, for the nominal load conditions specified the Francis configuration presents better performance. However, according to the same author, there are factors other than efficiency to ponder when choosing between Pelton and Francis configurations: elements subject to wear, disassembly time, maintenance time, plant operational costs and investment costs.

Overall, Pelton turbines are more likely to be exposed to wear due to the fact that it increases with increasing water velocity; Francis turbines have longer maintenance periods and are more difficult disassemble but these operations are not as frequently required as they are for a Pelton. Finally, investment costs for Francis turbines are usually lower given their higher rotational speeds and reduced weight, although replacement costs are higher.

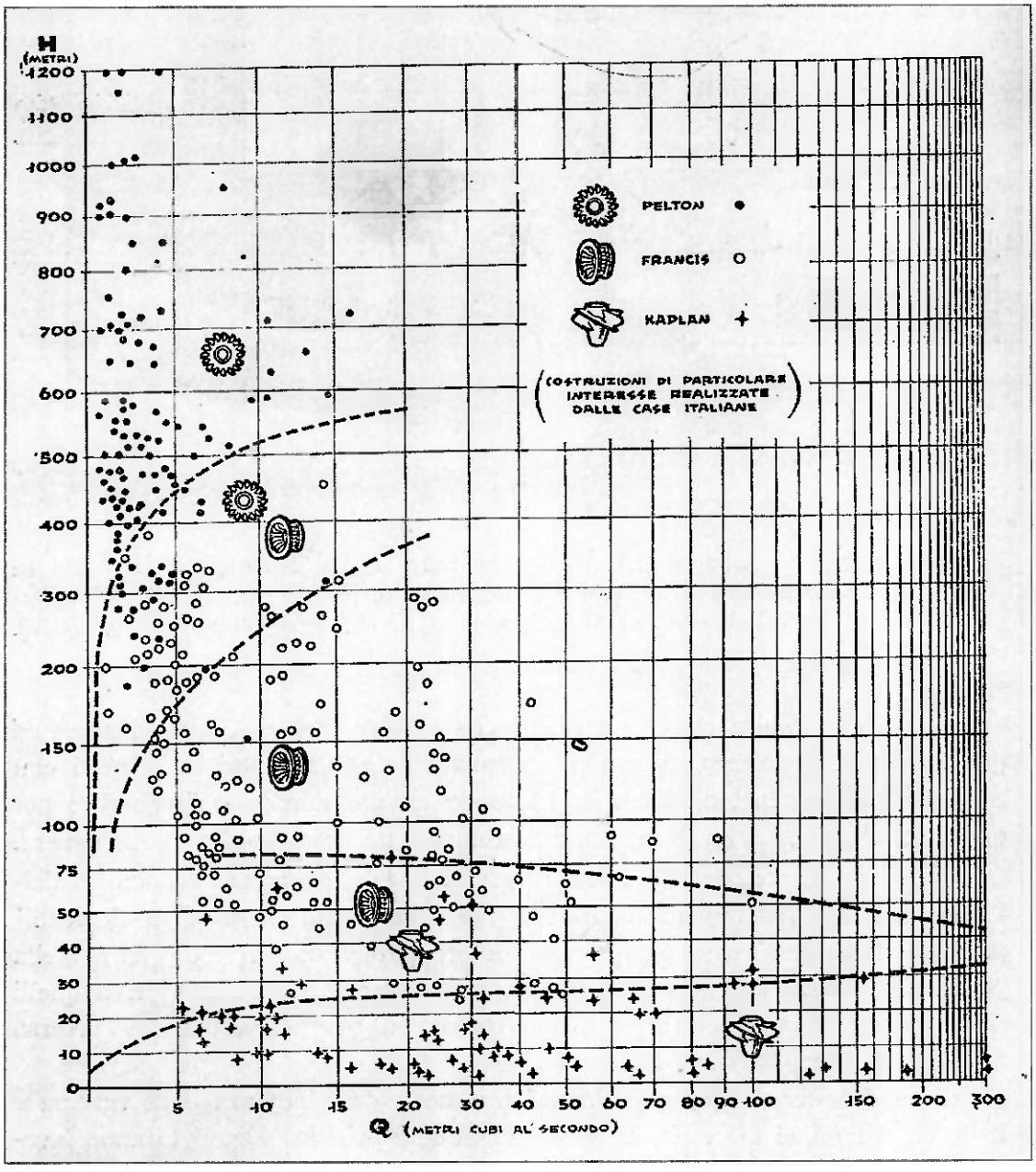

Figure 38: Division in all three characteristic parameters of the most important Italian turbines [41]

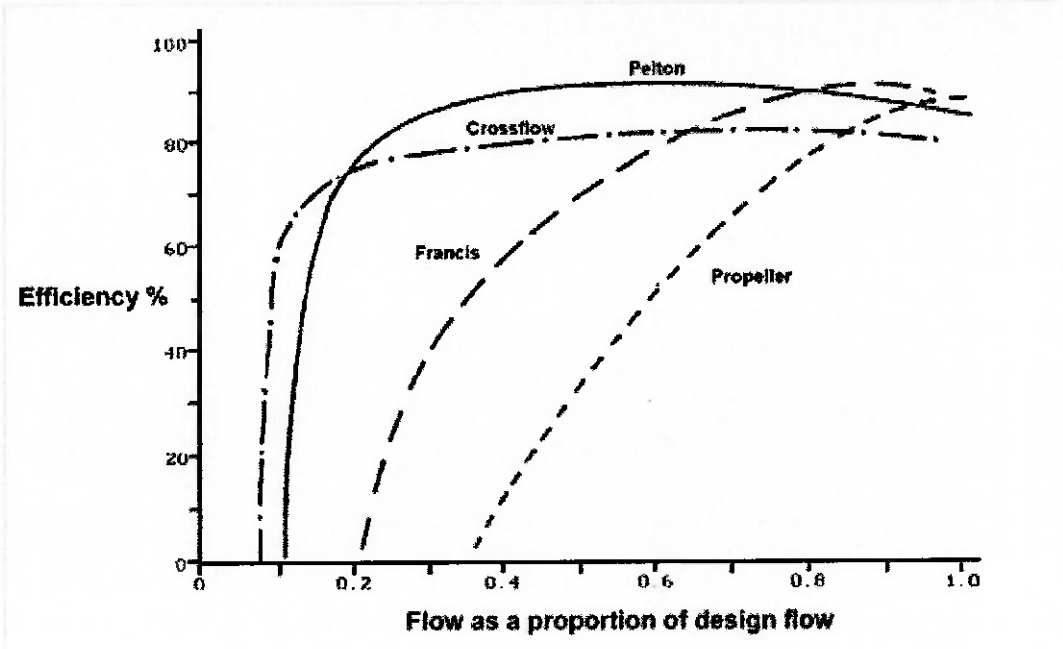

Figure 39: Efficiency as a function of load for different turbine configurations [40]

The conclusion is that the Francis configuration is progressively invading the operational field of Pelton turbines and are more suitable for medium-to-high power PRO processes. Sinchronous generators are connected to each of the 5 MW Francis turbines and to the electric grid. They are expected to work at rotational speeds of $1000\ rpm - 50\ Hz$.

5.4 External pipelines and pumping stations

The external pipeline was initially sized in assumption (I) with a constant pressure loss in Pa per meter of $\Delta p/m = 2$ and accounted for 1% reduction in power plant mechanical efficiency, which is an acceptable value. Freshwater intake for the whole $10\ MW$ power plant is around $65\,760\ m^3/h$ while that of seawater is $51\,090\ m^3/h$. If these flows were to be transported through a single pipeline the resulting pipe diameter would have to be very large, furthermore, having a single pipeline could compromise the power plant reliability and functioning. Thus, two pipelines will be used to transport the solutions into the plant.

In order to reduce pipe diameters without decreasing plant mechanical efficiency, a constant $\Delta p/m = 1$ was chosen this time. The pipelines will normally carry only half of the flows mentioned above $25\,545\,m^3/h$ and $32\,880\,m^3/h$; diameters of $1000\,mm$ for seawater and $1100\,mm$ for freshwater were employed. In case of rupture of one of the lines, the remaining one will transport the whole flow while repair is still in progress. Pressure losses in the overloaded line are expected to raise threefold, nevertheless, without causing significant drop in mechanical efficiency.

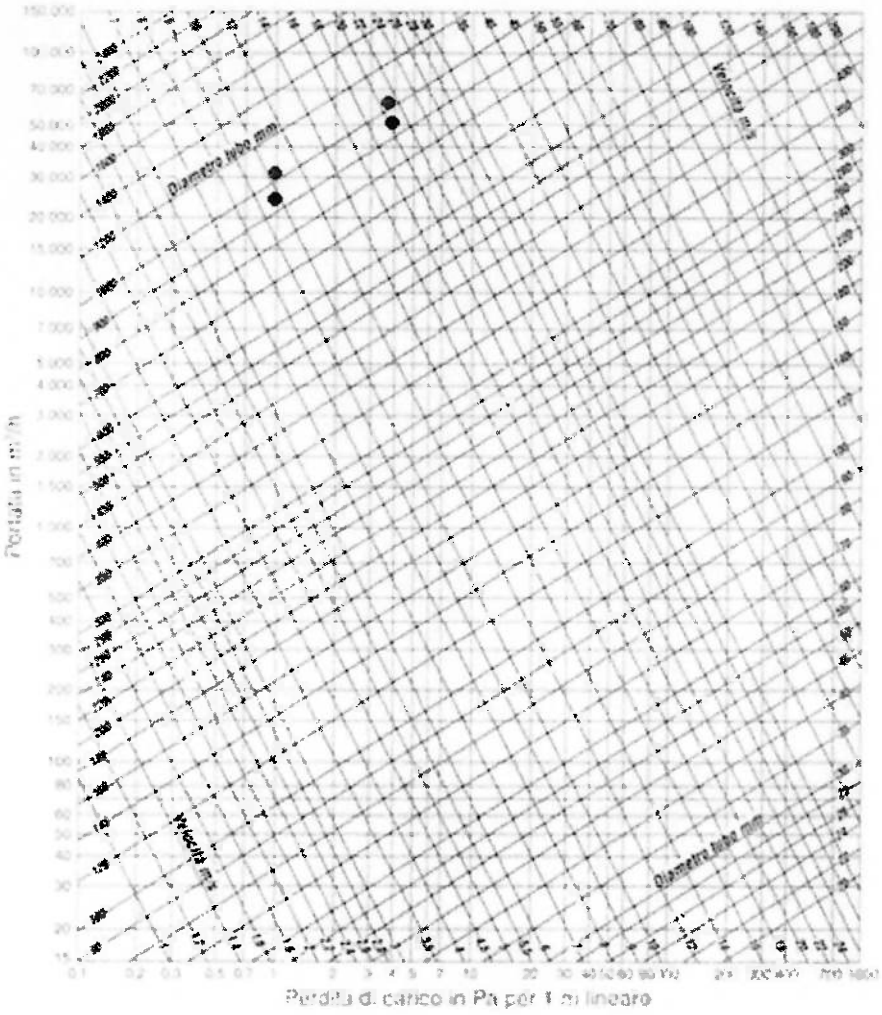

Figure 40: Diagram for pressure losses in pipelines

To make this single pipeline operation possible, three pumps will be used for each solution intake. They are sized to uphold half of the total flow each, the third one operating only when maintenace or repair activities are ongoing. Pumping requirements on the feed solution side are only to compensate pressure losses, both internal and

external. On the draw solution side, apart from losses in pipeline the pump must compensate the small pressure difference left, which the PX unit could not provide.

Pressure head (ΔH_p) and flow ($\dot{V}_p$) determines the operation conditons for the pumping system and serves as criteria for pump configuration selection. These quantities are calculated for both draw and feed solution systems:

$$\Delta H_{p,D} = \frac{\eta_p P_{p,D}}{\rho_D g \dot{V}_{p,D}} = \frac{\eta_p \dot{V}_{p,D}\left[\frac{1}{\eta_p}(p_s - p_{PX}) + \frac{0{,}007 p_s}{\eta_p} + \frac{\frac{\Delta p}{m} L_D}{\eta_p}\right]}{\rho_D g \dot{V}_{p,D}} \cong 4{,}065\ m$$

$$\Delta H_{p,F} = \frac{\eta_p P_{p,F}}{\rho_F g \dot{V}_{p,D}} = \frac{\eta_p \dot{V}_{p,F}\left[\frac{0{,}011 p_s}{\eta_p} + \frac{\frac{\Delta p}{m} L_F}{\eta_p}\right]}{\rho_F g \dot{V}_{p,D}} \cong 1{,}400\ m$$

$$\dot{V}_{p,D} = \frac{10\dot{V}}{2} = 7{,}097\ \frac{m^3}{s}$$

$$\dot{V}_{p,F} = \frac{10(\Delta\dot{V} + \dot{F}S)}{2} = 9{,}134\ \frac{m^3}{s}$$

Given that pressure head demand is modest whereas flow demand is high, the most suitable pump configuration is the axial type. For seawater, a submersible station was predicted to be placed as close to the water intake as possible, at a depth of around $30\ m$. Seawater is pumped to surface but, since it is already pressurized at intake, losses in the process are only of viscous nature. If we were to maintain the pressure level it had at that depth – $3\ atm$, there would be a further $30\ m$ head pressure pumping expense but in return a smaller flow of pressurized brackish solution would have to be deviated into the PX unit for energy recovery. However interesting this option seems to be, as the PX unit is much more efficient than the pump-motor pair, the resulting mechanical efficiency is lower than that of our configuration.

5.5 Storage tanks, pre-treatment and intake techniques

In Statkraft's prototype two storage tanks were put to use to secure water provision to the power plant so that it could operate continuously. This was necessary because the power plant relies on a very small stream to provide with sufficient water for its processes and, inasmuch as the stream flow seasonally changes, it was mandatory to have water stocked along the year to, afterwards, be used in dry periods. However, for a full-sized power plant this is impracticable; the amount of water to be stocked would be so high that the water storage system would prohibitively increase power plant investment cost.

Nevertheless, tanks are used during water pre-treatment processes but in a much smaller scale and not with the purpose of storing water for long periods. Tank size depends on how fast can the pre-treatment process be run and, ideally, it is done so that tank level do not rise nor fall abruptly and is kept almost constant. For water pre-treatment, there are many kinds of separation processes to be reviewed: screening, settling, decanting, centrifugation, filtration, hydro-cyclone, flotation, elutriation, flocculation, biological treatment. Most technologies were excluded for being overly expensive, having low fluxes and/or high residence times, demanding bigger storage tanks to function. Screening and filtration present themselves as the most cost effective options (POST, 2009), filtration being executed either mechanically or by river/sea bank techniques.

Peters and Pinto' (2008) compared the performances of different seawater bank intake techniques for RO plants, some of them adaptable for PRO processes: indirect intake with beach wells, indirect intake with seabed filtration based on buried pipes and indirect intake with Horizontal Drilled Drains HDD-based Neodren technology. All these indirect methods function by filtering seawater prior to its pumping into the power plant. Figures 42 and 43, from Peters and Pinto' (2008), illustrate how these technologies could be executed. At the depth in which seawater is being extracted $-30\,m$ – pollution levels are already expected to be lower, therefore any of the techniques mentioned could be employed.

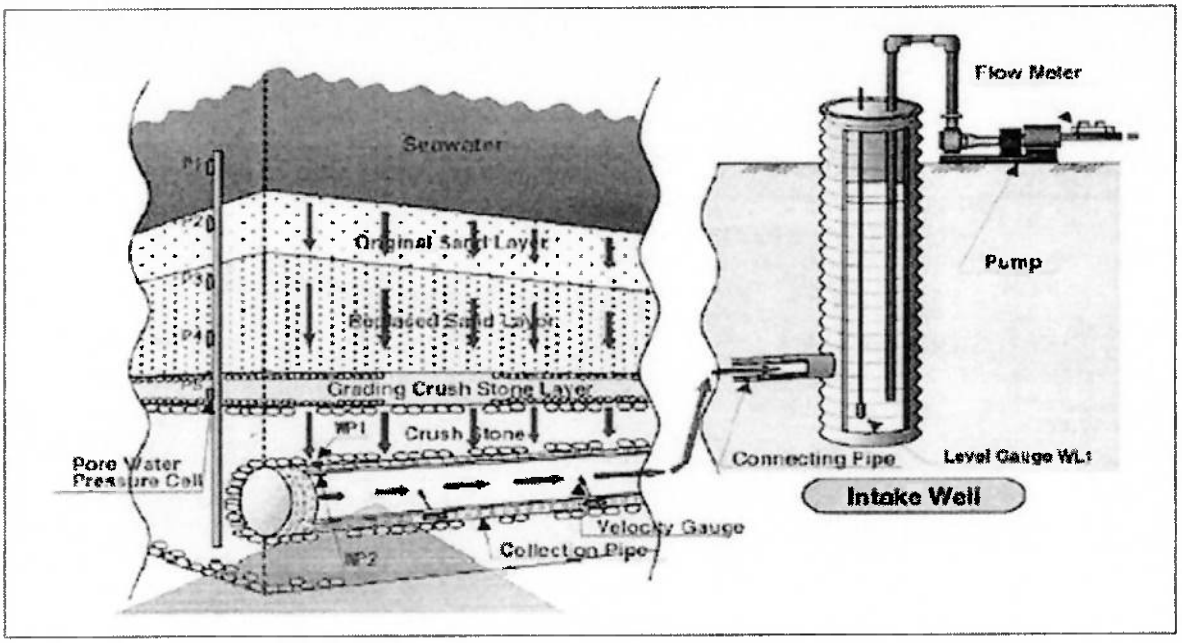

Figure 41: Cross-section of seabed intake system based on a filter bed [43]

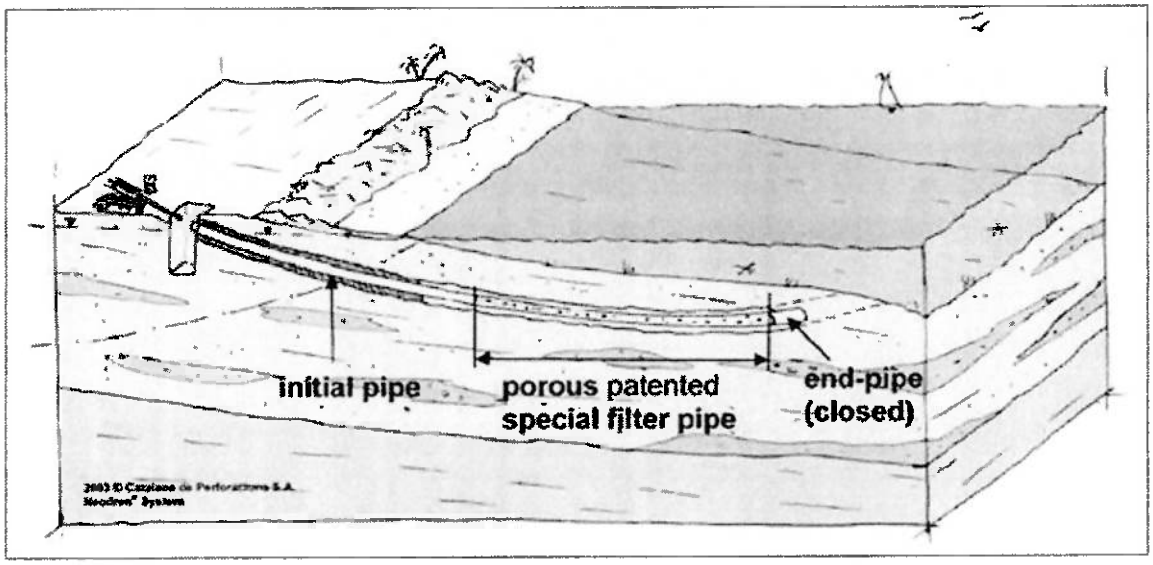

Figure 42: Schematic of the drains of the Neodren system [43]

Environmental and economic impacts shall then be used as criteria to which technology employ; the Neodren system is costly but environment-friendly, the beach well system has mild environmental impacts and costs, and the buried pipe seabed filtration has high costs and significant environmental impacts, especially during construction. The beach well intake system was chosen for being the most known of the

three methods, having no marine impacts during operation and using technologies that are fully developed and open to public.

Freshwater pre-treatment must be thought with special care, the membrane is more susceptible to fouling on the feed water side where it is more porous and permeable to fouling substances. Membrane fouling depends on the combined effects of chemical and hydrodynamic interactions, as already agreed by many authors. Post (2009) mentioned several potential sources of RED membrane fouling; most of them also presenting treat to PRO processes. They are: particles that may cause clogging, inorganic matter that may cause scale formation, organic matter that may adsorb to the membrane surface and biodegradable substances that may be used as feed for microorganisms in the vessel in order to grow a biofilm.

At intake, a screen is used to prevent floating coat waste and other macroscopic matter from entering the pipeline. Subsequently, the water passes through rotating drum filters which are known to obtain good results in RED processes from Post (2009). Biofilm formation cannot be prevented by filtration, but several studies showed that nutrient control by biological filtration can be effective to reduce the effects of biofouling.

Actions to be taken regarding membrane fouling control are either corrective or preventive. The most common corrective action is cleaning the membranes; the second most common is membrane substitution. To clean the membranes and restore the process performance, the biomass has to be physically removed generally by a two step cleaning strategy: weakening the biofilm matrix using chemicals – oxidants, enzymes, etc. – and then removing it using mechanical forces.

The chemicals commonly used are sodium hydroxide, sodium hypochlorite, peroxide and peroxyacetic acid. According to Bates (2008), the following properties define an ideal biocide for osmotic processes: does not damage the membrane; controls and kills all strains of bacteria and biofilms; physically breaks up existing biofilms; is compatible with all system components; is non-toxic and easy to handle; is easily disposed of and bio-degradable; is easily monitored and injected; is disinfectant and inexpensive. Eventually, even with all precautions and corrective actions taken, the membrane will lose its effectiveness and membrane substitution will take place. For well operated power plants membrane substitution is carried out each $3 - 7\ years$ and plays

a major role in plant operational and maintenance (O&M) costs, as will be shown in chapter 6.

Fouling preventive actions were developed from studies such as Bates (2008), which made evident the hydrodynamic dependence of membrane fouling to the rate of permeate flux, cross flow velocity and system idleness. According to him, fouling increases with increased permeate flow rate, decreased cross flow velocities and increased idleness. For the permeating flow, higher fluxes means higher drag forces perpendicular to the membrane surface, which benefit particle deposit. For the cross flow, higher velocity equals higher shearing actions parallel to the membrane surface, which flush away deposited matter.

When the system is idle and no water is flowing, the fouling rate can increase dramatically and provides insight on how start-up and shutdown operations should be carried on: with pre and post-operational solution flushing. Post (2009) concluded that a periodical feed water reversal in a RED system would have a potential retarding effect on the biofilm formation; another measure found to constrain the effects of fouling was the cross flow reversal. For PRO systems, feed water reversal is impracticable due to membrane asymmetry, the reversal process would cause permanent damage to the membrane (SOURIRAJAN, 1970); cross flow reversal is otherwise very possible, with only a few plant adaptations to perform. Organic matter is known to accumulate closer to the water intakes so that intermittently reversing cross flow would wash away previously deposited fouling substances.

To prevent high investment costs tanks are sized to provide the power plant with sufficient flow to maintain membrane qualities for ten hours, a period long enough so that repairs in water intake sub-systems are done. This maintenance flushing flow was estimated at 10% nominal permeating flux capacity, resulting in storage volumes of around $48\,000\,m^3$ for both feed and draw solutions; it was decided to use 4 tanks for each solution. Freshwater tanks are connected to 35 drum filters each, sized to provide altogether the total freshwater requirement of $65750\,m^3/h$.

5.6 Summary

A table is presented summarizing all information presented in this chapter. Data such as number of components and element operational point specifications are provided and will be used in the following chapter to estimate plant Primary Equipment Cost (PEC), total project cost and electricity production cost in $\$/kW$.

Table 11: PRO power plant equipment summary table

Membrane elements Achilli et al. (2009)	no. = 52500
	area = $90\ m^2$
	$J_w = 2{,}81E^{-6}\ m/s$
	$\dot{w} = 2{,}73\ W/m^2$
	$\eta = 0{,}5580$
Tubular vessels	no. = 7500
Racks	no. = 300
	footprint = $8\ x\ 2{,}7\ m$
	space between racks = $1{,}5\ m$
PX units	model: PX-300
	no. = 780
	High salinity inlet pressure = $9{,}7\ atm$
	High salinity outlet pressure = $0\ atm$
	Low salinity inlet pressure = $0\ atm$
	Low salinity outlet pressure = $9{,}409\ atm$
	$\eta_{PX} = 0{,}97$
	High salinity flow = $65{,}5\ m^3/h$
	Low salinity flow = $65{,}5\ m^3/h$
Turbines	configuration: Francis
	no. = 3
	$P_t = 5MW$
	$\Delta H \cong 105\ m$
	$\dot{Q}_t \cong 4{,}3\ m^3/s = 15480\ m^3/h$
	$\eta_t = 0{,}90$
Synchronous Generators	configuration: cylindrical rotor
	no. = 3
	$P_g = 5MW$
	$\eta_t = 0{,}95$
	no. of poles = 6
	rotational speed = $1000 - 1200\ rpm$
	frequency = $50 - 60\ Hz$

Transformers	no. = 3
	$P_{tf} = 5MW$
	$\eta_{tf} = 0{,}995$
Freshwater pumps	type: axial
	no. = 3
	$H \cong 1{,}400\ m$
	$\dot{Q} = 9{,}134\ m^3/s = 32882{,}4\ m^3/h$
	$\eta_p = 0{,}85$
Seawater pumps	type: submersible - axial
	no. = 3
	$H \cong 4{,}065\ m$
	$\dot{Q} = 7{,}097\ m^3/s = 35549{,}2\ m^3/h$
	$\eta_p = 0{,}85$
Freshwater Tanks	no. = 4
	volume $\cong 12000\ m^3$
	$Hmax = 4\ m$
	radius = $30\ m$
	footprint = $3000\ m^2$
Drum filters	no. = 70
	diameter = $1{,}7\ m$
	length = $4{,}5\ m$
	area = $31\ m^2$
	flux = $30\ m^3/m^2.h$
Seawater Tanks	no. = 4
	volume $\cong 12000\ m3$
	$Hmax = 4\ m$
	radius = $30\ m$
	footprint = $3000\ m^2$
Freshwater pipeline	no. = 2
	diameter = $1100\ mm$
	length = $1{,}5\ km$
	Total freshwater requirement = $65750\ m^3/h$
Seawater pipeline	no. = 2
	diameter = $1000\ mm$
	length = $2{,}5\ km$
	Total seawater requirement = $51090\ m^3/h$

PRO Power Plant	configuration: continuous flow – terrestrial power plant with PX unit
	$P_{net} = 10MW$
	$\dot{V}/\Delta\dot{V} = 1{,}08$
	$\dot{FS}/\Delta\dot{V} = 0{,}39$
	$\eta_m = 0{,}78137$
	$\eta_{II} = \eta_m.\eta = 0{,}4360$
	total membrane area = $4{,}725\ km^2$
	sub-site A total footprint = $25000\ m^2$

In this table we also introduced the thermodynamic second principle efficiency, or exergetic efficiency, of the PRO power plant. It is defined as the ratio between the net amount of net power produced and the theoretical amount of power available from the mixing of the two solutions at the specified proportion. It can be calculated by simple multiplication of the mechanical and the membrane energy recovery rate. As one can notice, the membrane is the most critical element in the continuous flow – terrestrial PP with PX configuration. It is possible to say that while the mechanical efficiency calculated is close to a technical limit and is not expected to raise much with further developments, membrane energy recovery rates could increase significantly with the development of new materials and production techniques.

This chapter presented a guideline to PRO power plant sizing, calculating major flows, working pressures and other conditions of the main components of such facility. One should remember that the results obtained here are fruit of various assumptions and data provided up to current date. As these assumptions change and new data are retrieved, the results vary. Nonetheless, the procedure presented can be easily adapted or simply brought up-to-date as it was conceived to be generally applicable.

C6. Pressure retarded osmosis economic evaluation

In this chapter we present a preliminary assessment to PRO economic analysis. No direct economic methodology was found regarding PRO technology; the study was carried on by adapting data from seawater reverse osmosis (SWRO) desalination plants and small hydro-electric plants. These evaluations usually consider power plants with higher capacities, making better use of scaling-up savings; nonetheless, there are two important reasons to why the $10\,MW$ power plant described in the previous chapter is used instead. The first one is to prevent data extrapolation inaccuracy from desalination costs; these are always referred to plant freshwater production capacity in m^3/d which can be considered equivalent to the daily permeating rate $\Delta\dot{V}$ in PRO processes. The Hadera SWRO desalination plant in Israel is the largest of its kind in the world with a capacity of around $350\,000\,m^3/d$, equivalent to only $3\,MW$ of power from PRO. A high capacity PRO power plant would certainly have a less accurate economic evaluation given its huge permeating rates.

The second reason is that $10\,MW$ power plants are already able to generate scaled-up demand for membrane elements and energy recovery units, with around $5\,km^2$ of membrane area and hundreds of energy recovery units required. Compared to and combined with the requirements of desalination facilities, the future market of these elements is enormous. The Freedonia Group, a leading international business research company, forecasted in 2006 a $US\$\,3{,}7\,billion$ membrane market demand for 2010, of which approximately 20% regarded to those for RO processes. This implies that an already significant share of this promising market is allocated to membrane technologies that are substantially similar to those applied in PRO.

The same promising scenario is observed globally. The Japanese company Toyobo, with expertise in polymerization, fibre modification, processing and biotechnology; identified water treatment membranes as one of three promising fields for growth. They recognized Africa and the Middle East as the global areas with most severe water supply problems but also pointed out the United States, Japan and Indonesia as strategic markets. Clearly, the inclusion of membrane demand for PRO

processes will push production rates to high levels, making it possible to develop new manufacturing technologies and significantly reduce costs.

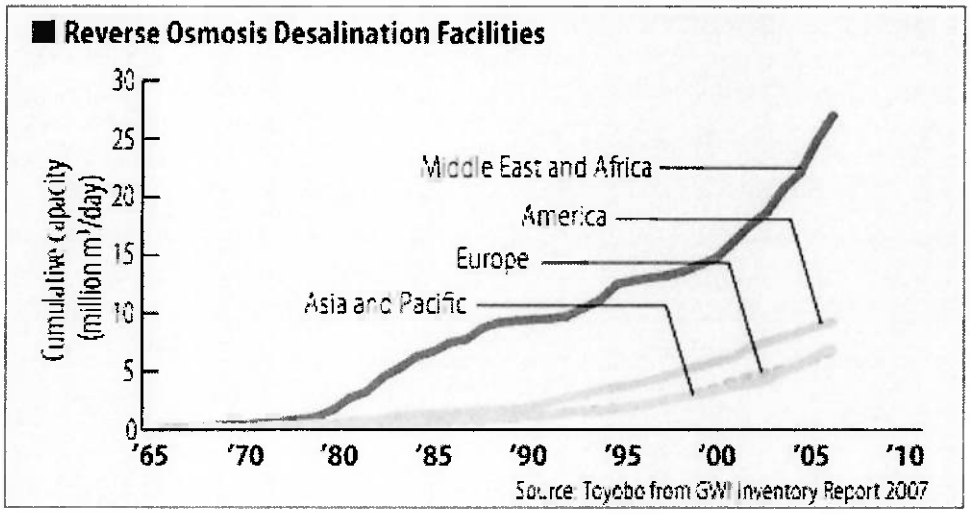

Figure 43: Future prospective for RO desalination. Source: Toyobo.

6.1 Preliminary economic analysis

In order to completely evaluate the economic feasibility of a power plant project it is important to know: (a) overall project cost; (b) electricity production cost; (c) annual revenue obtained; (d) depreciation rates and O&M costs; (e) the project's payback period/discount rate and their acceptability; (f) the regulatory environment; and (g) possible opportunities for subsidiary and other financial issues.

To estimate the items (a) overall project cost and (b) electricity production cost, we analysed data from existing desalination and small hydropower plants to estimate the magnitude of these parameters. These data are usually found with relative ease but, in order to have a more rigorous assessment, detailed studies such as that of Hafez and El-Manhawary (2002) are necessary. With the detailed cost components it is possible to evaluate which fraction of the total investment costs of desalination and small hydropower plants are relevant to PRO economic rating. As made visible in figure 45, provided by Frioui and Oumeddour (2008), there are several different cost items to be considered. We also display tables adapted from Hafez and El-Manhawary (2002),

where each cost item is presented and have its relevance to PRO processes determined.

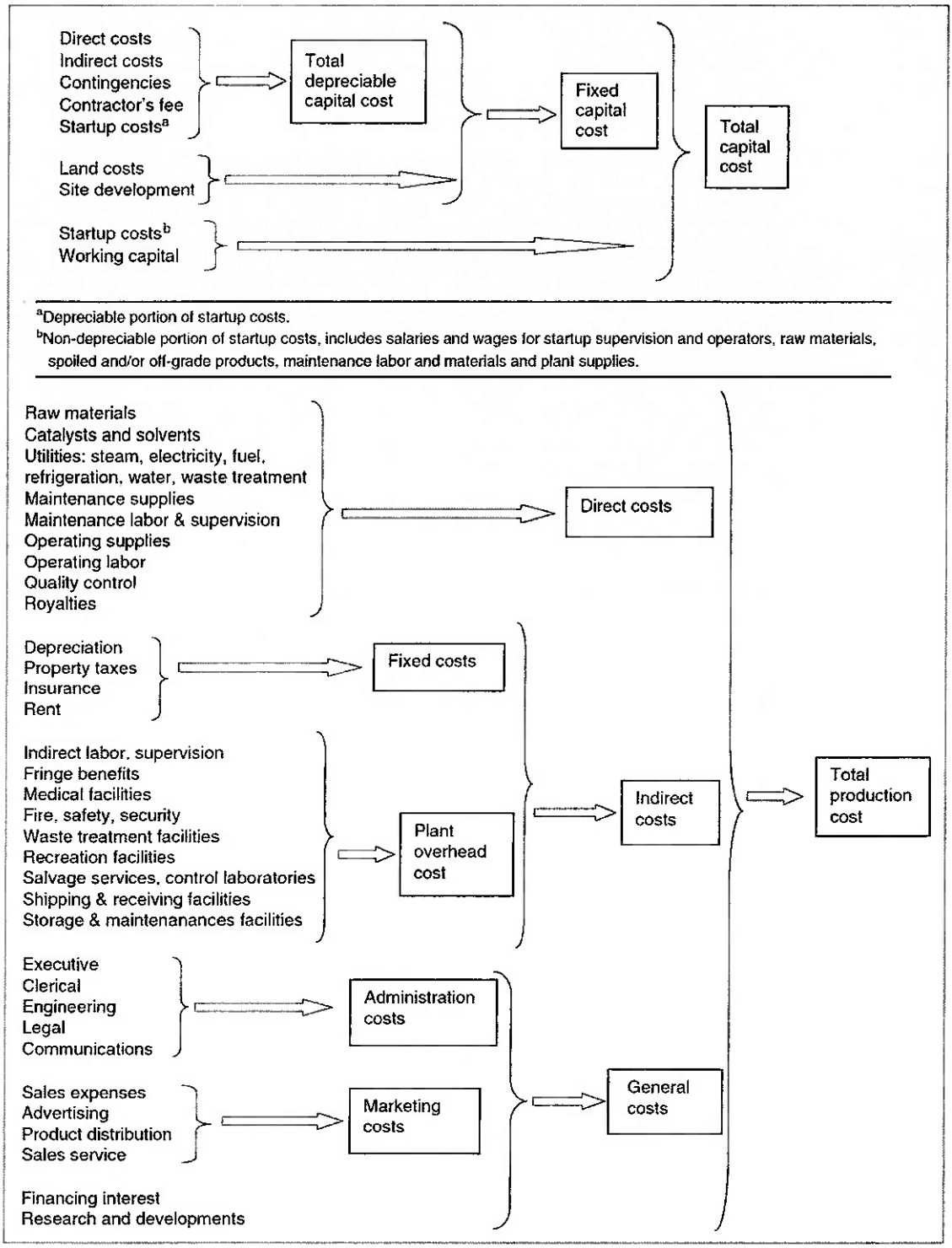

Figure 44: Different items for total investment and production costs [44]

Table 12: Reverse osmosis desalination investment cost analysis

REVERSE OSMOSIS DESALINATION INVESTMENT COST ANALYSIS		(HAFEZ, EL-MANHAWARY; 2002) US$ 2002					PRO RELEVANT?
Plant Capacity (m3/d)		250	500	2000	3500	4800	
Primary Equipment Costs							
	Intake system	180320	331010	870712	1403605	1118750	YES
	type	well	well	well	well	open-surface	
Detailed	Pre-treatment equipment	47652	123605	404504	695905	772003	NO
	of which filters	15677	40666	133082	228952	253989	YES
	of which testing equipment	6290	16316	53395	91859	101904	YES
	Energy recovery unit	8285	14531	51050	103065	109886	YES
	Pumps	28997	60047	164410	331929	353898	YES
	Post-treatment	2708	2933	3428	5898	6542	NO
	Internal pipes and valves	19436	29528	146459	451865	226032	YES
	Disposal pumping station	7011	15650	51214	88109	97743	YES
	Disposal pipeline	4524	10229	33474	57589	63887	YES
	Other	26216	45192	110111	201535	381671	NO
Sub-total		325149	632725	1835362	3339500	3130412	
Membrane Cost		36366	64495	300978	451466	737088	YES
Direct Costs							
Detailed	Measurement instruments	12062	21155	47296	95486	101806	YES
	Terrain	48194	93228	305092	524878	582274	YES
	Civic operations	3249	6285	20568	35385	39254	YES
	Distribution costs	126711	245115	802152	1380015	1530922	NO
Sub-total		190216	365783	1175108	2035764	2254256	
Indirect Costs							
Detailed	Project Planning	32491	62851	205680	353851	392544	YES
	Construction	12996	25140	82272	141540	157018	YES
Sub-total		45487	87991	287952	495391	549562	
Additional Costs							
	R&D + Financing	2708	5238	17140	29488	32712	YES
Sub-total		2708	5238	17140	29488	32712	
Total Capital Cost		599926	1156232	3616540	6351609	6704030	
	US$ 2010	731910	1410603	4412179	7748963	8178917	
Capital Unit Cost		2927,63	2821,21	2206,09	2213,99	1703,94	

Table 13: Reverse osmosis desalination production cost analysis

REVERSE OSMOSIS DESALINATION PRODUCTION COST ANALYSIS		(HAFEZ, EL-MANHAWARY; 2002) US$ 2002					PRO RELEVANT?
Plant Capacity (m3/d)		250	500	2000	3500	4800	
Annual depreciation							
Detailed	Intake system (10 years)	18032	33101	87071	140361	145896	YES
	Pre-treatment system (10 years)	4765	12361	40450	69591	77200	YES
	PEC (10 years)	12184	21369	75073	151566	161597	YES
	Post-treatment (10 years)	271	293	343	590	654	NO
	Disposal system (10 years)	2112	4714	15426	26539	29441	YES
	Infra-structure (40 years)	3533	6945	25539	40693	49232	YES
	Professional + financing (10 years)	2653	5133	22282	38334	42526	YES
Sub-total		43550	83916	266184	467674	506546	
Cost of membrane replacement		21670	39038	116274	185524	208611	YES
Operation & Maintenance ($/year)							
	Cost of repair and replacement	44412	80008	238302	380226	306787	YES
	Cost of labour	18863	33982	101214	161494	130302	YES
	Energy	85666	154329	459664	733425	824696	NO
	Chemical treatment	12353	22256	66288	105765	118928	NO
	Cost of insurance	16316	29394	87548	139689	112708	YES
	Others	3240	5838	17387	27742	31194	NO
Sub-total		180850	325807	970403	1548341	1524615	
Total depreciation + O&M (US$/year)		246070	448761	1352861	2201539	2239772	
Production cost (US$/m3)		2,6966	2,4590	1,8532	1,7233	1,2784	
Production cost (US$ 2010/m3)		3,2899	2,9999	2,2609	2,1024	1,5597	

It was observed that the fraction of cost items relevant to PRO processes remains reasonably constant, amounting to $65-70\%$ of the total investment value and up to $50-60\%$ of production costs, nevertheless, as plant capacity grows these fractions tend to vary and that is visible even with the modest amount of data presented in the tables above. Chemical pre-treatment and distribution systems are the two main PRO-

irrelevant parameters for overall investment. Pre-treatment capital expenses are expected to rise considerably with higher power plant capacities whereas the water distribution system cost may have lower impacts under this assumptions; the combined effect is that of maintaining the calculated interval of $65 - 70\%$ relevance.

The most significant PRO-irrelevant parameters from desalination plant production costs are energy and chemical treatment components, both expected to have a higher participation in total O&M annual costs with increasing plant capacities. Combined they are certain to reduce the estimated percentile relevance fraction of desalination production costs considerably; a reasonable guess value would be around $40 - 55\%$ for high capacity plants. Having these values in mind it is possible to estimate the fraction of total investment and production cost correspondent to desalination economics within PRO economic assessment.

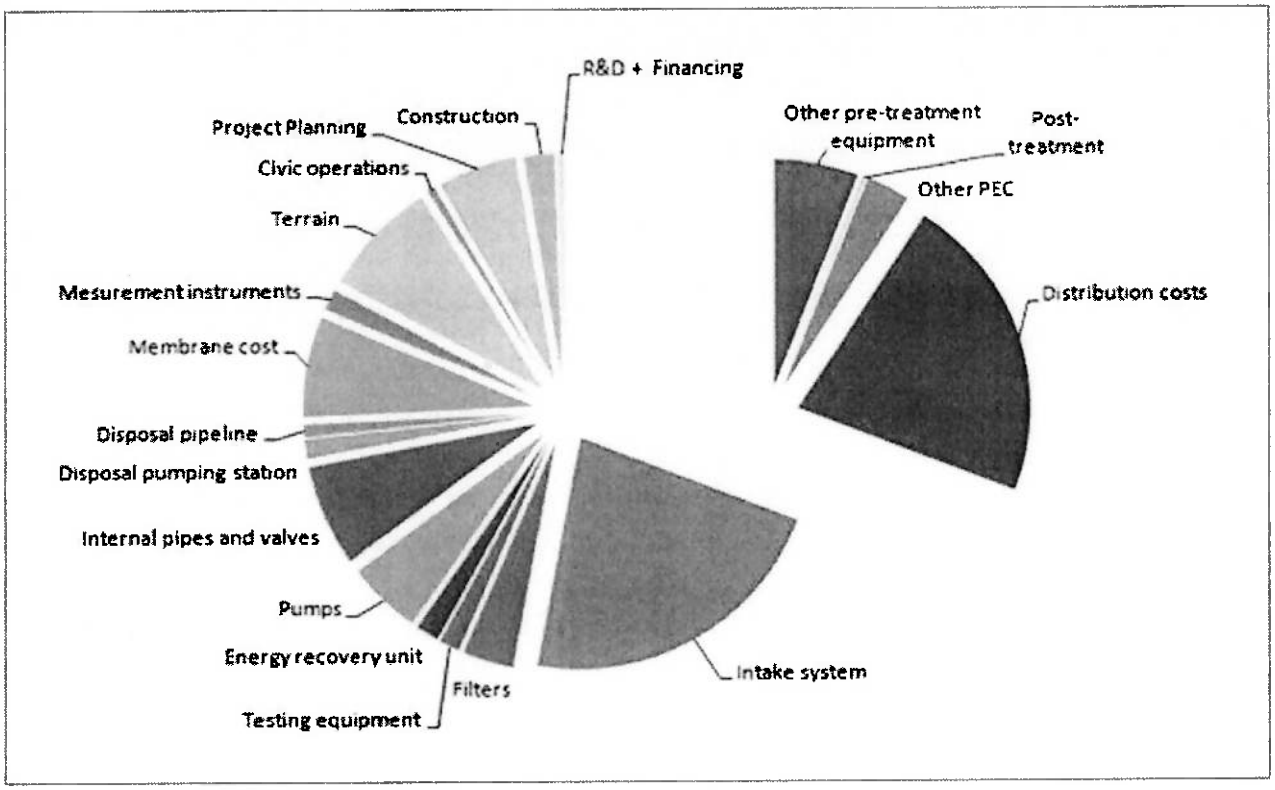

Figure 45: Relevant and irrelevant investment cost components for PRO processes

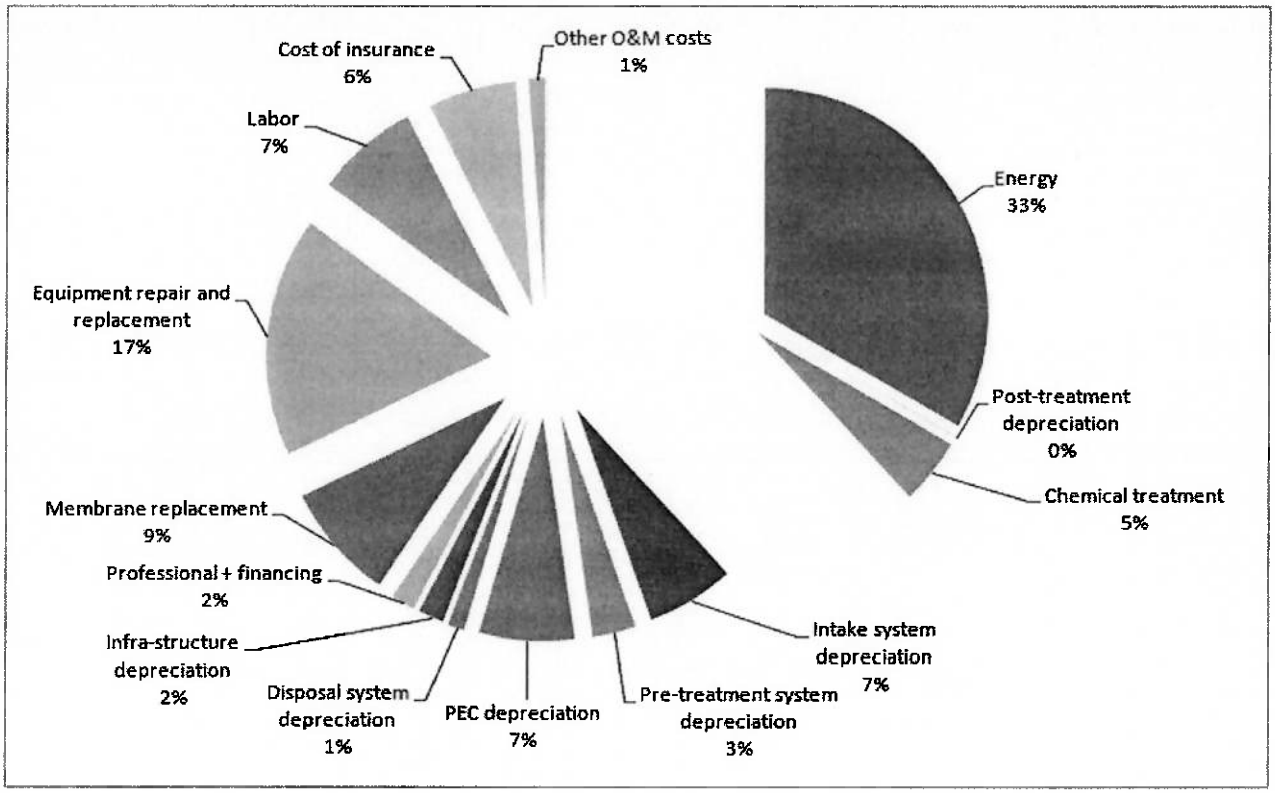

Figure 46: Relevant and irrelevant annual expenses cost components for PRO processes

Firstly, total capital cost and annual production expenses are extrapolated from a collection of data regarding various plants with different desalination capacities to the actual capacity of our PRO power plant. It was decided to use power interpolation in order to compare results with Rautenbach and Melin (2003) apud Fritzmann et al. (2007).

The results are also compared to those obtained applying the methodology proposed in Loeb (2002), a study in which preliminary economic analysis of a net $22{,}3\ MW$ alternating flow – terrestrial power plant is determined. In his assessment, Loeb considers a specific plant capital cost equivalent to $US\$\ 988{,}2\ per\ m^3/d$ – 2010 value, calculated with the introduction of an economy-of-scale factor as follows:

$$\frac{Project\ specific\ capital\ cost}{Existing\ specific\ capital\ cost} = \left(\frac{Existing\ plant\ capacity}{Project\ plant\ capacity}\right)^{0,2}$$

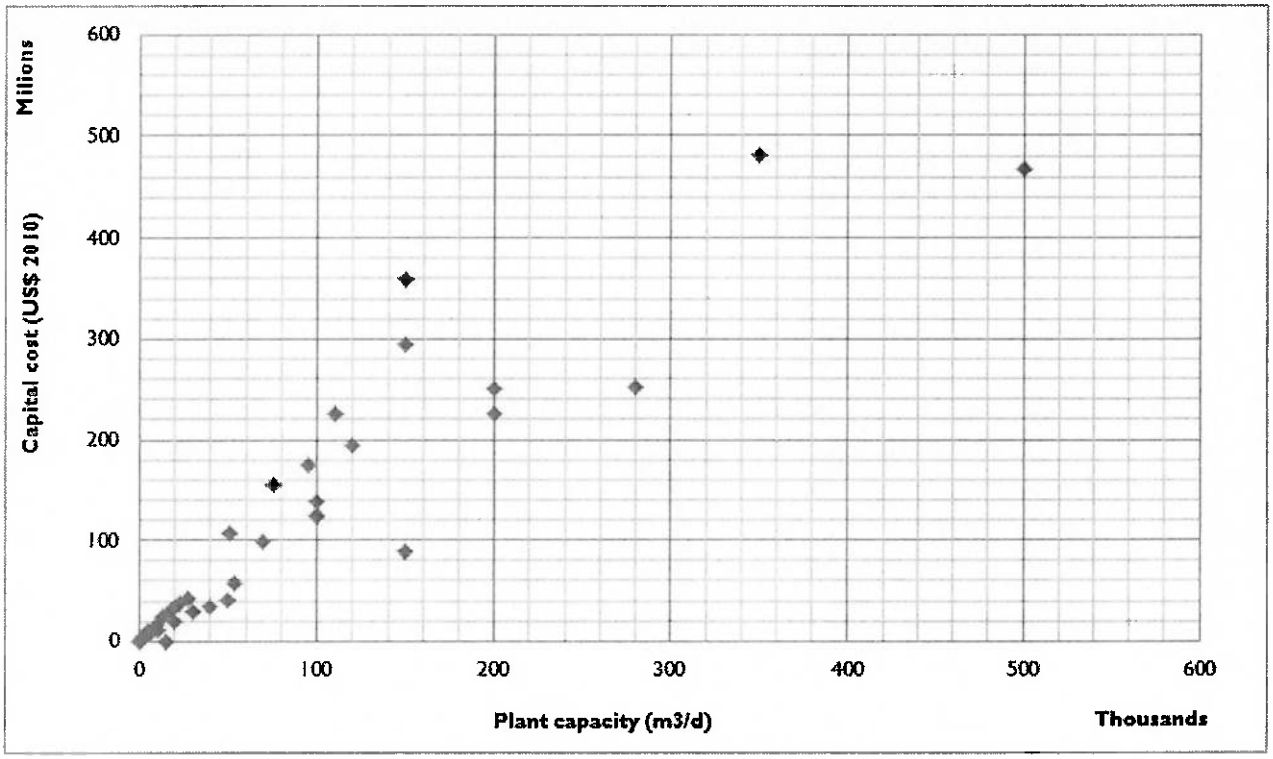

Figure 47: Total capital costs for several different SWRO desalination plant capacities

Applying the economy-of-scale factor to the data collected, an average specific capital cost of $US\$\ 901$ per m^3/d was calculated. All three possible estimating methods for PRO processes are presented; they consider a relevance factor of 70% regarding total capital costs of SWRO desalination plants.

(RAUTENBACH; MELIN, 2003 apud FRITZMANN et al., 2007)

$$TCC = 7100 * C^{0,85} \ for\ SWRO\ plants$$
$$TCC = 1850 * C^{0,82} \ for\ BWRO\ plants$$
$$TCC = 4970 * C^{0,85} \ for\ PRO\ plants \quad (adapted)$$

(LOEB, 2002) $TCC = 901 * C \ for\ PRO\ plants \quad (adapted)$

(This study)
$$TCC = 2345{,}9 * C^{0,9397} \ for\ SWRO\ plants$$
$$TCC = 1642 * C^{0,9397} \ for\ PRO\ plants$$

The PRO power plant has a total capacity of $1135250\ m^3/d$, which results in a total capital cost ranging at $US\$\ 697 - 1022\ million$. The results obtained from data extrapolation were consistent with formulas found in Rautenbach and Melin (2003) apud

Fritzmann et al. (2007) and with the methodology presented in Loeb (2002). Analogously, the desalination fraction of total annual depreciation and O&M expenses was estimated at around $US\$\ 79{,}4\ million/year$, considering relevant cost components to be 40% of total. All collected data corresponding to desalination plants are presented in table 15 at the end of this chapter.

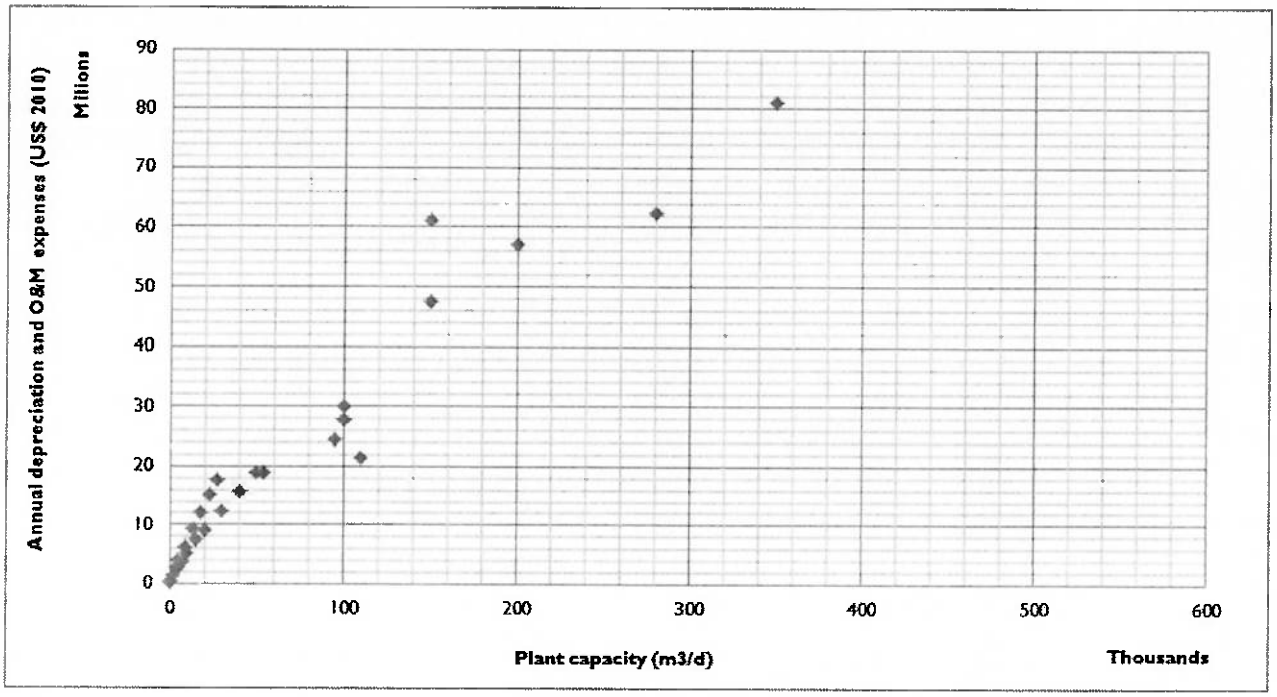

Figure 48: Annual depreciation and O&M expenses for several different SWRO desalination plant capacities

$$AM + O\&M = 5592{,}8.C^{0{,}752}\ for\ SWRO\ systems$$

The cost fraction corresponding to small hydropower equipment takes into account turbines, generators, switchyard equipment, connections to the power grid, powerhouse, machinery foundation civil costs, control and ancillary electric equipment. Cost components other than these are either irrelevant or were already considered in the desalination fraction. In PRO systems, as well as in small hydro projects, turbine and powerhouse costs are more closely correlated to huge flows than pressure heads and because of that equipment cost per kilowatt are relatively high compared to large hydropower facilities. On the other hand, transmission line costs should represent a

lesser portion of the total project cost since the availability of substations and transmission lines can handle an additional $10\ MW$ of power input.

Transmission and switchyard equipment costs are functions of plant capacity, transmission voltage and line length. Since PRO power plants are usually located close to populated areas, they can be connected directly to local medium voltage distribution grid; common voltages for the medium voltage distribution grids in Sweden are $10kV$ and $20kV$. Costs were estimated considering the power plant to be $18\ km$ away from the closest distribution substation in Göteborg and afterwards were brought up-to-date to 2010 dollars.

SWITCHYARD EQUIPMENT COST
(Thousand Dollars)

Plant Capacity	Transmission Voltage 13.8	34.5	69	115
1 MW	50	60	110	160
3 MW	85	100	120	175
5 MW	110	125	150	210
10 MW	150	170	210	280
15 MW	185	220	250	320

TRANSMISSION LINE COST
(Thousand Dollars)

Plant Capacity	Miles of transmission line 1	2	5	10	15
0.5 MW	30	60	150	—	—
5 MW	45	80	160	320	500
10 MW	60	100	180	380	600
15 MW	80	140	230	460	700

Figure 49: Switchyard equipment and transmission line costs, taken from [47]

Switchyard equipment expenses amounted to $US\$\,523\ thousand$ whereas transmission line investments sums up to $US\$\,1212\ thousand.$ In preliminary assessment of small hydropower projects it is usual to evaluate the lump sum capital cost of equipment: estimating different equipment costs altogether as a single value, without detailed breakdown of its cost components. Figure 49 was found in the small hydro report from the United States Army Corps of Engineers (1979) and used to estimate the lump sum cost of turbine/generator, appurtenant equipment, station electric equipment, miscellaneous power plant equipment, powerhouse, powerhouse

excavation, switchyard civil works, construction and installations. The details of cost estimation are explained in the figure as well. For 3 units of 5 MW of power each, the lump sum capital cost was estimated at around $US\$\ 17{,}4\ million$.

Small hydropower capital cost fraction totals $US\$\ 20\ million$, a modest contribution when compared to the desalination capital cost fraction of $US\$\ 697 - 1022\ million$. Operation and management costs are calculated as 4% of total capital cost, typical values ranging between $1{,}5 - 2{,}5\%$. Again, its contribution to total PRO plant O&M expenses is nearly negligible compared to that from the desalination fraction.

Therefore, for PRO power plants of smaller capacities – a few MW – total capital costs and electricity production costs are mostly defined from equivalent desalination plant operation data; the equivalency parameter of desalination capacity is total membrane permeation rate, usually expressed in m^3/d. For this study, 10 MW pilot plant total cost of investment and annual depreciation and O&M expenses were estimated at $US\$\ 825\ million$ and $79{,}4\ million\ US\$\ /year$ respectively. Considering the plant availability to be $7920\ hours\ per\ year$, electricity production cost is calculated at $1{,}0025\ US\$/kWh$. In his studies, Loeb (2002) obtained a value of $0{,}8203\ US\$/kWh$, nonetheless, he admits his assumptions of membrane performance to be rather optimistic. In any case, both values are much higher to what was considered to be an acceptable electricity production cost – $0{,}1586\ US\$/kWh$.

When projects economic assessment returns a prospect of unfeasibility, the evaluation of (c) annual revenue obtained should be changed into (c') minimum annual revenue requirements. Minimum revenue requirements for power plant operation is given by the power plant shutdown point, defined as the point at which revenues can only cover the variable and non-sunk fraction of annual expenses, that is, the fraction determined by total annual costs minus annual depreciation. Loeb (2002) considers a 3% interest rate in his analysis which is a relatively low interest scenario; instead, a rate of 8% will be used as current membrane market trends dictates. Annual depreciation is calculated from compounding total depreciable capital cost throughout power plant life according to the following formula:

$$A = TCC_{sunk}\left(\frac{r\,(1+r)^n}{(1+r)^n - 1}\right)$$

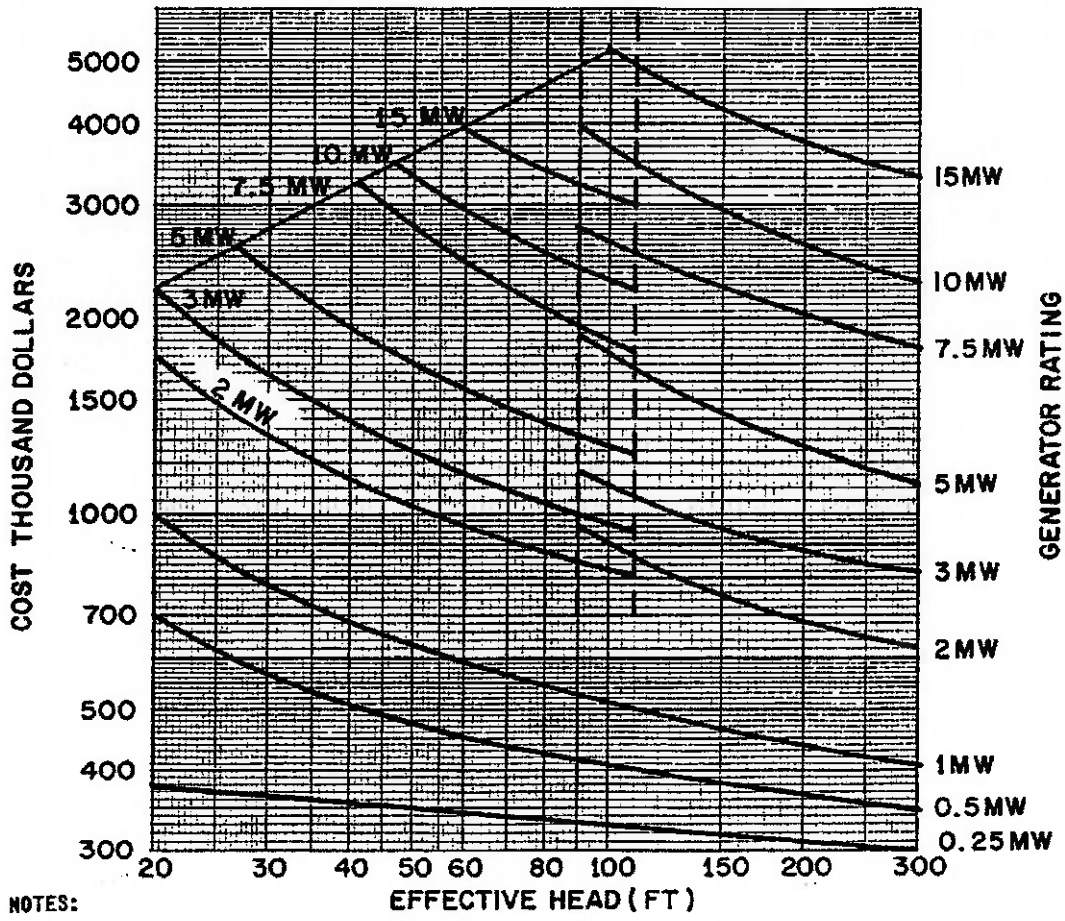

NOTES:

1. Estimated costs are based upon a typical or standardized turbine coupled to a generator either directly or through a speed increaser, depending on the type turbine used.
2. Costs include turbine/generator and appurtenant equipment, station electric equipment, miscellaneous powerplant equipment, powerhouse, powerhouse excavation, switchyard civil works, an upstream slide gate, and construction and installation.
3. Costs not included are transmission line, penstock, tailrace construction and switchyard equipment.
4. Cost base July 1978.
5. The transition zone occurs as unit types change due to increased head.
6. For a Multiple Unit powerhouse, additional station equipment costs are \$20,000 + \$58,000x(n-1) where n is the total number of units.
7. Data for this figure was obtained from figures and tables in Volumes V and VI.

Figure 50: Lump sum capital cost of small hydropower plants [47]

From table 11 it is possible to estimate sunken capital costs as around $60 - 65\%$ of total for PRO systems. Item (d1) annual depreciation rate is calculated to be $US\$\,54{,}6\,million$ for 8% interest rate scenario, item (d2) annual O&M costs is determined according to references left by (LOEB, 2002) as $US\$\,20{,}9\,million$. Item (c') minimum revenue requirements were calculated by simple subtraction of depreciation rates from total annual costs and resulted $US\$\,24{,}8\,million/year$.

An analysis of (e) the project's payback period/discount rate and their acceptability is only possible for projects that prove themselves economically feasible. The so called static evaluations, done without considering the time value of money, are only adequate for initial cost estimates. In preliminary assessment dynamic methods such as the net present value (NPV), benefit-cost ratio (BC) and internal rate of return (IRR) are preferred.

The NPV is calculated from discounting cashflows, either positive or negative, throughout the whole plant life taking into account timely interest rates. Revenues correspond to positive values of cashflows whereas costs and investments correspond to negative values. Thus, the project is economically interesting for positive NPV values.

$$NPV = \sum_{1}^{n} \frac{CF_k}{(1+r_k)^k} = \sum_{1}^{n} \frac{R_k - C_k - I_k}{(1+r_k)^k}$$

The IRR is defined as the interest rate which makes $NPV = 0$ calculated for a time period equal to the plant life-time. It is compared to a minimum acceptable rate of return for the investment, over which the process is considered to be economically interesting. The BC also derives from the NPV; it compares plant revenues and investments in a ratio basis such that projects with $BC < 1$ are considered to be uninteresting.

$$BC = \frac{\sum_{1}^{n} \frac{R_k}{(1+r_k)^k}}{\sum_{1}^{n} \frac{C_k + I_k}{(1+r_k)^k}}$$

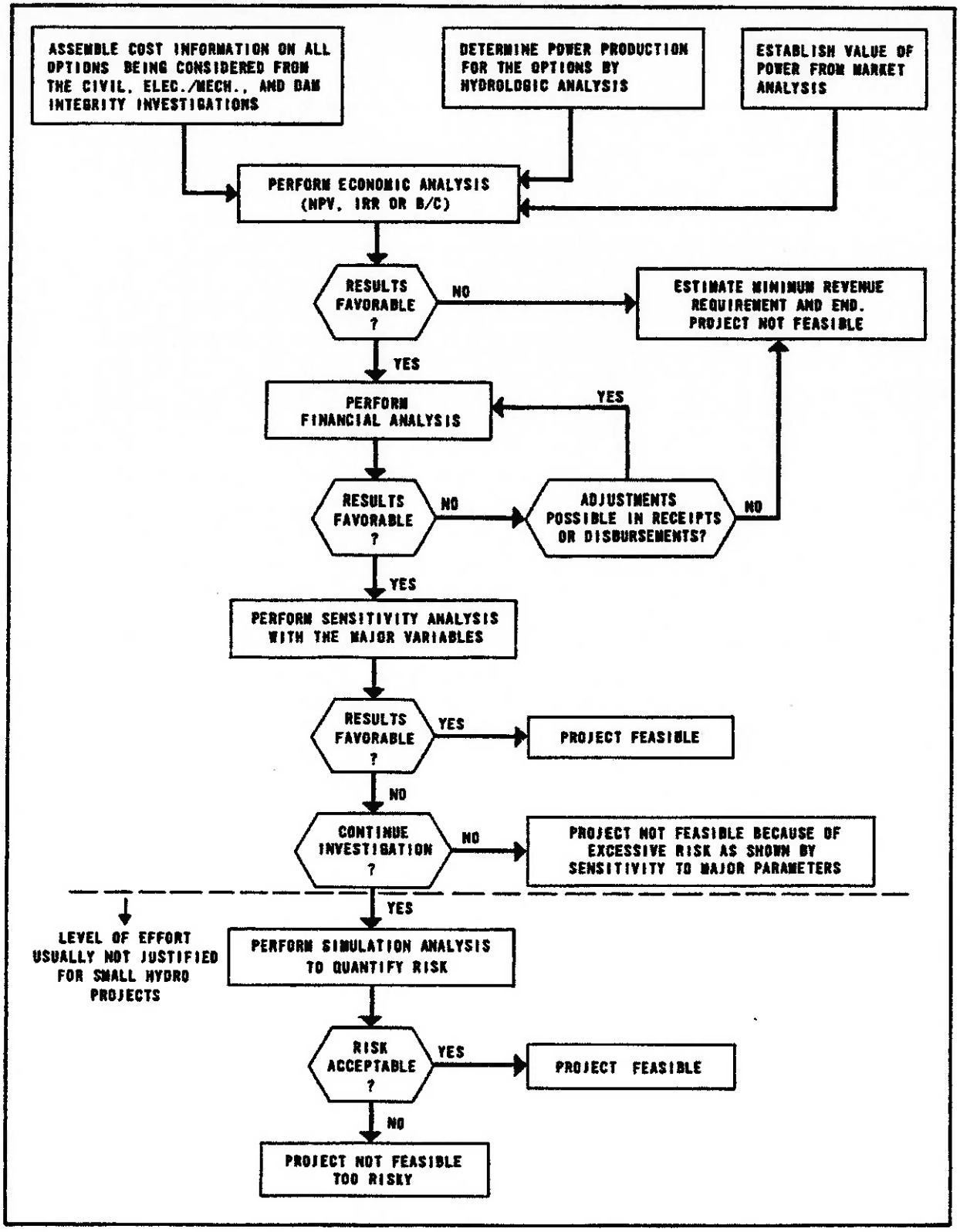

Figure 51: Summary procedure for small hydropower economic assessment [47]

To what regards items (f) the regulatory environment and (g) possible opportunities for subsidiary and other financial issues, it is important to remember that our results were obtained for current technology application under a no-incentive policy scenario, they should be considered more as an upper limit than as an average reference. The evaluation must account for possible revenues, savings and opportunity costs generated from energy taxes, emission taxes, green certificates, energetic efficient titles and carbon emission titles; all being instruments from which PRO is certain to benefit.

A summary table is presented in attachment; it contains all numeric information gathered throughout the economic analysis. We included the original preliminary cost evaluation found in Loeb (2002); a second evaluation showing the results that would be obtained if our power plant data were used instead of his; the results from this study; and the gradual effects of using the 2015 targeted values for membrane performance, increasing power plant capacity and reducing plant capital cost in 50%. A considerable coherence level is observed, for current technology application PRO electricity would cost from $0{,}8203 - 1{,}0025\ US\$/kWh$ whereas for the future it would be possible to produce at a fourth of this value.

6.2. Future economic prospectives

The results obtained demonstrated that the current status of PRO processes application to produce eletricity is that of economic unfeasibility. Nontheless, with new advancements in membrane manufacturing tecnology, it would be possible to produce energy at a fourth of the current estimated value. This analysis takes into account the effects of such development in the economic evaluation of the technology, which are presumed to be achieved around 2015. Furthermore, the importance of scaling-up plant capacities and reducing the investment costs, which are bound to occur later, are also assessed.

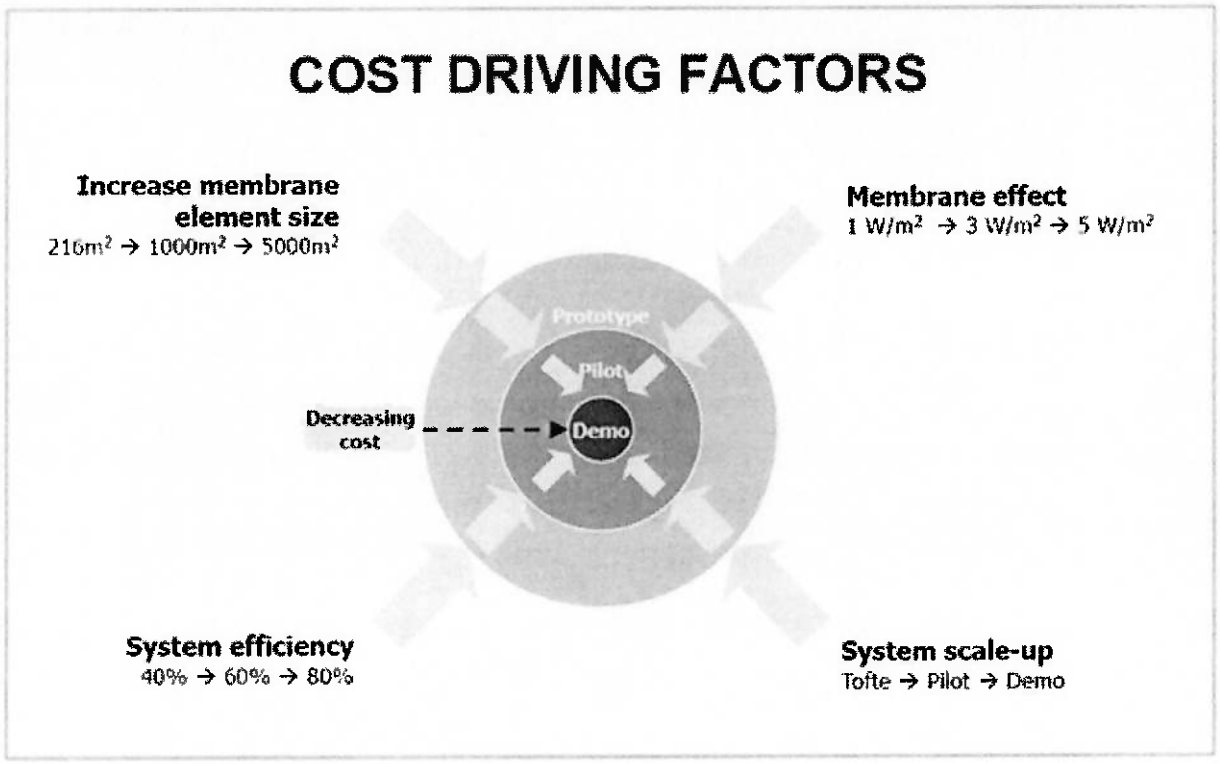

Figure 52: Cost driving factors in PRO processes. Source: Statkraft.

Assuming that by 2015 typical values of power density for membranes modules and energy recovery rates are around $5\,W/m^2$ and 80%, respectively; the permeating water flux per square meter of membrane area will result:

$$J_w = \frac{\dot{w}}{\eta \Delta G_{mix}} = 3{,}52E^{-6}\, m/s$$

With more efficient membrane modules it is possible to reduce the pumping expenses by reducing the values of $\dot{V}/\Delta\dot{V}$ and $\dot{FS}/\Delta\dot{V}$ without compromising the performance of the system. Given $\dot{V}/\Delta\dot{V} = 1{,}04$ and $\dot{FS}/\Delta\dot{V} = 0{,}2$, the major flow requirements for the power plant can be recalculated as follows:

$$\eta_m = \eta_T - \frac{1}{\eta_p}\left(1 - \frac{p_{PX}}{p_s}\right)\frac{\dot{V}}{\Delta\dot{V}} - \frac{0{,}007}{\eta_p}\frac{\dot{V}}{\Delta\dot{V}} - \frac{0{,}011}{\eta_p}\left(1 + \frac{\dot{FS}}{\Delta\dot{V}}\right) - \Delta\eta_{Dtube} - \Delta\eta_{Ftube}$$

$$\Delta\eta_{Dtube} = \frac{\frac{\Delta p}{m} L_D}{\eta_p p_s}\frac{\dot{V}}{\Delta\dot{V}} \qquad \Delta\eta_{Ftube} = \frac{\frac{\Delta p}{m} L_F}{\eta_p p_s}\left(1 + \frac{\dot{FS}}{\Delta\dot{V}}\right)$$

$$\eta_m = 0{,}7833 = \frac{net\ power}{gross\ power} = \frac{P_{net}}{P_{gross}}$$

$$P_{gross} = 12{,}7661\ MW = S\dot{w}$$

$$S = 2.553.232\ m^2 \qquad e \qquad \begin{bmatrix} \Delta\dot{V} = 8{,}987\ \frac{m^3}{s} = 32354\ \frac{m^3}{h} \\ \dot{V} = 9{,}347\ \frac{m^3}{s} = 33649\ \frac{m^3}{h} \\ \dot{FS} = 3{,}505\ \frac{m^3}{s} = 18450\ \frac{m^3}{h} \end{bmatrix}$$

The system will have a total capacity of $776500\ m^3/d$, a reduction of over 30% of the original requirements. In economic terms, the new values for total investment costs and annual expenses for electricity production will be:

$$TCC = 20 + \left(\frac{1642.C^{0{,}9397}}{10^6}\right) = US\$\ 582{,}7\ millions$$

$$AM + O\&M = 0{,}8 + 0{,}4\left(\frac{5592{,}8.C^{0{,}752}}{10^6}\right) = US\$\ 60{,}93\ \frac{millions}{year}$$

The final electricity cost given that membrane manufacturing technology has developed as previously mentioned results $0{,}7693\ US\$/kWh$, of which only $0{,}2821\ US\$/kWh$ represent expenses in maintenance and operation of the power plant. Compared to the original value of $1{,}0241\ US\$/kWh$ it is evident that new developments in membrane technology plays a major economic role for PRO processes.

It is possible to achieve further economies by scaling-up the system capacity, with the advantages obtained from the economy-of-scale when purchasing plant elements. In order to estimate such effect, the same previously mentioned formula, taken from Loeb (2002) was applied. Its application is as follows:

$$\frac{Project\ membrane\ substituition\ cost}{Existing\ membrane\ substituition\ cost} = \left(\frac{Existing\ plant\ capacity}{Project\ plant\ capacity}\right)^{0{,}2}$$

To calculate the total investment cost we used the formula given by Rautenbach and Melin (2003 apud FRITZMANN et al., 2008) instead of our own. That is beacuse the first one has a more pronounced economy effect as plant capacities increases and

reaches outstanding values. Therefore, for a PRO system with $100\ MW$ of net capacity and more advanced membrane modules, we have:

$$TCC = \left(\frac{4970.C^{0,85}}{10^6}\right) = US\$\ 3572{,}5\ millions$$

$$AM + O\&M = 0{,}8 + 0{,}4\left(\frac{5592{,}8.C^{0,752}}{10^6}\right) = US\$\ 340{,}5\ \frac{millions}{year}$$

The electricity cost in this case results $0{,}4299\ US\$/kWh$; again, depreciation costs are the main causes for increased electricity cost, corresponding to around 70% of the final value. With a 50% in investments, due to incentives and/or new tecnologic developments; it would be possible to produce at a cost of $0{,}2468\ US\$/kWh$, of which $0{,}0974\ US\$/kWh$ would correspondi to the O&M fraction of plant expenses.

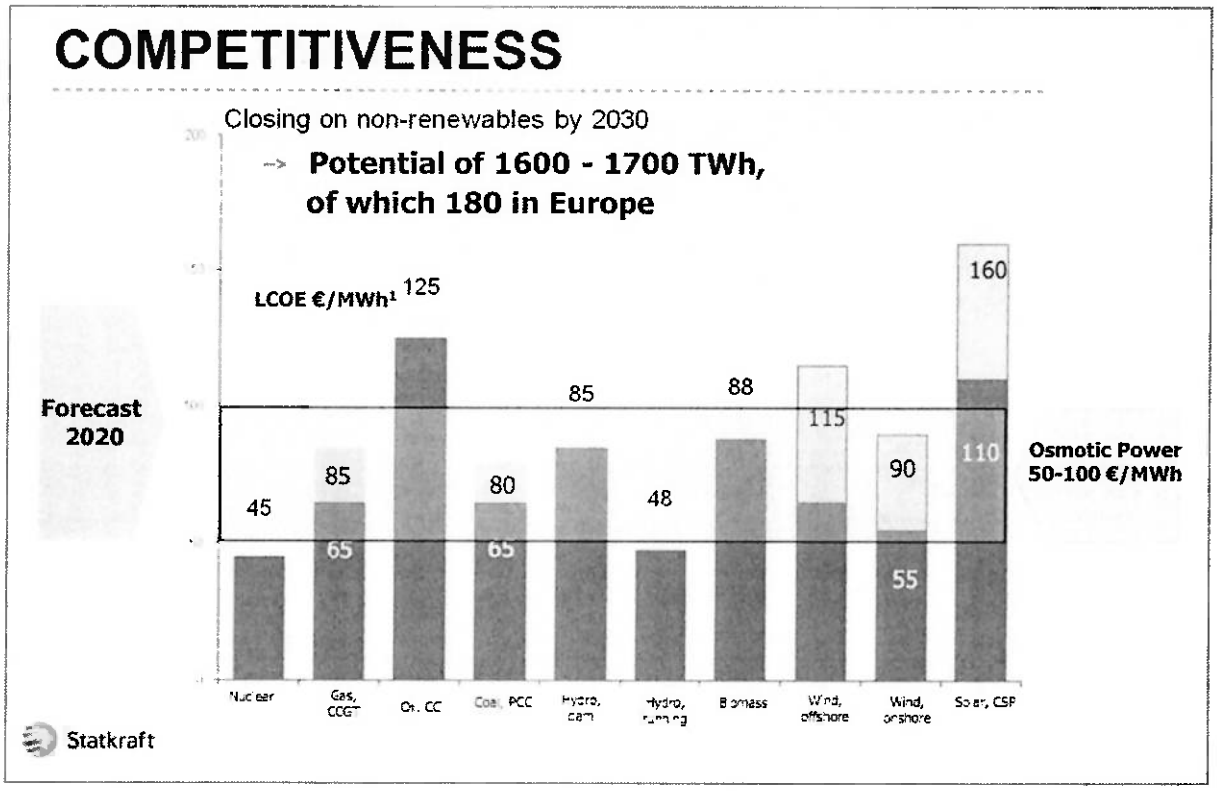

Figure 53: 2020 electricity cost forecast for several technologies. Source: Statkraft.

Forecasts for 2020 expect electricity costs to be greatly reduced and according to the results obtained it is an optimistic but possible scenario. Our most optimistic analysis

considered a 50% reduction in capital costs, scaled-up power plant and high-performance membranes and resulted in an electricity production cost of $0{,}2468\ US\$/kWh$ – equivalent to $171\ €/MWh$ and consistent with the forecasts presented in figure 53. Some points to be taken under consideration when making PRO more cost-efficient are:

(a) Developments in membrane performance should focus in reducing membrane thickness and increasing salt rejection, that is, in the direction of increasing the effective osmotic pressure difference between solutions. Improving efficiency and power density is also an effective method to shorten the contribution of plant capital amortization to kWh cost. For PRO the prospects are more promising than for RO processes as membrane pressurization is lower and, consequently, so are membrane structural requirements;

(b) Economy-of-scale production shall play a major role in reducing membrane manufacturing cost. PRO power plants will certainly accelerate the scaling-up process as they currently generate a demand of around $0{,}5\ km^2$ per MW installed, a membrane area equivalent to that of a $100000\ m^3/d$ desalination plant;

(c) The effect of improving membrane performance and manufacturing costs altogether is non-linear and, consequently, generate huge differences in cost analysis;

(d) It is of utmost importance to direct efforts in reducing other-equipment related capital costs as annual amortization is responsible for around 70% of electricity production cost. Plant design towards cost-effectiveness and suitable siting are critical to this matter. The study proved that, economically, a PRO power plant can be seen as a fraction of a SWRO desalination plant; so that developments in one area are easily transmitted to the other. Nonetheless, it is important to develop a detailed economic evaluation method specific for PRO processes rather than adapted from any other system.

In conclusion, it is important to bear in mind that the results obtained in this study, although calculated as accurately as possible, are limited. A reduced time span, expected membrane development and no-incentive policy were considered in almost all scenarios in order to assess PRO viability. This is an unusual practice in new renewable energy sources evaluation since those incentives play an important role in providing economic support. Nonetheless, even without considering these complex incentive mechanisms, PRO technology proved to be a valid alternative with competitive forecasted costs.

Table 14: Summary table for economic assessment

ECONOMIC ASSESSMENT SUMMARY TABLE	(LOEB, 2002) original calculation (US$ 2002 value)	(LOEB, 2002) original calculation (US$ 2010 value)	(LOEB, 2002) original cost data application	(RAUTENBACH; MELIN, 2003)	(This study)	2015 target membrane 10MW plant	2015 target membrane 100MW plant	2015 target membrane 100MW plant + 50% reduction in desalination plant cost
Plant capacity (m3/d)	2.000.000,00	2.000.000,00	1.140.966,00	1.140.966,00	1.140.966,00	776.500,00	7.765.000,00	7.765.000,00
Plant net power (MW)	22,3	22,3	10	10	10	10	100	100
Interest rate	0,03	0,03	0,03	0,08	0,08	0,08	0,08	0,08
Amortization period (years)	20	20	20	20	20	20	20	20
Total capital cost (US$ million)	1617,388	1973,213	1028,166	697,000	825,000	582,781	3572,536	1786,268
Capital cost per kW (US$)	72528,607	88484,901	102816,642	69700,000	82500,000	58278,055	35725,361	17862,681
Total annual expenses (US$ million)	118,763	144,890	76,938	65,164	81,108	60,928	340,484	195,432
Annual plant amortization costs (US$ millions)	83,295	101,620	52,951	46,144	54,618	38,582	236,516	118,258
Membrane replacement, labor, and O&M annual cost as proposed in (LOEB, 2002) (US$ millions)	35,467	43,270	23,988	19,020	20,940	14,461	96,296	69,502
Other annual costs (US$ millions)					5,550	7,884	7,672	7,672
Electricity production cost (US$/kWh)	0,6724	0,8204	0,9714	0,8228	1,0241	0,7693	0,4299	0,2468
Shutdown electricity production cost (US$/kWh)	0,2008	0,2450	0,3029	0,2402	0,3345	0,1826	0,1216	0,0878

ECONOMIC ASSESSMENT AS SEEN IN (LOEB, 2002)	(LOEB, 2002) original calculation (US$ 2002 value)	(LOEB, 2002) original calculation (US$ 2010 value)	(LOEB, 2002) cost data application	(RAUTENBACH; MELIN, 2003)	(This study)	2015 target membrane 10MW plant	2015 target membrane 100MW plant	2015 target membrane 100MW plant + 50% reduction capital cost
Plant capacity (m3/d)	2.000.000,00	2.000.000,00	1.140.966,00	1.140.966,00	1.140.966,00	776.500,00	7.765.000,00	7.765.000,00
Plant net power (MW)	22,3	22,3	10	10	10	10	100	100
total membrane area (km2)	6,9	6,9	4,75	4,75	4,75	2,55	25,5	25,5
membrane replacement cost (US$/m2)	7,3108	8,9192	9,9787	9,9787	9,9787	10,7771	6,7999	6,7999
membrane life (years)	7	7	7	7	7	7	7	7
membrane areal power (kW/m2)	0,00323	0,00323	0,00211	0,00211	0,00211	0,00392	0,00392	0,00392
membrane energy production during entire life (kWh/m2)	179,2	179,2	116,7	116,7	116,7	217,4	217,4	217,4
Total capital cost (US$ million)	1617,388	1617,388	1028,166	697,000	825,000	582,781	3572,536	1786,268
Capital cost per kW (US$ thousant)	72,529	72,529	102,817	69,700	82,500	58,278	35,725	17862,681
contribution of amortization to kWh cost	0,4716	0,5754	0,6686	0,5826	0,6896	0,4872	0,2986	0,1493
contribution of membrane replacement to kWh cost	0,0408	0,0498	0,0855	0,0855	0,0855	0,0496	0,0313	0,0313
contribution of labor to kWh cost	0,0226	0,0276	0,0226	0,0226	0,0226	0,0226	0,0226	0,0226
contribution of O&M to kWh cost	0,1374	0,1676	0,1947	0,1320	0,1563	0,1104	0,0677	0,0338
contribuition of other costs to kWh cost					0,0701	0,0995	0,0097	0,0097
Electricity production cost (US$/kWh)	0,6724	0,8204	0,9714	0,8228	1,0241	0,7693	0,4299	0,2468
Shutdown electricity production cost (US$/kWh)	0,2008	0,2450	0,3029	0,2402	0,3345	0,2821	0,1313	0,0974

C7. Conclusion

In this study we calculated that 17701 *TWh* per year could be produced from salinity gradient technologies worldwide; that is equivalent to a power potential of 2,245 *TW* when a power plant availability of 90% is assumed. Technically, only a fraction of that value – 60% – is exploitable, that is due to the common misconception of supposing that locations at the mouths of powerful rivers and hypersaline basins are the most promising sites for salinity power. As Post (2009) noticed, hypersaline basins are usually associated with low river discharges whereas huge rivers with lower coastal salinities; both effects reduce the technical viability of projects.

Six different technologies that could harness this potential were introduced and explained, none of which has completely matured. The electric double-layer capacitive method was only recently discovered and reported in 2009, its validity was proven only in laboratory scale. The reverse vapour compression process, reported since 1979, has already been tested in laboratory scale and already had some studies determining its preliminary economic viability. Another technology at that same development level is the hydrocratic generator, patented in 2001. These were the least mature technologies presented.

The submarine hydro-electric-osmotic power plant actually has never left the conceptual stage. However, it is included amongst the more mature salinity power techniques, given its similarity to pressure retarded osmosis; a process already studied at prototype scale and on its way to launching a pilot plant. Both processes are so similar that a land-based variation of the submarine hydro-electric-osmotic power plant was presented in this study as a possible configuration for pressure retarded osmosis. At last, the reverse electrodialysis technique has also been developed, reported and tested at prototype scale with a future pilot plant construction scheduled.

An in-depth characterization of the pressure retarded osmosis process was presented. We identified concentration polarization across the membrane support layer as the most significant cause of reduction in the effective osmotic pressure between solutions. The pressure exchanger device was briefly introduced as a promising element regarding improvements in plant efficiency. Four power plant configurations were

evaluated; the continuous flow terrestrial power plant configuration proved to be unfeasible with an extremely low mechanical efficiency even when an ideal membrane was considered. Other configurations proved to be over twice as much effective, with efficiencies ranging from $0{,}6 - 0{,}75$ for real membrane performances. A common trade-off for higher efficiency is higher capital cost; we identified the continuous-flow terrestrial power plant with pressure exchanger configuration as the most cost-effective.

Afterwards, PRO power plant siting criteria were established by adapting methodologies from desalination processes. The optimal location must be geologically and topographically suitable for the construction of the power plant and located where access to the power grid, freshwater and seawater are technically and economically feasible. Quality water provision plays an important role in extending membrane life; attention must be given to micro-organisms levels since biofouling is the major cause for premature membrane replacement. In order to secure the salinity levels of feed and draw solutions it is necessary to develop a salinity intrusion model of the river estuary and to position water intakes accordingly. An example that considers all technicalities involving PRO siting was provided: a fictional $10\,MW$ pilot plant was placed at the Nordre älv estuary, in the western coast of Sweden.

A guideline for power plant sizing was developed using the same fictional net $10\,MW$ power plant; the continuos flow – terrestrial power plant with pressure exchanger configuration was considered throughout the analysis. Mechanical efficiency was estimated at $0{,}7831$; plant requirements of $4{,}725\,km^2$ of membrane area and 780 pressure exchanger units were calculated. Francis turbines and axial pumps were defined as the most adequate configurations to dealing with the modest working pressure of $9{,}7\,atm$ and huge permeating rate of $1135250\,m^3/d$ of the power plant.

The economic feasibility of the fictional pilot plant was assessed. The methodology used was adapted from sea water reverse osmosis desalination plants. Only the cost components relevant to PRO processes were considered during the estimative of capital and electricity production costs. Current technology could be employed to produce electricity at a cost of $1.0025\,US\$/kWh$; forecasts for 2020 expect costs to be reduced to a fourth of this value. This study proved that with the combined effects of increased membrane performance (80% energy recovery rate) and reduced

capital costs (50% reduction) those forecasts could be met. We then identified power plant siting and design as critical phases to reaching this goal.

Techno-economic viability is just the first obstacle that salinity-gradient energy technologies must surpass. There are several other types of barriers to their penetration in the electricity market that may define whether or not a project is viable. The major barriers to the progression of salinity-gradient energy research and development were identified and divided into these categories: financial, institutional, social, political, market imperfection, and regulatory barriers.

Considering what is known of the possible environmental impacts, public acceptance of osmotic technologies is presumed to be broad. Attention over this matter focused on how the disposed brackish water and power plant construction would affect the local marine environment. Uncertainty in governmental policies and regulations may also hinder project schedule but can be easily surpassed by adapting and studying what has already been done in the desalination framework.

Regarding the market imperfection category, it is pointed out that the high investment requirements of these technologies act as an entry barrier for entrepreneurs and in such cases it is important to assess the possibility and feasibility of joint ventures or public-private partnerships. Furthermore, as mentioned throughout this study, only a few companies hold the state-of-art of critical components to the operation of salinity-gradient energy systems; this restricted access to the technology and lack of competition increases cost and obstruct investments.

In addition to the severe effect of everything mentioned above, on the short term, two other barriers are preventing R&D advancements in salinity-gradient energy: the lack of information/awareness over these processes and the lack of institutions or mechanisms to disseminate this information. The fact that these technologies were only recently discovered partly contributes to maintaining a low profile, but in reality, there were just a handful of conferences that presented and discussed the possibility of harnessing salinity-gradient energy. Therefore, it is important to have in mind not only how these technologies are promoted but also through which means the promotion is carried out.

As these technologies are developed, we expect them to become increasingly visible in both the academic and entrepreneur environments. The year 2015 may mark salinity-gradient energy research with the inauguration of the first pressure retarded osmosis and reverse electrodyalisis pilot plants. Until then it is important to promote publications in order to update results and refresh memories of this promising alternative.

C8. Bibliography

[1] POST, J. W. **Blue Energy:** electricity production from salinity-gradients by reverse electrodialysis. Wageningen, 2009. 224 p.. Thesis. (Doctor's degree in Socio-Economic and Natural Sciences of the Environment) - Wageningen University.

[2] PATTLE, R. E. Production of electric power by mixing fresh and salt water in the hydroelectric pile. **Nature**, 174, p. 660-660, 1954.

[3] WICK, G. L.; SCHMITT, W.R. Prospects for Renewable Energy from the Sea. **Marine technology society journal,** vol. 11, n. 3, p. 16-21, jul./ago. 1977.

[4] DAI, A., et. al. Changes in continental freshwater discharge from 1948-2004. **Journal climate**, vol. 22, p. 2773-2791, mai. 2009. Avaiable at: <http://www.cgd.ucar.edu/cas/catalog/surface/dai-runoff/index.html>. Accessed: 18 abril 2011.

[5] DAI, A.; TRENBERTH, K. E. Estimates of freshwater discharge from continents: Latitudinal and seasonal variations. **Journal hydrometeorol**, vol. 3, p. 660-687, dez. 2002. Avaiable at: <http://www.cgd.ucar.edu/cas/catalog/surface/dai-runoff/index.html>. Accessed: 18 abril 2011.

[6] UNITED STATES OF AMERICA. Energy Information Administration. Department of Energy. Office of integrated analysis and forecasting. **International energy outlook 2010.** Washington D.C., 2010. Avaiable at: <http://ei-01.eia.doe.gov/oiaf/ieo/pdf/0484(2010).pdf>. Accessed: 17 abril 2011.

[7] IEA, International Energy Agency. Head of Communication and Information Office. **Key world energy statistics 2009**. Paris, 2009. Avaiable at: <http://www.iea.org/textbase/nppdf/free/2009/key_stats_2009.pdf>. Accessed: 17 abril 2011.

[8] BROGIOLI, D. Extracting renewable energy from salinity difference using a capacitor. **Physical review letters**, vol. 103, jul. 2009.

[9] TIKHOMOLOVA, K. **Electro-osmosis**. New York: Horwood, 1993.

[10] OLSSON, M.; WICK, G. L.; ISAACS, J. D. Salinity-gradient power - utilizing vapor-pressure differences. **Science**, vol. 206, p. 452-454, out. 1979.

[11] BREWBAKER, P. **Design and economics of a Reverse-Vapour-Compression (RVC) salinity-gradient engine**, 2007. Avaiable at: <http://www.philsinventions.com/philsinventions_htm_files/Design%20&%20Economics%20of%20an%20RVC%20engine_for_web.pdf>. Accessed: 16 abril 2011.

[12] BREWBAKER, P. **A heat transfer element for a reverse vapor compression salinity-gradient engine**, 2006. Avaiable at: <http://www.philsinventions.com/philsinventions_htm_files/PA-heat%20transfer%20element%20for%20web.pdf>. Accessed: 16 abril 2011.

[13] BREWBAKER, P. Calculations of performance of an example FBHX RVC plant. In **PPA:** Foil-based heat-exchanger for RVC engines, 2006. Avaiable at: <http://www.philsinventions.com/philsinventions_htm_files/salinity_engine_physics_discussion_for_web.pdf>. Accessed: 16 abril 2011.

[14] BREWBAKER, P. **Philsinventions:** A Reverse-Vapor-Compression Salinity-Gradient engine, 2006. Available at: <http://www.philsinventions.com/philsinventions_htm_files/PA-RVC%20engine%20for%20web.pdf>. Accessed: 16 abril 2011.

[15] FINLEY, W.; PSCHEIDT, E. **Hydrocratic Generator**. Patent US 7898102 B2, Assignee: Wader, LCC, Laguna Beach, USA, 2011.

[16] FINLEY, W.; PSCHEIDT, E. **Hydrocratic Generator**. World Intellectual Property Organization Patent WO/2000/053924. Applicant: Wader, LCC, Laguna Beach, USA, 2000.

[17] PSCHEIDT, E.; FINLEY, W. **Deriving useful power from the osmotic potential between solutions.** Wader, LCC internal report. Available at: <http://www.waderllc.com/Finley/deriving%20useful%20power%20paper.pdf>. Accessed: 29 abril 2011.

[18] REALI, M. Submarine hydro-electric-osmotic power plant for an efficient exploitation of salinity-gradients. ENEL-DSR-CRIS, Milano. **Energy**, 6, p. 227-231, 1981.

[19] ESTADOS UNIDOS. DOE, Department of Energy. **Handbook of methods for the analysis of the various parameters of the carbon dioxide system in sea water.** DICKSON, A. G.; GOYET, C.; ORNL/CDIAC-74, 1994.

[20] POST, J. W., et al. Salinity-gradient power: Evaluation of pressure-retarded osmosis and reverse electrodialysis. **Journal of membrane science**, vol. 288, p. 218-230, 2007.

[21] VEERMAN, J., et al. Reducing power losses by ionic shortcut currents in reverse electrodialysis stacks by a validated model. **Desalination**, vol. 205, p. 67-74, 2007.

[22] ACHILLI, A.; CHILDRESS, A. E. Pressure retarded osmosis: From the vision of Sidney Loeb to the first prototype installation – Review. **Desalination**, vol. 261, p. 205-211, 2010.

[23] ACHILLI, A; CATH, T. Y.; CHILDRESS, A. E. Power Generation with pressure retarded osmosis: An experimental theoretical investigation. **Journal of membrane science**, vol. 343, p. 42-52, jul. 2009. Available at: <http://aqwatec.mines.edu/publications/CathPub/Power_generation_with_PRO.pdf>. Accessed: 19 abril 2011.

[24] LOEB, S. The Loeb-Sourarijan membrane: how it came about. In: **Synthetic Membranes:** Desalination. TURBAK, A. Washington DC: American Chemical Society, 1981. (ACS Symposium Series).

[25] LOEB, S. Large-scale power production by pressure retarded osmosis, using river water and sea water passing through spiral modules. **Desalination**, vol. 143, p. 115-122, jul. 2002 (see also: Desalination, 150, p. 205, 2002).

[26] LOEB, S.; HONDA, T.; REALI, M. Comparative mechanical efficiency of several plant configurations using a pressure-retarded osmosis energy converter. **Journal of membrane science**, vol. 51, p. 323-335, ago. 1990.

[27] SOURIRAJAN, S. **Reverse Osmosis.** Londres: Logos Press Limited, 1970.

[28] LEE, K.; BAKER, R.; LONSDALE, H. Membranes for power generation by pressure-restarted osmosis. **Journal of membrane science**, vol. 8, p. 141-171, 1981.

[29] HONDA, T. Development of a four-partitioned permeator for salinity power generation. **Bulletin society of sea water science**, 42, p. 233-240, 1989.

[30] STOKER, R. L. **Rotary Pressure Exchanger.** U.S. Patent 7201557 B2. Assignee: Energy Recovery, Inc. San Leandro, USA, 2007.

[31] STOKER, R. L. Development of a fourth generation energy recovery device. A 'CTO's Notebook'. **Desalination**, vol. 165, p. 313-321, 2004.

[32] TSIOURTIS, N. X. Criteria and procedure for selecting a site for a desalination plant. **Desalination**, vol. 221, p. 114-125, 2008.

[33] ZHAN, C. **A Three-Dimensional Model of Göta Älv for Water Quality Simulation**. Gothenburg, 2009. 50 p.. Master's Thesis (Master's degree in Civil and Environmental Engineering) – Chalmers University of Technology. Available at: <http://www.dricks.chalmers.se/files/exjobb/Exjobb_CZ-2009_7.Pdf>. Accessed: 19 abril 2011.

[34] MENDEL, V. M. **Raw Water Storage Case Study:** Göteborg's Water Supply. Gothenburg, 2005. 59 p.. Master's Thesis (Master's Thesis in Applied Environmental Measurement Techniques) – Chalmers University of Technology. Available at: <http://publications.lib.chalmers.se/records/fulltext/21669.pdf>. Accessed: 19 abril 2011.

[35] CA, V. T. **Salinity Intrusion in the Red River Delta.** 1996. Available at: <http://coombs.anu.edu.au/~vern/env_dev/papers/pap08.html>. Accessed: 20 abril 2011.

[36] LIU, W. C., et. al. The influence of river discharge on salinity intrusion in the Tanshui Estuary, Taiwan. **Journal of coastal research,** vol. 17, n. 3, p. 544-552, 2001. Available at: <http://ntur.lib.ntu.edu.tw/bitstream/246246/176164/1/07.pdf>. Accessed: 20 abril 2011.

[37] SELMER, J. S.; RYDBERG, L. Effects of nutrient discharge by river water and waste water on the nitrogen dynamics in the archipelago of Göteborg, Sweden. **Marine ecology progress series**, vol. 92, p. 119-133, jan. 1993. Available at: <http://www.int-res.com/articles/meps/92/m092p119.pdf>. Accessed: 18 abril 2011.

[38] DHI INSTITUT FOR VAND OG MILIØ. **Investigation of the effects of phosphorus emissions from Ryaverket.** Bohuskustens Vattenvårdsförbund, 2005. Available at: <http://www.gryaab.se/admin/varor/docs/DHISlutrapportrecipientdel12005UWA.pdf>. Accessed: 18 abril 2011.

[39] NASCO, NORTH ATLANTIC SALMON CONSERVATION ORGANIZATION. **Protection, restoration and enhancement of salmon habitat, focus area report.** EU-Sweden, 2009. Available at: <http://www.nasco.int/pdf/far_habitat/HabitatFAR_Sweden.pdf>. Accessed: 18 abril 2011.

[40] THAKE, J. **The micro-hydro pelton turbine manual:** design, manufacture and installation for small-scale hydropower. Londres: ITDG Publishing, 2000.

[41] RUBBO, V. **Turbine idrauliche:** regolazione – progetti. Milão: Edizioni Bignami, 1967.

[42] BATES, W. T. Reducing the fouling rate of surface and waste water RO systems. **Hydranautics, IWC-98-08,** p. 1-7. Available at: <http://www.membranes.com/docs/trc/fouling.pdf>. Accessed: 18 abril 2011.

[43] PETER, T.; PINTO', D. Seawater intake and pre-treatment / brine discharge – environmental issues. **Desalination**, vol. 221, p. 576-584, 2008.

[44] FRIOUI, S.; OUMEDDOUR, R. Investment and production costs of desalination plants by semi-empirical method. **Desalination**, vol. 223, p. 457-463, 2008. Available at: < http://www.desline.com/articoli/9046.pdf>. Accessed: 18 abril 2011.

[45] HAFEZ, A.; EL-MANHAWARY, S. Economics of seawater RO desalination in the Red Sea region, Egypt. Part1. A case study. **Desalination**, vol. 153, p. 335-347, 2002. Available at:
<http://www.desline.com/articoli/4938.pdf>. Accessed: 18 abril 2011.

[46] AKASHAN, S., et. al. Cost and economic analysis of Doha Reverse Osmosis plant (Kuwait). **Desalination**, vol. 64, p. 65-82, 1987.

[47] UNITED STATES ARMY CORPS OF ENGINEERS. Hydrology Engineering Center. **A feasibility study for small scale hydropower additions, a guide manual**. USA, 1979.

[48] FRITZMANN, C., et. al. State-of-the-art of reverse osmosis desalination. **Desalination**, vol. 216, p. 1-76, 2007. Available at:
<http://www.desline.com/articoli/8671.pdf>. Accessed: 18 abril 2011.

[49] JONES, A. T.; FINLEY, W. Recent developments in salinity gradient power. p. 2884-2887, 2004. Available at:
<http://waderllc.com/2284-2287.pdf>. Accessed: 18 abril 2011.

[50] WICK, G.L.; SCHMITT, W.R. Prospects for renewable energy from the sea. **Marine technology society journal**, p. 16-21, 1977.

Other subject-related references

MI, B.; ELIMELECH, M. Chemical and physical aspects of organic fouling of forward osmosis membranes. **Journal of membrane science**, 320, p. 292-302, 2008.

PAISH, O. Small hydro power: technology and current status. **Renewable and sustainable energy reviews**, 6, p. 537-556, 2002.

LOEB, S. **Method and apparatus for generating power utilizing pressure-retarded osmosis.** Patent US 4193267. Assignee: Ben-Gurion University of the Negev Research and Development Authority, Beersheba, Israel, 1978.

PAINULY, J. P. Barriers for renewable energy penetration; a framework for analysis. **Renewable energy**, 24, p. 73-89, 2001.

Internet references

http://www.stromstad.se – accessed May 6th 2011
http://www.uddevalla.se – accessed May 6th 2011
http://www.munkedal.se – accessed May 6th 2011

http://www.kungavl.se – accessed May 6th 2011
http://www.goteborg.se – accessed May 6th 2011

Statkraft
www.statkraft.com – accessed May 13th 2011
http://www.statkraft.com/energy-sources/osmotic-power/ – accessed May 13th 2011
http://www.osmosefilmer.com/engelsk2.html – accessed May 13th 2011

Wader, LCC
http://www.waderllc.com/technical.htm – accessed May 13th 2011

Sveriges Vattenorganizationer
http://www.vattenorganisationer.se/ – accessed May 13th 2011

Swedish Meteorological and Hydrological Institute
http://www.smhi.se/en – accessed May 13th 2011

Google maps
http://www.maps.google.com – accessed July 5th 2011

http://www.kochmembrane.com/pdf/megamag_bro_lores1.pdf – accessed June 2nd 2011
http://www.energyrecovery.com/ – accessed June 2nd 2011
http://www.ide-tech.com/media-center/downloads – accessed June 2nd 2011
http://www.africacncl.org/downloads/Algeria_Desalination_Plant.pdf
– accessed June 2nd 2011
http://www.gewater.com/pdf/Case%20Studies_Cust/Americas/English/CS1338EN.pdf
– accessed June 2nd 2011
http://www.freedoniagroup.com/brochure/20xx/2033smwe.pdf
– accessed June 2nd 2011
http://www.toyobo.co.jp/e/annai/zaimu/annual/2008/p08-11.pdf
– accessed June 2nd 2011
http://www.ecw.org/ecwresults/425-1.pdf – accessed June 2nd 2011
http://www.aquatechnology.net/reverse_osmosis.html – accessed June 2nd 2011
http://www.engineering.lancs.ac.uk/lureg/nwhrm/engineering/turbine_costs.php?#tab
– accessed June 2nd 2011
http://www.water-technology.net/projects/ – accessed June 2nd 2011
http://www.ges.co.il/files/GES_ProjPage_Palmachim_Eng.pdf – accessed June 2nd 2011
http://h2oreuse.blogspot.com/2007/09/israels-desalination-industry.html
– accessed June 2nd 2011

Attachments

A) Technical datasheet of the pressure exchanger energy recovery unit PX-300

ERI
1717 Doolittle Dr.
San Leandro, CA
94577, USA
Phone: 1-510-483-7370
FAX: 1-510-483-7371

Energy Recovery, Inc. Specifications Sheet PX-300

Sheet Page 1 of 1

Document number: **80179-01**

REV	BY	CKD	REVISION	DATE
0	JMP	RLS	Preliminary release	7/2/09
1	JMP	RLS	Performance update	9/30/2009
2	JGM	RBC	Performance update	6/8/2010

DESCRIPTION: TECHNICAL DATA SHEET, POSITIVE DISPLACEMENT ENERGY RECOVERY DEVICE

1.Part number **40027** | 2. Service | 3. Reference

4	OPERATING CONDITIONS	Liquid	Seawater
5		Operating Temperature	33°F-120°F (0.6-49°C)
6		Max. Temperature	120°F (49°C)
7		Specific Gravity	1.03
8		Viscosity	1.060 cP @ 70°F (21.1°C)
9		Flow range	200 - 300 gpm (45 - 68m3/h)
10		Maximum High-Pressure Inlet Flow	300 gpm (68 m3/h)
11		Maximum Low-Pressure Outlet Flow	300 gpm (68 m3/h)
12		Maximum Outlet High Pressure	1200 psi (82.7 bar)
13		Maximum Outlet Low Pressure	300 psi (20.7 bar)
14		Maximum Inlet High Pressure	1200 psi (82.7 bar)
15		Minimum Inlet Low Pressure	N/A
16		Minimum Discharge Pressure	12 psi (0.8 bar)
17		Filtration Requirement (Nominal)	10 µm
18			
19	PERFORMANCE	Peak Effiency	98%
20		Maximum High Pressure Differential	14.5 psi (1 bar) @ 300 gpm
21		Maximum Low Pressure Differential	14.5 psi (1 bar) @ 300 gpm
22		Maximum Lubrication Flow	4.4 gpm (1 m3/h) @ 300 gpm
23		Maximum Rotational Speed	600 rpm @ 300 gpm
24		Maximum Salinity Increase at Membranes	3% @ 40% Recovery
25		Sound level	93 dBA
26			
27	MATERIALS	Housing	GRP**
28		Rotor, Sleeve, Endcover Assembly	Ceramic-alumina
29		Low Pressure Inlet Port Fitting	PVC
30		Low Pressure Outlet Port Fitting	PVC
31		High Pressure Inlet Port Fitting	Superduplex
32		High Pressure Outlet Port Fitting	Superduplex
33		Internal Low Pressure Interconnector	Titanium
34		Fasteners/Hardware (non-wetted)	316SS
35		Tension Rod Assembly	AL-6XN* / C-276
36		O-rings	EPDM
37			
38	PIPING CONNECTIONS	Low Pressure Inlet Port Fitting	4" (DN100) Grooved-end Flexible Pipe Coupling
39		Low Pressure Outlet Port Fitting	
40		High Pressure Inlet Port Fitting	3" (DN80) Grooved-end Flexible Pipe Coupling
41		High Pressure Outlet Port Fitting	
42			
43			
44			

45	TESTS	Performance	Standard
46		Case Hydrotest	Standard
47		Rotation Speed Test	Standard
48		Die Penetrant Test (ceramics)	Standard
49		Cavitation Test	Standard
50		Witnessed Test	Optional
51			
52			
53			
54			
55			
56			
57	INSPECTION	Outside Dimensions	Standard
58		Internal Components	Standard
59		Housing Dimensions	Standard
60		Ceramic Dimensions	Standard
61		Material Certificates	Standard
62		Visual	Standard
63		Packing and Crating	Standard
64			
65			
66			
67			
68			
69	SHIPPING WEIGHT AND DIMENSIONS	PX-300 unit Shipping Dimensions	47x17x17 inch 119x43x43 cm
70		PX-300 unit Shipping Weight	205 lbs. (93 kg)
71		Dry PX-300 unit weight	195 lbs. (88 kg)
72		Cartridge Shipping Dimensions	20x12x12 inch 51x31x31 cm
73		Cartridge Weight	44 lbs. (20 kg)
74		Shipping and Storage Temperature	33°F-120°F (0.6-49°C)
75			
76			
77	MISCELLANEOUS		
72			
79			
80			
81			
82			
83			

*AL-6XN is a registered trademark of Allegheny Ludlum
**Housing designed in accordance with the engineering standards of the Boiler and Pressure Vessel Code of the American Society of Mechanical Engineers.
ERI RESERVES THE RIGHT TO MAKE SPECIFICATION CHANGES AT ANY TIME WITHOUT PRIOR NOTICE.

PRICE: sales@energyrecovery.com

MANUFACTURER: Energy Recovery Inc | **MODEL:** PX-300

B) Economic database from SWRO desalination plants

Power plant / reference	Plant capacity (m3/d)	Capital cost (US$)	Unit Cost ($.d/m3)	Water production cost (US$)	Annual expenses (US$)	Year	Capital Cost (US$ 2010)	Unit Cost 2010 ($.d / m3)	Annual expenses (US$ 2010)
(HAFEZ, EL-MANHAWARY; 2002)	250	541500	2166,00	2,700	243000	2002	660630	2642,52	296460
	500	1047500	2095,00	2,460	442800		1277950	2555,90	540216
	2000	3428000	1714,00	1,850	1332000		4182160	2091,08	1625040
	3500	5897500	1685,00	1,720	2167200		7194950	2055,70	2643984
	4800	6542400	1363,00	1,280	2211840		7981728	1662,86	2698445
	7000	7917000	1131,00	1,210	3049200		9658740	1379,82	3720024
	10000	9620000	962,00	1,180	4248000		11736400	1173,64	5182560
	15000	13560000	904,00	1,150	6210000		16543200	1102,88	7576200
	20000	16640000	832,00	1,040	7488000		20300800	1015,04	9135360
	30000	23640000	788,00	0,930	10044000		28840800	961,36	12253680
	40000	28520000	713,00	0,890	12816000		34794400	869,86	15635520
	50000	33350000	667,00	0,860	15480000		40687000	813,74	18885600
(AKASHAN et al.; 1987)	4546	5009676	1102,00	1,230	2013395	1987	9768869	2148,89	3926121
	9092	8790641	966,85	1,003	3281901		17141750	1885,37	6399707
	13638	12347051	905,34	0,969	4758804		24076750	1765,42	9279668
	18134	15882876	875,86	0,960	6263935		30971608	1707,93	12214674
	22730	19147830	842,40	0,941	7702576		37338268	1642,69	15020023
	27276	22228118	814,93	0,925	9085647		43344830	1589,12	17717012
Alicante SWRO - Spain	50700	90500000	1785,01			2003	107695000	2124,16	
Lanarca SWRO - Cyprus	54000	47000000	870,37	0,790	15357600	2001	58280000	1079,26	19043424
Palm Jumeirah SWRO - UAE	70000	90000000	1285,71			2006	99000000	1414,29	
Paraguana SWRO - Venezuela	75000	150000000	2000,00			2008	154500000	2060,00	
Tampa Bay SWRO - USA	95000	158000000	1663,16	0,650	22230000	2006	173800000	1829,47	24453000
Skikda SWRO - Algeria	100000	110600000	1106,00	0,740	26640000	2005	124978000	1249,78	30103200
Cap Djinet SWRO - Algeria	100000	120000000	1200,00	0,750	27000000	2008	123600000	1236,00	27810000
Qingdao SWRO - China	100000	135000000	1350,00			2008	139050000	1390,50	
Tuas SWRO - Singapore	110000	200000000	1818,18	0,480	19008000	2005	226000000	2054,55	21479040
Tipaza Fouka SWRO - Algeria	120000	189000000	1575,00			2008	194670000	1622,25	
Palmachim SWRO - Israel	150000	180000000	1200,00	0,690	37260000	2006	198000000	1320,00	40986000
Perth SWRO - Australia	150000	317000000	2113,33	1,000	54000000	2005	358210000	2388,07	61020000
Sur SWRO - Oman	150000	275000000	1833,33			2007	294250000	1961,67	
Hamma SWRO - Algeria	200000	200000000	1000,00	0,702	50544000	2005	226000000	1130,00	57114720
Llobregat SWRO - Spain	200000	250000000	1250,00			2011	250000000	1250,00	
Ashkelon SWRO - Israel	280000	212000000	757,14	0,520	52416000	2003	252280000	901,00	62375040
Hadera SWRO - Israel	350000	425000000	1214,29	0,570	71820000	2005	480250000	1372,14	81156600
Magtaa RO - Algeria	500000	468000000	936,00			2011	468000000	936,00	